

ファイル番号	候補者	候補者所属	業績の題目	推薦者	論文査読者
No.19-1	NGUYEN QUANG HUNG Vietnamese	Institute of Research and Development, Duy Tan University	The award is given to Dr. Nguyen Quang Hung for his contributions in the field of nuclear structure theory, particularly for the description of level density and $\gamma$ -ray strength function	Nguyen Dinh Dang Nishina Center Research Scientist Quantum Hadron Physics Laboratory (理研 仁科加速器センター)	福島, 田村
No.19-2	Bumjoon Kim Korea	Department of Physics Pohang University of Science and Technology	The discovery and experimental study of an unconventional Mott insulating state induced by relativistic spin-orbit coupling in iridates.	Soo-Bong Kim Professor of Physics Seoul National University	前野, 伊藤
No.19-3	Hao Zhang Chinese	Department of Physics, Tsinghua University, Beijing	Outstanding contribution to the Majorana nanowire experiments and topological quantum computation	Ke He Department of Physics, Tsinghua University, Beijing	村尾, 風間
No.19-4	Donghun Lee Korea	Department of Physics, Korea University, South Korea	Contribution to the observation of quantum phenomena in macroscopic mechanical objects	Cheol Eui Lee Department of Physics, Korea University, South Korea	永長, 村尾
No.19-5	Sungjay Lee Korea	School of Physics Korea Institute for Advanced Study	Discovery of a new class of d=3 gauge theories, with M-theory applications, and pioneering works that revolutionized study of d=2, 3 gauge theories and their conformal limit.	Piljin Yi Professor of Physics & Vice President Korea Institute for Advanced Study	風間, 佐々木
No.19-6	Chen Fang China	Institute of Physics, Chinese Academy of Sciences	For developing the theory of topological classification and diagnosis for non-magnetic materials.	Hongming WENG Institute of Physics, Chinese Academy of Sciences	押川, 前野
No.19-7	Bohm-Jung Yang Korea	Department of Physics and Astronomy, Seoul National University	for his contribution to uncovering topological of three-dimensional Dirac semimetals	Doochul Kim, Naoto Nagaosa	押川, 磯
No.19-8 受賞	Chao Yang Lu China	Professor of Physics, Hefei National Laboratory for Physical Sciences at Microscale, University of Science and Technology of China	For his outstanding contributions to quantum information science with single photons	Ruibao Tao Department of Physics, Fudan University	村尾, 佐々木

No.19-9	Elmer Estacio Philippine	National Institute of Physics University of the Philippines Diliman	Dr.Estacio performed extensive work on the investigation of the optical and terahertz properties of semiconductors,as well as their possible application in the development of novel terahertz ptoelectronic devices.	Arnel A.Salvador Professor of Physics National Institute of Physics University of the Philippines Diliman	前野, 永長
No.19-10	Seunghwan Shin Korea	PLS-II accelerator division,Pohang Accelerator Laboratory	For his remarkable contributions to the commissioning of PLS-II and the understanding of current-dependent nonlinear beam dynamics on storage rings for synchrotron radiation.	In Soo Ko Director, Pohang Accelerator Laboratory and Professor Emeritus,POSTECH	中家, 山内
No.19-11	Jeng-Da Chai Taiwan	Department of Physics, National Taiwan University	For his development of accurate density functional methods for nanoscale application,	Yuan-Huei Chang Professor and Chairman National Taiwan University	押川, 伊藤
No.19-12	Yanchao Wang China	State Key Lab of Superhard Materials, Jilin University, China	For his development of efficient method(named as CALYPSO) for the prediction of crystal structures with the only given information of chemical compositions,	Yanming Ma College of Physics, Jilin University, China	永長, 中家
No.19-13	Yi-Bo Yang China	Institute of Theoretical Physics, Chinese Academy of Science (ITP-CAS), Beijing, China	Advancement of Lattice QCD efforts to understand the importance of the gluon in the proton	Hai-Jun Zhou Institute of Theoretical Physics, Chinese Academy of Science (ITP-CAS), Beijing, China	福島, 磯
No.19-14	Jun Zhao China	Xie Xide Junior Chair Professor, Dept. of Physics, Fudan University, Shanghai, China	The elucidation of magnetic properties of iron-based superconductors.	Yuanbo Zhang Professor of Physics, Fudan University, China	伊藤, 山内
No.19-15	Feng-Kun Guo China	Institute of Theoretical Physics, Chinese Academy of Sciences	For his outstanding theoretical contributions to understanding the nature of new hadrons discovered since 2003.	岡 眞 Advanced Science Research Center, Japan Atomic Energy Agency	福島, 田村



# Nomination form for the 2019 Nishina Asia Award

Candidate (name, affiliation, curriculum vitae including the date of the degree of Ph.D., nationality, address, email and telephone)	
Name: NGUYEN QUANG HUNG (*)	Date of birth: July 24, 1980
Nationality: Vietnamese	Sex: male
<b>Affiliation:</b> Institute of Fundamental and Applied Sciences (IFAS), Duy Tan University, 03 Quang Trung, Danang City, Vietnam	
<b>Position:</b> Associate Professor, Director of IFAS	
<p>(*) Re-nominated for the fourth time. Previous nominations: 2013, 2017, 2018. Please see the materials of his nomination for the Nishina Asia Award 2018 (NAA 2018).</p> <p>The only revision here is the replacement of the Ref. 3 (in list of key references) with</p> <p><b>3) N. Quang Hung, N. Dinh Dang, and L.G. Moretto</b></p> <p><i>Pairing in excited nuclei: a review</i>, invited review to appear in Rep. Prog. Phys. in 2019.</p> <p>Abstract:</p> <p>The present review summarizes the recent studies on the thermodynamic properties of pairing in many-body systems including superconductors, metallic nanosized clusters and/or grains, solid-state materials, focusing on the excited nuclei, that is nuclei at finite temperature and/or angular momentum formed via heavy-ion fusion, alpha-induced fusion reactions, or inelastic scattering of light particles on heavy targets. Because of the finiteness of the systems, several interesting effects of pairing such as nonvanishing pairing gap, smoothing of superfluid-normal phase transition, first and second order phase transitions, pairing reentrance, etc., will be discussed in detail. Influences of exact and approximate thermal pairing on some nuclear properties such as temperature-dependent width of the giant dipole resonance, total level density, and radiative strength function of the gamma-rays emission will also be analyzed. Finally, the first experimental evidence of the pairing reentrance phenomenon in a <math>^{104}\text{Pd}</math> nucleus as well as its solid-state counterpart of ferromagnets under strong magnetic field will be presented.</p>	
Citation for the Award (within 30 words)	
Please see his nomination for NAA 2018.	



Description of the work

Please see his nomination for NAA 2018.

Key references (up to 3 key publications\*)

- 1) **N. Quang Hung, N. Dinh Dang, L.T. Quynh Huong,**  
*Simultaneous microscopic description of nuclear level density and radiative strength function,*  
Phys. Rev. Lett. **118** (2017) 022502.
- 2) **N. Quang Hung and N. Dinh Dang,**  
*Thermodynamic properties of hot nuclei within the self-consistent quasiparticle random phase approximation,* Phys. Rev. C **82** (2010) 044316.
- 3) **N. Quang Hung, N. Dinh Dang, and L.G. Moretto**  
*Pairing in excited nuclei: a review,* invited review to appear in Rep. Prog. Phys. in 2019.

\*) Copy of one most significant publication should be attached.



Nominator (name, affiliation, email, telephone and relation to the candidate)

Nguyen Dinh Dang

Nishina Center Research Scientist

Quantum Hadron Physics Laboratory

RIKEN Nishina Center for Accelerator-Based Science

Main Research Bldg., R. 430

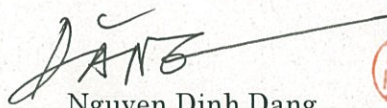
RIKEN, 2-1 Hirosawa, Wako city, 351-0198 Saitama, Japan

Tel: 81-48-462-1111, Extension: 3447

Fax: 81-48-462-4698

Email: dang@riken.jp

Signature



Nguyen Dinh Dang



Date 9 January 2019

## Nomination form for the 2018 Nishina Asia Award

Candidate (name, affiliation, curriculum vitae including the date of the degree of Ph.D., nationality, address, email and telephone)
<p>Bumjoon Kim Department of Physics Pohang University of Science and Technology</p> <p>77 Cheongam-Ro Nam-Gu Pohang Gyeongbuk Korea 37673 Tel: +82 (0)54 279 9882 Fax: +82 (0)52 279 9889 Mobile: +82 (0)10 5128 5122</p> <p>Nationality: Korean</p> <p>Career history:</p> <p>December 2016 - present Associate Professor Pohang University of Science and Technology Department of Physics</p> <p>July 2013 - November 2016 Group Leader Max Planck Institute for Solid State Research Neutron Scattering Group, Solid State Spectroscopy Department</p> <p>September 2010 - June 2013 Assistant Physicist Argonne National Laboratory Materials Science Division</p> <p>February 2010 - September 2010 Postdoctoral Research Fellow Argonne National Laboratory Materials Science Division</p> <p>April 2008 - January 2010</p>

Postdoctoral Research Fellow  
University of Michigan, Ann Arbor  
Prof. James W. Allen  
October 2006 - March 2008  
Visiting scientist  
University of Tokyo  
Prof. Hidenori Takagi

08.2005  
Ph. D. in physics  
New approach to angle-resolved photoemission spectroscopy using high photon energy  
Prof. Se-Jung Oh  
Seoul National University

02.2001  
M. S. in physics  
Seoul National University

02.1999  
B. A. in physics  
Korea Advanced Institute of Science and Technology

Award:  
Brian R. Coles Prize 2013  
30 Young Scientists of Korea (2016)

Citation for the Award (within 30 words)

The discovery and experimental study of the spin-orbit Mott insulating state induced by relativistic spin-orbit coupling in iridates.

Description of the work

B. J. Kim discovered a new phase of quantum matter in the 5d transition-metal oxide  $\text{Sr}_2\text{IrO}_4$  now widely known as “spin-orbit Mott insulator”. Using angle-resolved photoemission, x-ray absorption, and resonant x-ray diffraction, he established that the electronic ground state in this material has a highly nontrivial spin-orbit entangled structure with effective total angular momentum one-half ( $J_{\text{eff}}=1/2$ ). These results were published in Physical Review Letters (2008) and Science (2009), which have a combined citation exceeding 1600 (as of 3/3/2018). The study of spin-orbit Mott insulator has now become one of the mainstreams in condensed matter physics.

The discovery of the  $J_{\text{eff}}=1/2$  ground state is significant because it is parent to a plethora of unconventional electronic orders. One of the most exciting possibilities is the realization of the cuprate physics in a non-cuprate material; namely, spin-1/2 Mott insulator on a square lattice with  $J_{\text{eff}}=1/2$  moments playing the role of spin-1/2 moments. Following the initial work, B. J. Kim showed that  $\text{Sr}_2\text{IrO}_4$  exhibits spin dynamics in remarkable similarity with that in high temperature superconducting cuprates, heightening the prospect of finding a new high temperature superconductor. This work is also a major breakthrough in x-ray science because it is the first demonstration of using hard x-ray to probe momentum-resolved dynamic spin structure over the full Brillouin zone, which has previously been only accessible by inelastic neutron scattering.

B. J. Kim has further shown that the  $J_{\text{eff}}=1/2$  state develops a high temperature pseudogap and a low-temperature d-wave gap upon carrier doping, reproducing the complete phenomenology of the cuprates. This work used surface sensitive techniques to dope the surface layer of  $\text{Sr}_2\text{IrO}_4$  and at present whether the d-wave gap represents unconventional superconductivity remains an open question, but at the least it established a new material platform to study the elusive relationship between the pseudogap and the d-wave gap. Contributions from other groups have further strengthened the analogy to cuprates by showing the existence of competing symmetry broken phases in the pseudogap region of the phase diagram that are also very much reminiscent of the cuprate phase diagram. All the evidence collectively point to a high probability of finding high temperature superconductivity in iridate in the near future.

In another related material  $\text{Na}_2\text{IrO}_3$ , B. J. Kim showed that the  $J_{\text{eff}}=1/2$  state leads to a strong magnetic frustration and a magnetic phase in close proximity to the Kitaev spin liquid.

This is first direct evidence that the Kitaev magnetic interaction can be realized in a condensed matter setting. This shows that  $J_{\text{eff}}=1/2$  states can lead to very different types of magnetic interactions depending on the bonding and lattice geometry and thus can have wide applications beyond reproducing cuprate physics. Other interesting directions include topological phases of matter combining magnetism, for which pyrochlore iridates (also based on  $J_{\text{eff}}=1/2$  states) are now under active discussions.



In summary, the discovery of the  $J_{\text{eff}}=1/2$  ground state by B. J. Kim has opened a new field and had a broad impact in condensed matter physics in the last decade. Given the fact that the conventional Mott insulator since its discovery in 1930's has been a central paradigm of correlated electron physics for nearly a century, it is extremely interesting to see a new spin on the Mott insulators and the future it will bring.

Key references (up to 3 key publications\*)

B. J. Kim et al., Novel  $J_{\text{eff}}=1/2$  Mott insulator induced by relativistic spin-orbit coupling in  $\text{Sr}_2\text{IrO}_4$ , Physical Review Letters **101**, 076402 (2008).

B. J. Kim et al., Phase-sensitive observation of a spin-orbital Mott state in  $\text{Sr}_2\text{IrO}_4$ , Science **323**, 1329 (2009).

Y. K. Kim et al., Fermi arcs in a doped pseudospin-1/2 Heisenberg antiferromagnet, Science **345**, 187 (2014).

\*) Copy of one most significant publication should be attached.

Nominator (name, affiliation, email, telephone and relation to the candidate)

Soo-Bong Kim

Department of Physics and Astronomy

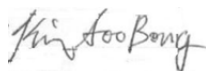
Seoul National University

sbk@snu.ac.kr

+82-2-880-5755 (O), +82-10-3896-3530 (Mobile)

I know him by his impressive research achievements although he is in other University and other physics field.

Signature



Date March 7, 2018

Candidate (name, affiliation, curriculum vitae including the date of the degree of Ph.D., nationality, address, email and telephone)
<p><b>Name:</b> Hao Zhang</p> <p><b>Affiliation:</b> Department of Physics, Tsinghua University, Beijing</p> <p><b>Nationality:</b> Chinese. <b>Email:</b> hzquantum@tsinghua.edu.cn</p> <p><b>Telephone:</b> +8618518088943</p> <p><b>Address:</b> Department of Physics, Tsinghua University, Meng-minwei Science and Technology Building S715, Beijing, 100084, China</p> <p><b>Curriculum Vitae:</b></p> <p>Education &amp; Working experience:</p> <p>2006.09 – 2010.07, B.S. in Physics, Peking University Minor in Economics, Peking University</p> <p>2010.08 – 2014.07, M.S. in Electrical Engineering, Duke University PhD in Physics, Duke University (date: 2014.09.01) Advisor: Albert Chang Thesis: Electron correlation effects in quantum point contacts</p> <p>2014.08 – 2018.07, Postdoc Researcher, Delft University of Technology, Netherlands Leo Kouwenhoven Group Research subject: Majorana fermions and topological quantum computation</p> <p>2018.08 – present, Associate Professor, Tsinghua University Joint Professor, Beijing Academy of Quantum Information Sciences</p> <p>Research Interests: Experimental condensed matter physics, quantum transport Majorana zero modes and topological quantum computing</p> <p>Awards:</p> <ul style="list-style-type: none"> <li>2018 National Thousand Young Talents Plan</li> <li>2018 Alibaba DAMO Academy Young Fellow</li> <li>2013 Outstanding Physics Teachers, American Association of Physics Teachers (AAPT)</li> </ul>
Citation for the Award (within 30 words)
Outstanding contributions to the Majorana nanowire experiments and topological quantum computation
Description of the work

Majorana zero-modes is the key building block for topological quantum computing. Topological quantum computing can in principle solve error problems, i.e. decoherence, in a fundamental way due to the unique topological properties of Majorana modes. Among all different Majorana proposals based on various topological systems, semiconductor nanowires coupled to a superconductor is the leading platform due to the tremendous experimental breakthroughs over the last few years, in which the candidate is a main contributor.

In 2012, Kouwenhoven group in Delft University of Technology (Netherlands) reported the first experimental signatures of Majorana modes (Science 336, 1003 (2012)), which raised enormous interest, but also along with heavy debates on whether Majorana zero-modes have been unambiguously observed. The candidate joined the Delft group as a postdoc to settle these debates and fully establish Majoranas in this system. The candidate spends four years to develop a new nano-fabrication recipe (a new experimental approach), which solves the disorder problem. This not only helps to rule out alternative explanations of the Majorana experiment, but also leads to the first quantization of Majorana conductance (Nature 556, 74 (2018)), which was the biggest discrepancy between previous experiment and Majorana theory. This work is “A hallmark experiment towards topological qubit” (Nature Physics 14, 334 (2018)).

Besides the quantized Majorana zero-mode experiment, the candidate also made great contributions to develop the Majorana braiding circuit, i.e. semiconductor-superconductor nanowire network, which is the foundation for a scalable topological quantum computer.

Up to now, the candidate’s work has resulted in 11 published papers including 2 Natures, 1 Nature Nanotechnology, 1 Nature Communications and 1 PRL (editor’s suggestion).

#### Key references (up to 3 key publications\*)

- 1, Quantized Majorana conductance, **Nature** 556, 74 (2018) (contribution: first author, co-corresponding author), **H. Zhang\***, C.-X. Liu, S. Gazibegovic, D. Xu, J. Logan, G. Wang, N. van Loo, J. Bommer, M. de Moor, D. Car, R. Op het Veld, P. van Veldhoven, S. Koelling, M. Verheijen, M. Pendharkar, D. Pennachio, B. Shojaei, J. Lee, C. Palmstrom, E. Bakkers, S. Das Sarma & L. Kouwenhoven,
- 2, Ballistic Majorana nanowire devices, **Nature Nanotechnology** 13, 192 (2018) (co-first author, co-corresponding author), O. Gul\*, **H. Zhang\***, J. Bommer\*, M. de Moor, D. Car, S. Plissard, E. Bakkers, A. Geresdi, K. Watanabe, T. Taniguchi and L. Kouwenhoven,
- 3, Epitaxy of advanced nanowire quantum devices, **Nature** 548, 434 (2017) (co-first author), S. Gazibegovic\*, D. Car\*, **H. Zhang\***, S. Balk, J. Logan, M. de Moor, M. Cassidy, R. Schmits, D. Xu, G. Wang, P. Krogstrup, R. Op het Veld, K. Zuo, Y. Vos, J. Shen, D. Bouman, B. Shojaei, D. Pennachio, J. Lee, P. van Veldhoven, S. Koelling, M. Verheijen, L. Kouwenhoven, C. Palmström & Erik Bakkers,



\*) Copy of one most significant publication should be attached. (see attachment)

Nominator (name, affiliation, email, telephone and relation to the candidate)

**Name:** Ke He

**Affiliation:** Department of Physics, Tsinghua University, Beijing

**Email:** kehe@tsinghua.edu.cn

**Telephone:** +8615110263128

**Relation to the candidate:** Colleague

Signature 

Date March 7, 2019

# Nomination form for the 2019 Nishina Asia Award

Candidate (name, affiliation, curriculum vitae including the date of the degree of Ph.D., nationality, address, email and telephone)
<p>First &amp; Last Name: Donghun Lee</p> <p>Affiliation: Department of Physics, Korea University, South Korea</p> <p>Education:</p> <ul style="list-style-type: none"> <li>- Ph.D., Physics, Ohio State University, USA (06/13/2010) Advisor: Jay Gupta</li> <li>- B.S. cum laude, Material Science and Engineering, Pohang University of Science and Technology, South Korea (02/2002)</li> </ul> <p>Professional Appointments:</p> <ul style="list-style-type: none"> <li>- Associate Professor at Dept. of Physics, Korea University (Sep 2018 – present)</li> <li>- Assistant Professor at Dept. of Physics, Korea University (Mar 2016 – Aug 2018)</li> <li>- Associate Specialist at Dept. of Physics, Univ. of California at Santa Barbara (Aug 2014 – Dec 2015) Advisor: Ania Jayich</li> <li>- Post Doctoral Researcher at Dept. of Physics, Yale University (Mar 2011 – Aug 2014) Advisor: Jack Harris</li> </ul> <p>Nationality: Republic of Korea</p> <p>Mailing Address: Asan Science Building Rm404, Anam-dong 5, Sungbuk-gu, Seoul, South Korea</p> <p>Email Address: donghun@korea.ac.kr</p> <p>Phone Number: (82) 02-3290-3095</p>
Citation for the Award (within 30 words)
Contribution to the observation of quantum phenomena in macroscopic mechanical objects
Description of the work
<p>The field of cavity optomechanics studies quantum mechanical phenomena from macroscopic mechanical objects. It is based on the interaction between laser light inside a high quality optical resonator (i.e. cavity) and the motion of a highly compliant mechanical oscillator. It is a rapidly emerging field, as it can be a test bed for fundamental quantum mechanics, particularly the boundary between classical and quantum mechanics. It can be also used for ultrasensitive mass, force and displacement sensing, and for quantum information processing. Due to the promising aspects both in fundamental and application, the field of cavity optomechanics has been recognized as one of the 'milestones' in laser and quantum science.</p> <p>Realizing such optomechanical devices to observe miniscule quantum signatures, however, is very demanding and requires overcoming many technical challenges. This includes suppressing the</p>

classical noise in lasers and the seismic and acoustic noise that can couple to the oscillator's motion. It also generally requires working in cryogenic environment to avoid thermal fluctuations while achieving high quality optical cavities and mechanical oscillators.

Professor Donghun Lee built experimental devices capable of the quantum measurements and successfully observed quantum behaviors from the heaviest mechanical objects by the time (i.e. 43 ng, mm size mechanical oscillator) [1]. He studied both linear and non-linear optomechanical interactions. With the linear coupling combined with cryogenics and resolved-sideband laser cooling, he was able to cool the mechanical motion close to its quantum ground state and observed a strong asymmetry in the mechanical sidebands which is a signature of quantum phenomena in mechanical oscillators [1]. On the other hand, he also demonstrated a non-linear optomechanical interaction with a thorough characterization of its dynamics and full comparison with a theoretical model [2]. Such interaction can provide more striking quantum effects such as quantum nondemolition (QND) measurements of mechanical oscillators and the production of non-classical mechanical states such as Schrodinger cat states in macroscopic objects.

More recent years, Prof. Lee has focused on hybrid quantum systems consisting of mechanical oscillators, cavity photons, and two-level systems such as diamond defect-based spin qubits [3]. Such hybrid systems are expected to bring stronger non-linear interaction and can serve as a universal quantum interface between diverse qubit systems. Quantum interfaces are crucial for quantum information processing and quantum communications, but, realizing such interfaces between disparate quantum systems is a pressing challenge in current research. The hybrid mechanical system is a promising solution to this challenge and Prof. Lee's work lies at the frontiers of this field.

Prof. Lee has successfully demonstrated quantum measurements in the field of cavity optomechanics and deepened our understandings on quantum physics in macroscopic objects. His contribution is indispensable in this outstanding research and, based on his achievement and future prospect, Prof. Lee is very well qualified as a recipient of the Nishina Asia Award 2019.

Key references (up to 3 key publications\*)

1. M. Underwood, D. Mason, D. Lee\*, H. Xu, L. Jiang, A. B. Shkarin, K. Børkje, S. M. Girvin, J. G. E. Harris, "Measurement of the motional sidebands of a nanogram-scale oscillator in the quantum regime", *Physical Review A (Rapid Communications)* 92, 061801 (2015)
2. D. Lee\*, M. Underwood, D. Mason, A. B. Shkarin, S. W. Scott and J. G. E. Harris, "Multimode optomechanical dynamics in a cavity with avoided crossings", *Nature Communications* 6, 6232 (2015)



3. Donghun Lee<sup>\*,†</sup>, Kenneth W. Lee<sup>†</sup>, Preeti Ovartchaiyapong, Jeff Cady, and Ania C. Bleszynski Jayich, "Topical Review: Spins and mechanics in diamond", Journal of Optics 19, 033001 (2017)

<sup>†</sup> Equal contributions

\*) Copy of one most significant publication should be attached.

Nominator (name, affiliation, email, telephone and relation to the candidate)

First & Last Name: Cheol Eui Lee

Affiliation: Department of Physics, Korea University, South Korea

Email Address: rscel@korea.ac.kr

Phone Number: (82) 02-3290-3098

Relation to the candidate: expert in similar fields and a department colleague of the candidate

Signature



Date

03/12/19

Nomination form for the 2019 Nishina Asia Award

Candidate (name, affiliation, curriculum vitae including the date of the degree of Ph.D., nationality, address, email and telephone)

**Nominee**

Dr. Sungjay Lee

School of Physics

Korea Institute for Advanced Study

85 Hoegiro, Dongdaemun-Gu, Seoul 20455

Republic of Korea

Phone: +82-2-958-3708

E-mail: sjlee@kias.re.kr

**Academic Employment**

2015 - Present: Professor at Korea Institute for Advanced Study, Seoul, Korea

2013 - 2015: Enrico Fermi Fellow at Enrico Fermi Institute, Univ. of Chicago, Illinois, USA

2012 - 2015: STFC Ernest Rutherford Fellow at DAMTP, Univ. of Cambridge, United Kingdom

2010 - 2012: Research Associate at DAMTP, Univ. of Cambridge, United Kingdom

2010 - 2010: KIAS Assistant Professor at Korea Institute for Advanced Study, Seoul, Korea

2008 - 2010: Research Fellow at Korea Institute for Advanced Study, Seoul, Korea

**Education and Qualifications Received**

Ph.D., March 2004 – February 2008

Department of Physics and Astronomy, Seoul National University, Korea

Thesis: Studies on three dimensional superconformal theories and their gravity duals

M.S., March 2002 – February 2004

Department of Physics and Astronomy, Seoul National University, Korea

B.S., March 1998 – February 2002

School of Chemical Engineering / School of Physics, Seoul National University, Korea

**Prizes and Awards**

2017 Baekcheon Physics Prize, Korean Physical Society, Korea.

2016 Young Scientist Award (Presidential), Ministry of Science and ICT, Korea.

2016 Junior Fellowship, Fondation Science Mathématique de Paris, France.

2012 Ernest Rutherford Fellowship, Science and Technology Facilities Council, UK.

2012 Enrico Fermi Fellowship, University of Chicago.

2009 Research Excellence Award, Korea Institute for Advanced Study.

## Recent Invited Talks (Selected)

*“Modular Constraints on (S)CFTs”*, East Asia Joint Workshop on Fields and Strings 2018, November 6 (2018), Korea Institute for Advanced Study, Korea.

*“Modular Constraints on (S)CFTs”*, Workshop on New Frontiers in String Theory, July 25 (2018), Yukawa Institute for Theoretical Physics, Japan.

*“Modular Constraints on CFTs with Currents”*, Workshop on SCFTs in 6 and Lower Dimensions, January 16 (2018), Tsinghua Sanya International Mathematics Forum, China.

*“Bootstrapping Pure Quantum Gravity”*, Strings and Fields 2016, August 12 (2016), Yukawa Institute for Theoretical Physics, Japan.

*“Three-Charge Black Holes and Quarter BPS States in Little String Theory”*, Recent Developments in M-theory, February 16 (2016), CERN, Switzerland.

*“Three-Charge Black Holes and Quarter BPS States in Little String Theory”*, KIAS-YITP Joint Workshop 2015, September 15 (2015), Korea Institute for Advanced Study, Korea.

*“Ramond-Ramond Charges and the Gamma Class”*, Strings Conference 2014, June 25 (2014), Princeton University, United States.

*“Sphere Partition Function and Its Applications”*, Strings Conference 2013, June 25 (2013), Sogang University, Korea.

*“Exact results in 2d SUSY theories and Applications”*, Workshop on Geometry and Physics of Gauged Linear Sigma Model, March 07 (2013), University of Michigan, United States.

More than 90 invited talks at universities and research centers in Belgium, Canada, France, Germany, Netherlands, Italy, Japan, Korea, Spain, UK, and US.

## Publication Statistics (InspireHEP database, as of Mar. 4<sup>th</sup>, 2019)

Papers Published in SCI Journals:	<b>34</b>
Papers Cited More than 250 times:	<b>3</b>
Papers Cited More than 100 times:	<b>4</b>
Papers Cited More than 50 times:	<b>5</b>
Total Accumulated Citations:	<b>2,250</b>



Citation for the Award (within 30 words)

Discovery of a new class of  $d=3$  gauge theories, with M-theory applications, and pioneering works that revolutionized study of  $d=2, 3$  gauge theories and their conformal limit.

Description of the work

Dr. Sungjay Lee is the most prominent Ph.D. that emerged from the Korean high energy theory community during the last two decade or so, and belong to the very top echelon of young string theorists worldwide today. In less than seven years since graduation, he became a major player and a leader in supersymmetric gauge theories in low dimensions. Dr. Lee has either initiated, or contributed a key ingredient to, several new burgeoning research subjects repeatedly, including multi-M2-brane dynamics, ab initio Wall-Crossing for Seiberg-Witten theory, S-duality wall,  $S^3$  partition functions of 3d CFT's. One of the most recent and perhaps the most significant such contribution is computation of exact 2d GLSM partition functions on  $S^2$  and understanding of how Gromov-Witten invariants are embedded in those partition functions. I know of not too many Ph.D.s in the 21<sup>st</sup> century era who has achieved so much so early in their career.

Dr. Lee made an impressive entrance to the worldwide string theory community in 2008 with a set of works in three dimensional conformal field theories. Since 2007, many string theorists began to take serious interests in multi-M2 brane worldvolume theory, which is now believed to be described by a Chern-Simons theory called Aharony-Bergman-Jafferis-Maldacena (ABJM). An important precursor of this was a study of  $N=4$  superconformal Chern-Simons gauge theories with hypermultiplets by Gaiotto and Witten. Having worked on AdS4/CFT3 related issue in the previous year, Sungjay was motivated to study these systems, and at the end bridged the gap between Gaiotto-Witten theories and the M2 brane worldvolume theory. In a collaboration with four others (K. Hosomichi, K. Lee, S. Lee, J. Park), Sungjay managed to formulate the most general three-dimensional  $N=4,5,6$  superconformal field theories of Chern-Simons type, where the crucial element was how to include the twisted hypermultiplets as well consistently.

This work, in particular, provided very simple prescriptions on how to construct all such  $N=4$  theories, and thus produced ABJM model itself and many generalizations, including the symplectic and the orthogonal models with  $N=5$  supersymmetries, for an analog of orientifold for multi-M2 branes. In my view, their contribution here represents the most significant progress for M2-brane physics, next to the Bagger-Lambert, the Gaiotto-Witten, and the ABJM proposal. Let me emphasize that their construction in fact preceded that of ABJM. The

most astounding of this story is that he was apparently a key contributor to this project despite that he was the youngest of the collaboration team.

Since then, Dr. Lee made several other crucial contributions for  $d=2$  and  $d=3$  supersymmetric gauge theories by computing their sphere partition functions and also unraveling their physical meaning. Until very recently, there has been little progress in our understanding of strongly interacting conformal field theories in  $d=3$ . This is related to the fact that there is no efficient and systematic tool to control the long-distance behavior of the 3d theories such as 't Hooft anomaly matching condition in even-dimensional theories.  $S^3$  SUSY partition functions, computed by Sungjay in collaboration with Hama and Hosomichi in 2010-2011, provided for the first time an efficient and systematic tool to study the strong infrared (IR) physics of the 3d (SUSY) gauge theories analytically: confirm detailed predictions of the AdS4/CFT3 correspondence and answer to a long-standing question of defining a measure counting the number of degrees of freedom in 3d, analogous to Zamolodchikov's theorems in 2d CFTs.

This work paved the way for his perhaps most important set of works, namely  $S^2$  partition function of  $d=2$  Gauged Linear Sigma Models and its interpretation via Gromov-Witten invariants for Calabi-Yau GLSM's. An exact computation of  $S^2$  partition functions with several collaborators was followed by an even more important paper with Jaume Gomis, where the pair proved a conjecture that the  $S^2$  partition function of  $D=2$  (axial-anomaly-free) Gauge Linear Sigma Models computes the fully quantum corrected A-model Kaehler potential of the corresponding Calabi-Yau manifold.

In more mathematical terms, these  $S^2$  partition functions compute the famed Gromov-Witten invariants directly, without any help from the mirror symmetry. The conjecture that this might be true was actually suggested by David Morrison and company a few months earlier. This proposal was motivated by Sungjay's exact computations of  $S^2$  partition functions a few months prior, to begin with, but Sungjay and Jaume came back to the problem and managed to find a very simple, intuitive, and convincing proof of the conjecture, closing the loop themselves. Of many exact computation of partition functions via the localization method during last ten years, this is probably the most significant result, thanks to which the entire subject of  $d=2$  GLSM has come under new attentions of numerous string theorists and geometers.

Most recently, Sungjay has extended his scope to the (numerical) conformal bootstrap in various dimensions with emphasis on understanding generic features of quantum gravity. In particular, he has shown that any unitary two-dimensional CFT with global symmetry should contain a light charged state. This numerical study provides a nontrivial evidence toward a proof of the Weak Gravity Conjecture, which leads to a number of intriguing implications to cosmology

and particle physics.

Dr. Sungjay Lee's contribution to  $d=3$  and  $d=2$  supersymmetric gauge theories since 2008 have been all class-leading and right at the forefront of the worldwide string theory community. In terms of his scientific contribution to the community, which has been singularly stellar among string theorists of Asian origin, I find very few comparable, say, under the age of forty. Prof. Yuji Tachikawa of Tokyo University is the only person I can think of, with comparable or higher level of achievement at the similar stage of career.

Key references (up to 3 key publications\*)

*$N=5,6$  Superconformal Chern-Simons Theories and M2-branes on Orbifolds*

Kazuo Hosomichi, Ki-Myeong Lee, Sangmin Lee, Sungjay Lee, Jaemo Park,  
JHEP 0809 (2008) 002

*SUSY Gauge Theories on Squashed Three-Spheres*

Naofumi Hama, Kazuo Hosomichi, Sungjay Lee  
JHEP 1105 (2011) 014

\*\* Exact Results in  $D=2$  Supersymmetric Gauge Theories

Nima Doroud, Jaume Gomis, Bruno Le Floch, Sungjay Lee  
JHEP 1305 (2013) 093

\*\* attached as the most significant paper

Nominator (name, affiliation, email, telephone and relation to the candidate)

Piljin Yi ( piljin@kias.re.kr )

Professor of Physics

& Vice President

Korea Institute for Advanced Study

☎ 82-2-958-3757

I served as Dr. Sungjay Lee's mentor during his postdoctoral stay at KIAS, right after his Ph.D. from Seoul National University.

Signature

Piljin Yi



Date

2019.03.14

# Nomination form for the 2019 Nishina Asia Award

Candidate (name, affiliation, curriculum vitae including the date of the degree of Ph.D., nationality, address, email and telephone)
<u>Name</u> Chen Fang <u>Affiliation</u> Institute of Physics, Chinese Academy of Sciences <u>Contact</u> 8 Zhongguancun South 3 <sup>rd</sup> St., Beijing 100190, China +86-1082649073 cfang@iphy.ac.cn <u>Citizenship</u> China <u>Education</u> Oct. 2011    Ph.D.    Purdue University (USA)
Citation for the Award (within 30 words)
For developing the theory of topological classification and diagnosis for non-magnetic materials.
Description of the work
<p>The research on topological materials is one of the major topics in condensed matter physics. These materials are known to host interesting phenomena such as the negative linear magnetoresistance in the bulk of topological semimetals, and the robust, gapless modes on the surface of topological insulators. The nominee and his group have solved two important problems in this field, the problems of “classification” and “diagnosis”.</p> <p>A key concept in this field is the “topological invariant”, a global quantum number that distinguishes topological materials from non-topological ones, and distinguishes different types of topological materials. In fact, all topology-related phenomena in a material are fully determined by this quantum number(s). The types and forms of all topological invariants depend and only depend on two factors: symmetry and dimensionality. Identifying all invariants for a given dimension and symmetry group of interest is, therefore, an important mission for theorists, known as the “classification problem”.</p> <p>The nominee’s recent work in Ref.[1,2] for the first time identifies four new <math>Z_2</math> topological invariants in 3D for the following spatial symmetries: rotation, screw rotation, roto-reflection and inversion. These new invariants in hand and, using a theoretical tool called “layer construction”, in Ref.[2] they list all independent topological invariants when the symmetry is time reversal plus any one of the 230 space groups in 3D, solving the classification problem for the cases that are most relevant in condensed matter physics.</p> <p>While classification is a purely theoretical topic, the “diagnosis problem” is more concerned</p>



with realistic materials: it asks for a given real material what are the actual values of the above invariants, based on first-principle calculations. Direct computation of topological invariants is notoriously difficult in many real materials, and this difficulty has so far been hindering the discovery of more topological materials. In Ref.[2], nominee and his group develop a new method that greatly simplifies the calculation, by which people can extract most information on topology only from the symmetry eigenvalues of the bands at several high-symmetry momenta in the Brillouin zone. Based on this method, they in Ref.[3] design an automated diagnosis process that automatically and efficiently finds all topological properties for any given non-magnetic material. This process is then applied to ~40000 materials in a materials database in Ref.[3], and they predict ~8000 materials to be topological semimetals and insulators, exceeding by an order of magnitude the total number of such materials theoretically discovered in the past ten years. The work does not fully solve the diagnosis problem and the method has its limits, but it still marks so far the biggest step forward in this direction.

Key references (up to 3 key publications\*)

1. Z. Song, Z. Fang and C. Fang, “*(d-2)-Dimensional Edge States of Rotation Symmetry Protected Topological States*”, Phys. Rev. Lett. **119**, 246402 (2017).
2. Z. Song, T. Zhang, Z. Fang and C. Fang, “*Quantitative mappings between symmetry and topology in solids*”, Nature Communications **9**, 3530 (2018).
3. T. Zhang, Y. Jiang, Z. Song, H. Huang, Y. He, Z. Fang, H. Weng and C. Fang, “*Catalogue of Topological Electronic Materials*”, Nature **566**, 475 (2019).

\*) Copy of one most significant publication should be attached.

Nominator (name, affiliation, email, telephone and relation to the candidate)

**Name:** Hongming WENG

**Affiliation:** Institute of Physics, Chinese Academy of Sciences

**Address:** Institute of Physics, Chinese Academy of Sciences P.O.Box 603, Beijing 100190, China

**Phone:** +86-10-6284-9941 (office); +86-138-1157-0964(cell)

**Fax:** +86-10-6255-3698

**Email:** hmweng@iphy.ac.cn

**Relation to the candidate:** colleague

Signature\_\_\_\_\_

Date\_\_\_\_\_

## Nomination form for the 2019 Nishina Asia Award

<p>Candidate (name, affiliation, curriculum vitae including the date of the degree of Ph.D., nationality, address, email and telephone)</p>
<ul style="list-style-type: none"> <li>✓ Name : Bohm-Jung Yang</li> <li>✓ Affiliation: Department of Physics and Astronomy, Seoul National University</li> <li>✓ Nationality: Republic of Korea</li> <li>✓ Address: Department of Physics and Astronomy, 56-526, Seoul National University, 1 Gwanak-ro, Gwanak-gu, Seoul, Korea</li> <li>✓ Telephone : 82-2-880-6604</li> <li>✓ Email:bjyang@snu.ac.kr</li>   <li>✓ Research Experience</li> <li>① August 2008: Doctor of Philosophy in Physics, Seoul National University (Seoul, Korea; Advisor: Prof. Jaejun Yu)</li> <li>② October 2008 – June 2010: Postdoctoral Researcher, Department of Physics, University of Toronto (Toronto, Canada; Advisor: Prof. Yong Baek Kim and Prof. Hae-Young Kee)</li> <li>③ July 2010 – March 2015: Postdoctoral Researcher, RIKEN Center for Emergent Matter Science (Saitama, Japan; Advisor: Prof. Naoto Nagaosa)</li> <li>④ April 2015 – August 2015: Research Scientist, RIKEN Center for Emergent Matter Science (Saitama, Japan; Advisor: Prof. Naoto Nagaosa)</li> <li>⑤ September 2015 – present: Assistant Professor, Department of Physics, Seoul National University (Seoul, Korea)</li> </ul>
<p>Citation for the Award (within 30 words)</p>
<p>For his contribution to uncovering topological properties of three-dimensional Dirac semimetals</p>

## Description of the work

Prof. Bohm-Jung Yang has published a series of important papers about topological semimetals. In particular, he made a significant contribution to uncovering topological properties of three-dimensional (3D) Dirac semimetals. In certain condensed matter systems, the low energy electronic excitations can be described by massless Dirac fermions with relativistic energy dispersion. Graphene and the surface of topological insulators are the representative systems possessing two-dimensional (2D) massless Dirac fermions. Because of this characteristic energy band structure, 2D Dirac materials can exhibit various novel physical properties. On the other hand, 3D massless Dirac fermions have been considered more unstable than its 2D counterpart, and its discovery is achieved only very recently. Na<sub>3</sub>Bi and Cd<sub>3</sub>As<sub>2</sub> are the first materials in which 3D massless Dirac fermions are predicted by first-principle calculations and experimentally confirmed after that. At that time, although there were few theories proposing the symmetry protection of 3D massless Dirac fermions, a general theoretical framework describing stable 3D Dirac semimetals and their topological properties were absent. Prof. Yang conceived the idea that a unified theoretical description of 3D Dirac semimetals can be achieved by investigating the relation between the band topology and symmetry eigenvalues of symmorphic and non-symmorphic rotations. In collaboration with Prof. Naoto Nagaosa, Prof. Yang successfully constructed a general theoretical framework describing stable 3D Dirac semimetals with nontrivial topological properties, which is reported in Ref.[1]. In this paper, Prof. Yang explained how crystalline symmetries, stable Dirac points, and band topology are related to each other, and classified stable 3D Dirac semimetals into two distinct classes, class I and class II, protected by symmorphic and nonsymmorphic rotation symmetries, respectively. This paper has provided a fundamental theoretical basis for describing 3D topological Dirac semimetals, and has been considered as one of the most influential papers in the study of 3D Dirac semimetals.

According to Ref.[1], a 3D Dirac semimetal system has to satisfy time-reversal (T), inversion (P) symmetries in the presence of spin-orbit coupling. For further generalization of the theory to embrace wider classes of 3D Dirac materials, it is essential to understand the influence of P, T symmetry breaking and the effect of weak spin orbit coupling. In Ref.[2], Prof. Yang and his student studied the topological properties of PT symmetric Dirac semimetal systems with negligible spin orbit coupling in which electrons can be described by spinless fermions and a Dirac point can be deformed to a nodal line. In this paper, Prof. Yang showed that the band topology of spinless PT symmetric systems is endowed with the characteristic mathematical structure, so-called the Stiefel Whitney class. When a Dirac point or a

nodal line carries nontrivial Stiefel Whitney numbers, a single node has topological stability and nodal line pairs develop linking structure with other nodal lines below the Fermi level. The idea of Stiefel Whitney classes is extended further to 2D insulators, based on which Prof. Yang proposed a new 2D topological insulator, dubbed a 2D Stiefel Whitney insulator. Ref.[2] is the first work in which novel topological phases associated with Stiefel Whitney classes are proposed in condensed matter systems. Considering the tremendous impact of the notion of Chern classes defined by complex wave functions to condensed matter physics, the notion of Stiefel Whitney classes defined by real wave functions proposed in Ref.[2] is expected to play a critical role in the future study of topological states.

Finally, Prof. Yang also examined the influence of time-reversal symmetry breaking on PT symmetric Dirac semimetals. In particular, focusing on a van der Waals ferromagnet Fe<sub>3</sub>GeTe<sub>2</sub>, Prof. Yang and his student performed careful theoretical analysis. It is shown that when spin orbit coupling is neglected, this material can be considered as a PT symmetric Dirac semimetal with stable nodal lines. Introduction of ferromagnetic ordering opens a tiny gap along nodal lines, which significantly enhances the anomalous Hall conductivity in Fe<sub>3</sub>GeTe<sub>2</sub> as shown in Ref.[3]. In collaboration with experimental groups, Prof. Yang successfully identified Fe<sub>3</sub>GeTe<sub>2</sub> as the first example of ferromagnetic nodal line semimetals in which the interplay between the symmetry protected nodal structure and ferromagnetism gives rise to novel topological responses of magnetic topological Dirac materials.

To sum up, Prof. Yang constructed a general theoretical framework to understand stable 3D Dirac semimetals and unveiled the fundamental relationship between crystalline symmetry and band topology of Dirac semimetals [1]. Also, his study of PT symmetric Dirac semimetals in spinless fermion systems has established the central role of Stiefel Whitney classes on new topological phenomena in condensed matter systems [2]. Moreover, his study of a magnetic Dirac semimetal system Fe<sub>3</sub>GeTe<sub>2</sub> showed that the interplay of ferromagnetism and band topology can induce new topological magnetic state, leading to the first discovery of a ferromagnetic topological nodal line semimetal [3]. Considering his contribution to uncovering novel topological properties of 3D Dirac materials, I believe that Prof. Yang deserves to be the winner of the Nishina Asia Award in 2019.



Key references (up to 3 key publications\*)

1. **Bohm-Jung Yang\*** and Naoto Nagaosa, “Classification of stable three-dimensional Dirac semimetals with nontrivial topology”, Nature Communications 5, 4898 (Sep. 2014).
2. J. Ahn, D. W. Kim, Y.K.Kim and **Bohm-Jung Yang\***, “Band topology and linking structure of nodal line semimetals with Z<sub>2</sub> monopole charges”, Phys. Rev. Lett. 121, 106403 (2018).
3. Kyoo Kim, Junho Seo, Eunwoo Lee, K.-T. Ko, B. S. Kim, Bo Gyu Jang, Jong Mok Ok, Jinwon Lee, Youn Jung Jo, Woun Kang, Ji Hoon Shim, C. Kim, Han Woong Yeom, Byung Il Min, **Bohm-Jung Yang\*** & Jun Sung Kim\* “Large anomalous Hall current induced by topological nodal lines in a ferromagnetic van der Waals semimetal”, Nature Materials. 17, 794-799 (2018).

\*) Copy of one most significant publication should be attached.

Nominator (name, affiliation, email, telephone and relation to the candidate)

Nominator: Doochul Kim,

President, Institute for Basic Science, Daejeon, Korea, dkim@ibs.re.kr,

Professor Emeritus, Seoul National University, Seoul, Korea, dkim@snu.ac.kr

Tel: +82-10-4221-7155


Relation: The candidate was a graduate student while I was at Department of Physics and Astronomy, Seoul National University. The candidate's Ph.D. supervisor, Prof. Jaejun Yu, and the postdoc advisor, Prof. Yong Baek Kim are my long time colleagues and strong supporters of the candidate.

Signature



Date March, 22, 2019

Nomination form for the 2019 Nishina Asia Award

Candidate (name, affiliation, curriculum vitae including the date of the degree of Ph.D., nationality, address, email and telephone)
First Name: Chao Yang Last Name: Lu Affiliation: University of Science and Technology of China
Citation for the Award (within 30 words)
Description of the work
Key references (up to 3 key publications*)
*) Copy of one most significant publication should be attached.
Nominator (name, affiliation, email, telephone and relation to the candidate)
Ruibao Tao Fudan University rbtao@fudan.edu.cn +86 21 65642968, mobile: +86 18930576922
 Signature _____ Date 22 March, 2019 _____

# Nomination form for the 2019 Nishina Asia Award

Candidate (name, affiliation, curriculum vitae including the date of the degree of Ph.D., nationality, address, email and telephone)

Name: Elmer S. Estacio

Affiliation: National Institute of Physics, University of the Philippines Diliman

Curriculum Vitae:

## Education

June 2002 – November 2004	Doctor of Philosophy in Physics, University of the Philippines Diliman
June 1998 – May 2002	Master of Science in Physics, University of the Philippines Diliman
June 1991 – May 1007	Bachelor of Science in Applied Physics, University of the Philippines Diliman

## Work Experience

August 2015 - Present	Coordinator, Material Science and Engineering Program, College of Science, University of the Philippines Diliman
January 2015 - Present	Professor of Physics, National Institute of Physics, University of the Philippines Diliman
June 2012 – December 2015	Associate Professor of Physics, National Institute of Physics, University of the Philippines Diliman
September 2010 – April 2012	Specially-Appointed Assistant Professor, University of Fukui
September 2008 – August 2010	JSPS Postdoctoral Fellow, Institute of Laser Engineering, Osaka University
October 2006 – August 2008	Postdoctoral Fellow, Institute of Laser Engineering, Osaka University
April 2005 – September 2006	Postdoctoral Fellow, Institute of Molecular Science, Okazaki, Japan

## Honors and Awards

March 2019	National Research Council of the Philippines Achievement Award in Physics
2016-2018	Scientist I, University of the Philippines
2012 - 2014	Balik Scientist Program Awardee, Department of Science and Technology



<p>Nationality: Filipino</p> <p>Address: AA6402 Hardin ng Rosas, UP Campus, Quezon City</p> <p>Email: eestacio@nip.upd.edu.ph</p> <p>Telephone: +632-920-9749</p>
<p>Citation for the Award (within 30 words)</p> <p>Dr. Estacio performed extensive work on the investigation of the optical and terahertz properties of semiconductors, as well as their possible application in the development of novel terahertz optoelectronic devices.</p>
<p>Description of the work</p> <p>Terahertz (THz) refers to electromagnetic waves in the frequency range of 0.1 to 10 THz. It has been the primary motivation of scientists and researchers to provide solution to the so-called "THz gap", which refers to the absence of suitably strong THz emitters and detectors. THz technology has numerous possible applications, especially in nondestructive material evaluation, spectroscopic fingerprinting of molecules and compounds, and imaging. Dr. Elmer Estacio has made significant contribution in developing novel THz emitters based from molecular beam epitaxy (MBE)-grown semiconductor heterostructures such as InAs/GaAs quantum dots and GaAs-AlGaAs modulation-doped heterostructures. The investigation of carrier dynamics and transport in these semiconductor heterostructures has provided useful insights in the design considerations and optimization of novel terahertz optoelectronic devices such as photoconductive antenna emitters and detectors.</p>
<p>Key references (up to 3 key publications*)</p> <p>[1] E. Estacio, M.H. Pham, S. Takatori, M. Cadatal-Raduban, T. Nakazato, T. Shimizu, N. Sarukura, A. Somintac, M. Defensor, F.C.B. Awitan, R.B. Jaculbia, A. Salvador, and A. Garcia, "Strong enhancement of terahertz emission from GaAs in InAs/GaAs quantum dot structures", Applied Physics Letters, vol. 94 (23), art. no. 232104, 2009. 19 citations.</p> <p>[2] E. Estacio, H. Sumikura, H. Murakami, M. Tani, N. Sarukura, M. Hangyo, C. Ponseca, Jr., R. Pobre, R. Quiroga, S. Ono, "Magnetic-field-induced fourfold azimuthal angle dependence in the terahertz radiation power of (100) InAs", Applied Physics Letters, vol. 90 (15), art. no. 151915, 2007. 16 citations.</p> <p>[3] E. S. Estacio, M. Hibi, K. Saito, C.T. Que, T. Furuya, F. Miyamaru, S. Nishizawa, K. Yamamoto, M. Tani, "Saturation and polarization characteristics of 1.56 um optical probe pulses in a LTG-GaAs photoconductive antenna terahertz detector", Journal of Infrared, Millimeter, and terahertz Waves, vol. 34 (8), pp. 423-430, 2013. 6 citations.</p>

\*) Copy of one most significant publication should be attached.

Nominator (name, affiliation, email, telephone and relation to the candidate)

Name: Arnel Salvador, PhD (h-index = 34)

Affiliation: National Institute of Physics, University of the Philippines Diliman

Email Address: asalvador.nip@gmail.com

Telephone: +632-920-5490

Relation to the Candidate: I was the dissertation adviser of Elmer Estacio when he was still pursuing his graduate studies at the National Institute of Physics (2002-2004). After spending several years as a postdoc student abroad, he returned to the Philippines in 2012 to setup his own research facility. Now, we are both the senior faculty members of the Condensed Matter Physics Laboratory and co-faculties at the National Institute of Physics.



Signature: Arnel A. Salvador, Ph.D.

Date 25 March 2019

## Strong enhancement of terahertz emission from GaAs in InAs/GaAs quantum dot structures

Elmer Estacio, Minh Hong Pham, Satoru Takatori, Marilou Cadatal-Raduban, Tomoharu Nakazato, Toshihiko Shimizu, Nobuhiko Sarukura, Armando Somintac, Michael Defensor, Fritz Christian B. Awitan, Rafael B. Jaculbia, Arnel Salvador, and Alipio Garcia

Citation: [Applied Physics Letters](#) **94**, 232104 (2009); doi: 10.1063/1.3148670

View online: <http://dx.doi.org/10.1063/1.3148670>

View Table of Contents: <http://scitation.aip.org/content/aip/journal/apl/94/23?ver=pdfcov>

Published by the [AIP Publishing](#)

---

### Articles you may be interested in

[Plasmon-enhanced terahertz emission in self-assembled quantum dots by femtosecond pulses](#)  
J. Appl. Phys. **115**, 064304 (2014); 10.1063/1.4863781

[Terahertz emission from InAs/GaAs quantum dot based photoconductive devices](#)  
Appl. Phys. Lett. **98**, 181107 (2011); 10.1063/1.3586774

[Single quantum dot emission at telecom wavelengths from metamorphic InAs/InGaAs nanostructures grown on GaAs substrates](#)  
Appl. Phys. Lett. **98**, 173112 (2011); 10.1063/1.3584132

[Terahertz spectroscopy of shift currents resulting from asymmetric \(110\)-oriented GaAs/AlGaAs quantum wells](#)  
Appl. Phys. Lett. **95**, 151110 (2009); 10.1063/1.3249611

[Tuning the structural and optical properties of 1.3- \$\mu\$ m InAs/GaAs quantum dots by a combined InAlAs and GaAs strained buffer layer](#)  
Appl. Phys. Lett. **82**, 3644 (2003); 10.1063/1.1577827

---



Free online magazine

# MULTIPHYSICS SIMULATION

[READ NOW ►](#)

The COMSOL logo, consisting of a small red and blue square icon followed by the word 'COMSOL' in a bold, sans-serif font.



# Strong enhancement of terahertz emission from GaAs in InAs/GaAs quantum dot structures

Elmer Estacio,<sup>1,a)</sup> Minh Hong Pham,<sup>1</sup> Satoru Takatori,<sup>1</sup> Marilou Cadatal-Raduban,<sup>1</sup> Tomoharu Nakazato,<sup>1</sup> Toshihiko Shimizu,<sup>1</sup> Nobuhiko Sarukura,<sup>1</sup> Armando Somintac,<sup>2</sup> Michael Defensor,<sup>2</sup> Fritz Christian B. Awitan,<sup>2</sup> Rafael B. Jaculbia,<sup>2</sup> Arnel Salvador,<sup>2</sup> and Alipio Garcia<sup>3</sup>

<sup>1</sup>*Institute of Laser Engineering, Osaka University, 2-6 Yamadaoka, Suita, Osaka 565-0871, Japan*

<sup>2</sup>*National Institute of Physics, University of the Philippines, Diliman, Quezon City 1101, Philippines*

<sup>3</sup>*Department of Physical Sciences, University of the Philippines, Baguio City 2600, Philippines*

(Received 5 February 2009; accepted 13 May 2009; published online 11 June 2009)

We report on the intense terahertz emission from InAs/GaAs quantum dot (QD) structures grown by molecular beam epitaxy. Results reveal that the QD sample emission was as high as 70% of that of a *p*-type InAs wafer, the most intense semiconductor emitter to date. Excitation wavelength studies showed that the emission was due to absorption in strained undoped GaAs, and corresponds to a two order-of-magnitude enhancement. Moreover, it was found that multilayer QDs emit more strongly compared with a single layer QD sample. At present, we ascribe the intense radiation to huge strain fields at the InAs/GaAs interface. © 2009 American Institute of Physics. [DOI: 10.1063/1.3148670]

Terahertz science currently offers applications ranging from fingerprinting spectroscopy, semiconductor and medical imaging, and even law enforcement.<sup>1–4</sup> The rapid implementation of terahertz science as a mainstream technology, however, is hampered by the unavailability of sufficiently intense terahertz radiation sources. The generation of terahertz transients by way of surge current and optical rectification from semiconductor irradiated by femtosecond laser pulses has been well-studied in the context of searching for intense, pulsed terahertz emitters.<sup>5–8</sup> To date, the best material for this purpose is bulk InAs (Ref. 5) due to its reduced carrier effective mass, while GaAs pales in comparison due to its large carrier effective mass and lower mobility.<sup>7</sup> Previous reports on the application of terahertz science on semiconductor quantum dot (QD) structures have been concentrated on terahertz spectroscopy to probe electronic properties such as carrier/exciton relaxation and concentration dynamics, intraband absorption, and photoconductivity anisotropies.<sup>9–13</sup> Additionally, theoretical and experimental results on QD terahertz detectors and even possible emitter devices based on energy-level transitions have also been reported.<sup>14–21</sup> This work demonstrates intense terahertz emission from femtosecond laser-irradiated InAs/GaAs QD structures. The terahertz emission characteristics of single layer QD (SLQD) and a multilayer QD (MLQD) structures were compared with those of other semiconductors; *p*-type InAs (*p*-InAs), *n*-type InAs (*n*-InAs), semi-insulating (SI) GaAs, and undoped (UD) GaAs wafers.

The QD layers were grown on SI-GaAs substrates using a Riber<sup>32</sup> *P* molecular beam epitaxy (MBE) machine. The SLQD was initiated with the growth of a 1  $\mu\text{m}$  thick UD GaAs buffer layer at 640 °C followed by a three-layer GaAs/AlAs superlattice to smoothen out the surface prior to succeeding epitaxial growth. The growth temperature was then ramped down to 490 °C before the growth of 300 Å UD GaAs layer on which a single layer of InAs QDs was

grown. The QD formation was monitored by reflection high energy electron diffraction. The QD layer is capped with a 600 Å GaAs, with the top half, doped with Si. The MLQD consists of eight layers of InAs QDs separated by 330 Å UD GaAs layers. The thickness of the separation layers ensures that no vertical coupling of dots will ensue. The first five QD layers were grown at 490 °C and the remaining three layers, at 520 °C. Terahertz emission measurements were performed at room temperature using a mode-locked Ti: sapphire laser delivering  $\sim 100$  fs pulses at  $\sim 80$  MHz repetition rate as the optical excitation. The laser was incident at a 45° angle with respect to the semiconductor surface and the terahertz emission was collected at the specular direction using paraboloid mirrors. The laser was then tuned from 800 to 895 nm to study the excitation wavelength dependence and terahertz emission spectroscopy was performed using a Fou-

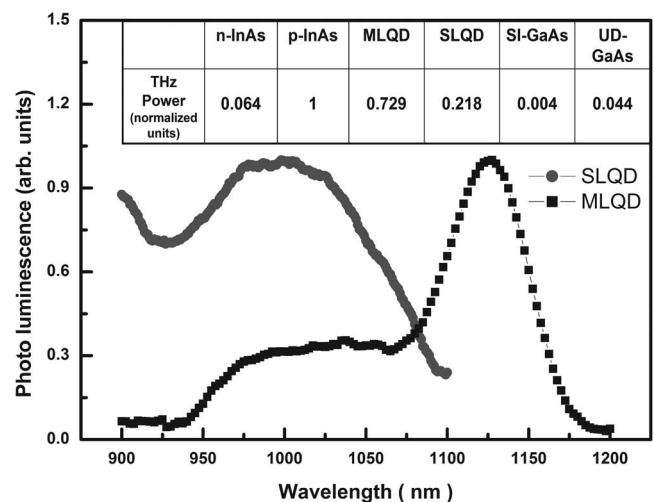


FIG. 1. Normalized 77 K PL of the SLQD and MLQD samples. Results reveal that more uniform and larger-sized QD structures dominate the MLQD. The inset shows a comparison of the normalized broadband terahertz radiation power from the MLQD, SLQD, *p*-InAs, *n*-InAs, and reference SI- and UD-GaAs samples. Both QD wafers emit more strongly than *n*-InAs and the MLQD radiation power reaches up to 70% of that of *p*-InAs.

<sup>a)</sup>Author to whom correspondence should be addressed. Electronic mail: estacio-es@ile.osaka-u.ac.jp.



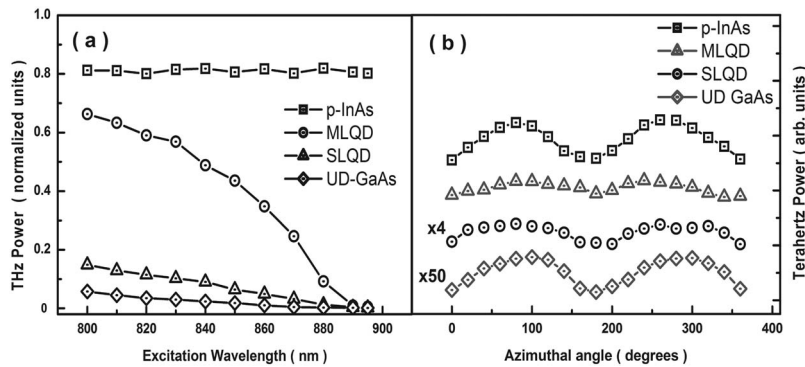


FIG. 2. (a) The excitation wavelength spectra comparison for the QD samples, *p*-InAs, and UD-GaAs. The QD samples' terahertz emission is due photocarriers from UD GaAs absorption and not from the QD structures. (b) The azimuthal angle dependence of the terahertz radiation power in the QD samples show the dominance of an angularly independent surge current mechanism as in the reference samples, surmised to be due to the transient current as the photocarriers are swept across the strain field of the GaAs/InAs interface region.

rier transform far infrared spectrometer. A liquid He-cooled Si bolometer and a lock-in amplifier were employed to detect the terahertz radiation.

Figure 1 shows the 77 K photoluminescence (PL) spectra of the QD layers. The difference in PL peaks is due to variation in QD size distribution. In the MLQD, the majority of the QDs are larger (less carrier quantum confinement, thus the band edge sits at a lower energy). Variations in size distribution are expected of QDs grown at various temperatures. Moreover, the narrower PL linewidth of the MLQD shows that the dot size distribution for this sample is relatively uniform. In the inset of Fig. 1, the comparison of the measured broadband terahertz emission power (at  $4 \mu\text{J}/\text{cm}^2$  excitation fluence) for the six semiconductor samples, namely, *n*-InAs, *p*-InAs, MLQD, SLQD, SI-GaAs, and UD-GaAs are shown. The values are the broadband terahertz power values normalized with respect to *p*-InAs emission. The UD-GaAs and SI-GaAs samples' terahertz emission was taken as reference for the contribution from the substrate and GaAs layers in the QD wafers. As expected, the most intense terahertz emission is from InAs. The *p*-InAs terahertz emission power is at least two orders of magnitude greater compared with either of the GaAs wafers. Currently, *p*-InAs is reputed to be the most intense terahertz emitter among wafer semiconductors, primarily due to reduced carrier screening and low carrier effective mass.<sup>22–24</sup> Additionally, *n*-InAs is considered to be another intense terahertz emitter while GaAs has been shown to suffer from higher carrier effective mass.<sup>22</sup> It can be seen that the MLQD can emit up to 70% of the terahertz power of *p*-InAs; even emitting more strongly compared with *n*-InAs. The SLQD emission, although not as intense as the MLQD, is also comparable. It has the third most intense emission; likewise emitting more strongly than the *n*-InAs.

In order to ascertain the origin of the intense terahertz radiation in the QD layers, the excitation wavelength and azimuthal angle dependence of the radiation were then stud-

ied and compared with standard samples. Shown in Fig. 2(a) are the excitation wavelength spectra of the QD layers, *p*-InAs, and UD-GaAs. The excitation wavelength dependence of the terahertz emission from *p*-InAs and UD-GaAs are initially compared. The *p*-InAs terahertz emission ( $E_{\text{gap}} = 3.4 \mu\text{m}$ ) is relatively independent of the excitation wavelength within the range covered by the experiment. The GaAs excitation spectra, on the other hand, follow the GaAs density of states, lending evidence that the radiation mechanism is caused by photogenerated carriers ( $E_{\text{gap}} = 870 \text{ nm}$ ).<sup>25</sup> The terahertz emission from the QD layers resembles the density of states of bulk GaAs. Interestingly, this plot confirms that the terahertz emission in the InAs/GaAs QD layers is from GaAs carrier absorption and not from the QD structures, themselves. Moreover, the radiation mechanism is surmised to be the surge current from the acceleration of GaAs photocarriers as they are swept across the InAs/GaAs interface, possibly due to an interfacial strain field.<sup>26,27</sup> Note that for short excitation wavelengths, the MLQD terahertz emission intensity approaches that of *p*-InAs. The azimuthal angle dependence of the terahertz emission for these four samples was also measured and is shown in Fig. 2(b). It can be seen that the angular-dependent emission comprises only about 7%–15% of the total radiation power; with the majority originating from an angular-independent signal. It has been previously reported that at low excitation fluence, the surge current dominates.<sup>28</sup> These results affirm that the QDs emit by a surge current mechanism.

The application of semiconductor QD structures in terahertz devices have been previously suggested.<sup>29,30</sup> However, these reports did not involve ultrafast excitation of the wafer surface. Recently, an enhancement on the terahertz emission of surface-irradiated InAs/GaAs QD-based terahertz emitter was reported and a 25% increase was observed.<sup>31</sup> The authors attributed this enhancement to a modification of the

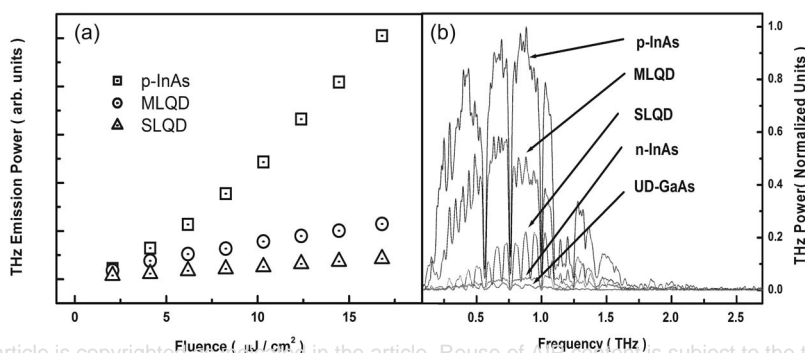


FIG. 3. (a) Excitation fluence dependence comparison for the samples that were studied. At low fluence excitation, the MLQD emission is comparable to that of *p*-InAs. (b) The terahertz emission spectra show that the MLQD terahertz bandwidth is similar to the *p*-InAs. The presence of Fabry-Perot oscillations is attributed to GaAs being transparent at terahertz frequencies and to the multilayer structures in the QD samples. It can be noted that both the MLQD and the SLQD emit more strongly than *n*-InAs.

Fermi level pinning brought about by the presence of the QD structures on the GaAs substrate. This was surmised to have resulted in increased carrier acceleration. This modification of a semiconductor's band structure to enhance terahertz emission in surface-irradiated wafers was also demonstrated in a more recent report. Takeuchi *et al.*<sup>32</sup> demonstrated a factor of 10 enhancement in the terahertz emission amplitude of GaAs embedded in an *i*-GaAs/*n*-GaAs epitaxial structure. Their results showed that the UD GaAs layer modifies the Fermi-level pinning and the depletion width at the *i*-GaAs/*n*-GaAs interface. This causes an increase in the photocarrier acceleration, thereby enhancing the terahertz emission intensity. In this current work, the photocarriers from GaAs absorption were determined to cause the terahertz emission from the MLQD and the SLQD via surge current. Moreover, the huge enhancement in the UD GaAs-based radiation is attributed to an intense electric field at the GaAs/InAs interface. The lattice-mismatch will result in an interfacial strain field that will undoubtedly modify the band structure of the sample and enhance photocarrier acceleration. In comparing the terahertz emission intensities between the two QD samples, the MLQD is presumed to have greater optical absorption resulting into stronger terahertz emission simply because of the multiple GaAs/InAs interfaces. The penetration depth of the 800 nm optical excitation in bulk GaAs was estimated to be 1  $\mu\text{m}$  while it is only about 100 nm in bulk InAs.<sup>7</sup> Even so, the InAs QD structures are only a few monolayers thick compared with bulk InAs and therefore it is highly expected that more than one interfaces were optically excited. The PL spectra in Fig. 1 differentiate the QD size distribution between the two samples. In the MLQD, the GaAs layer is more highly strained compared to the SLQD not only due to the larger dots but the GaAs spacer layer is also sandwiched by QD layers above and below it. The QDs in the MLQD sample strain the GaAs layer directly above it; a mechanism that is absent in the SLQD.<sup>27</sup> The QD size distribution in the MLQD is also more uniform; possibly improving the interface quality and enhancing emission due to reduced scattering.

Finally, the fluence dependence and terahertz emission spectra of the QD samples were also compared with the other wafers. The results are shown in Fig. 3. The fluence dependence in Fig. 3(a) shows that the *p*-InAs yields more intense emission for increasing excitation fluence, compared with the QD samples. However, at low excitation fluence values (4  $\mu\text{J}/\text{cm}^2$  and below), the terahertz emission power of the QD layers is very much comparable with *p*-InAs. In future compact applications, low fluence and low power excitations are likely to be utilized. As such, the InAs/GaAs QDs may rival the feasibility of *p*-InAs emitters. The frequency bandwidth of the MLQD terahertz emission is comparable with *p*-InAs at 4  $\mu\text{J}/\text{cm}^2$  excitation fluence, as shown in Fig. 3(b). The Fabry–Perot modes in the QD samples' emission spectra are attributed to the fact that the GaAs is not opaque to terahertz radiation. The underlying multilayers can form an optical cavity; in contrast to the surface generation case in the InAs and bulk GaAs samples.

This study demonstrates that the presence of the QDs can produce enhanced terahertz emission from UD GaAs possibly due to intense interfacial strain fields. With proper MBE growth parameters such as doping and QD size con-

trol, it may be possible to realize even more intense QD-based pulsed terahertz emitters.

E. Estacio thanks the JSPS Postdoctoral Fellowship for Foreign Researchers. A. Salvador and A. Garcia acknowledge support from DOST-PCASTRD and OVCAA—University of the Philippines, Baguio, respectively.

- <sup>1</sup>M. Walther, B. Fischer, M. Schall, H. Helm, and P. Uhd Jepsen, *Chem. Phys. Lett.* **332**, 389 (2000).
- <sup>2</sup>M. Yamashita, K. Kawase, C. Otani, T. Kiwa, and M. Tonouchi, *Opt. Express* **13**, 115 (2005).
- <sup>3</sup>P. Y. Han, G. C. Cho, and X.-C. Zhang, *Opt. Lett.* **25**, 242 (2000).
- <sup>4</sup>K. Kawase, Y. Ogawa, Y. Watanabe, and H. Inoue, *Opt. Express* **11**, 2549 (2003).
- <sup>5</sup>N. Sarukura, H. Ohtake, S. Izumida, and Z. Liu, *J. Appl. Phys.* **84**, 654 (1998).
- <sup>6</sup>M. B. Johnston, D. M. Whitaker, A. Corchia, A. G. Davies, and E. H. Linfield, *Phys. Rev. B* **65**, 165301 (2002).
- <sup>7</sup>P. Gu and M. Tani, in *Terahertz Optoelectronics, Topics in Applied Physics*, edited by K. Sakai (Springer, Berlin, 2005), Vol. 97, pp. 63–76.
- <sup>8</sup>M. Reid and R. Fedosejevs, *Appl. Opt.* **44**, 149 (2005).
- <sup>9</sup>S. J. Oh, C. Kang, I. Maeng, J.-H. Son, N. K. Cho, J. D. Song, W. J. Choi, W.-J. Cho, and J. I. Lee, *Appl. Phys. Lett.* **90**, 131906 (2007).
- <sup>10</sup>D. G. Cooke, F. A. Hegmann, Yu. I. Mazur, W. Q. Ma, X. Wang, Z. M. Wang, G. J. Salamo, M. Xiao, T. D. Mishima, and M. B. Johnson, *Appl. Phys. Lett.* **85**, 3839 (2004).
- <sup>11</sup>K.-C. Je and S.-H. Park, *Phys. Rev. B* **76**, 245318 (2007).
- <sup>12</sup>D. A. Yarotski, R. D. Averitt, N. Negre, S. A. Crooker, A. J. Taylor, G. P. Donati, A. Stintz, L. F. Lester, and K. J. Malloy, *J. Opt. Soc. Am. B* **19**, 1480 (2002).
- <sup>13</sup>P. Boucaud, K. S. Gill, J. B. Williams, M. S. Sherwin, W. V. Schoenfeld, and P. M. Petroff, *Phys. Status Solidi B* **224**, 443 (2001).
- <sup>14</sup>G. Huang, J. Yang, P. Bhattacharya, G. Ariyawansa, and A. G. U. Perera, *Appl. Phys. Lett.* **92**, 011117 (2008).
- <sup>15</sup>P. Kleinschmidt, S. P. Giblin, V. Antonov, H. Hashiba, L. Kulik, A. Tzalenchuk, and S. Komiyama, *IEEE Trans. Instrum. Meas.* **56**, 463 (2007).
- <sup>16</sup>N. Vukmirović, D. Indjin, Z. Ikonić, and P. Harrison, *IEEE Photonics Technol. Lett.* **20**, 129 (2008).
- <sup>17</sup>A. G. U. Perera, G. Ariyawansa, V. M. Apalkov, S. G. Matsik, X. H. Su, S. Chakrabarti, and P. Bhattacharya, *Opto-Electron. Rev.* **15**, 223 (2007).
- <sup>18</sup>Z. Y. Lai and W. Z. Shen, *J. Appl. Phys.* **94**, 367 (2003).
- <sup>19</sup>S. Pelling, R. Davis, L. Kulik, A. Tzalenchuk, S. Kubatkin, T. Ueda, S. Komiyama, and V. N. Antonov, *Appl. Phys. Lett.* **93**, 073501 (2008).
- <sup>20</sup>P. Hewageegana and V. Apalkov, *Physica E* **40**, 2817 (2008).
- <sup>21</sup>I. Vurgaftman, J. R. Meyer, D. H. Wu, K. Bussmann, and B. T. Jonker, *J. Appl. Phys.* **100**, 064509 (2006).
- <sup>22</sup>R. Adomavicius, G. Molis, A. Krotkus, and V. Sirutkaitis, *Appl. Phys. Lett.* **87**, 261101 (2005).
- <sup>23</sup>K. Liu, J. Xu, T. Yuan, and X.-C. Zhang, *Phys. Rev. B* **73**, 155330 (2006).
- <sup>24</sup>R. Mendis, M. L. Smith, L. J. Bignell, R. E. M. Vickers, and R. A. Lewis, *J. Appl. Phys.* **98**, 126104 (2005).
- <sup>25</sup>K. Zeeger, *Semiconductor Physics* (Springer, New York, 1973), Chap. 11.
- <sup>26</sup>N. N. Ledentsov, M. Grundmann, N. Kirstaedter, O. Schmidt, R. Heitz, J. Bohrer, D. Bimberg, G. V. M. Ustinov, and J. Heydenreich, *Solid-State Electron.* **40**, 785 (1996).
- <sup>27</sup>D. Bimberg, M. Grundmann, and N. N. Ledentsov, *Quantum Dot Heterostructures* (Wiley, Chichester, 1999) p. 96.
- <sup>28</sup>M. Reid and R. Fedosejevs, *Appl. Phys. Lett.* **86**, 011906 (2005).
- <sup>29</sup>W. E. Kerr, A. Pancholi, and V. G. Stoleru, *Physica E* **35**, 139 (2006).
- <sup>30</sup>V. G. Stoleru, E. Towe, C. Ni, and D. Pal, in *Progress in Compound Semiconductor Materials IV—Electronic and Optoelectronic Applications*, edited by G. J. Brown, R. M. Biefeld, C. Gmachl, M. O. Manasreh, and K. Unterrainer (Materials Research Society Series, Warrendale, PA, 2005), Vol. 829, p. B1.3.1.
- <sup>31</sup>H. Park, J. Kim, K. Moon, and H. Han, Proceedings of the I2006 Joint 31st International Conference on Infrared and Millimeter Waves and 14th International Conference on Terahertz Electronics Conference Digest, 2006 (unpublished), p. 543.
- <sup>32</sup>H. Takeuchi, J. Yanagisawa, T. Hasegawa, and M. Nakayama, *Appl. Phys. Lett.* **93**, 081916 (2008).

Nomination form for the 2019 Nishina Asia Award

Candidate (name, affiliation, curriculum vitae including the date of the degree of Ph.D., nationality, address, email and telephone)

1. Personal information

- Name: Seunghwan Shin
- Affiliation: PLS-II accelerator division, Pohang Accelerator Laboratory
- Address: Faculty APT 6-508, Jigokro-155, Namgu, Pohang, Gyeongbuk 37673, Korea
- Email: tlssh@postech.ac.kr
- Tel: 82-54-279-1468
- Nationality: Korea

2. Education

- Ph.D. in Accelerator physics, POSTECH, Korea (The date of the degree: August 2006)
- M.S. in Accelerator physics, POSTECH, Korea, March 2000 – February 2002
- B.A. in physics, Keimyung University, Korea, March 1993 – February 2000

3. Academic career

- Lecturer, Principles and technologies on accelerators, POSTECH, March 2018 –

4. Employment

- Senior Researcher at Accelerator Division, PAL, March 2009 –
- Sabbatical at Accelerator Division, APS, ANL, June 2016 – May 2017
- Scientific Fellow at Accelerator Division, Fermilab, March 2008 – March 2009
- Post-Doc, in Physics, Kyungpook National University, September 2006 – March 2008

5. Research interests

- Lattice design and beam dynamics for storage rings.
- Advanced beam dynamics (new concept and development).
- Beam based diagnostics on linear and nonlinear optics of storage rings.
- Beam dynamics and code development for cyclotrons.

Citation for the Award (within 30 words)

For his remarkable contributions to the commissioning of PLS-II and the understanding of current-dependent nonlinear beam dynamics on storage rings for synchrotron radiation.

## Description of the work

As a leader of the PLS-II beam dynamics group, Dr. Shin accomplished design of PLS-II lattice and of overall beam dynamics. In this work, he realized a new concept of double-bend structure, which has an additional straight section for insertion device between bends. As a result, 42 % of the circumference is available for a straight section and the total number of insertion devices was doubled to 20; these devices can be available to users. With the PLS-II commissioning team he attained the first beam store, systematic ring setup including establishment of a golden orbit, a 100-mA beam current (goal of commissioning), implementation of the orbit-feedback system, and support on 30 beamline commissioning within 6 months. As a result, PLS-II user service was started on schedule.

Recently he has performed important and high-impact research in the collaboration between PAL (Korea) and ANL (USA). He performed a benchmark study of collective and nonlinear dynamics in the Advanced Photon Source. Storage rings have nonlinear beam dynamics with intensity-dependent beam characteristics (i.e., 'collective effect'), but accurate prediction of this effect is extremely challenging. Many models have been proposed to predict it, but in many rings the predictions differ significantly from experimental results. To obtain simulations that describe phenomena observed of injections for fourth generation storage ring (4GSR), Dr. Shin integrated an existing impedance model with the 'Elegant' software program in APS and constructed an accurate model of a storage ring that has an intensity-dependent beam to simulate the kick aperture at various charges. As a result, the simulations agree well with experimental measurement. Based on the agreement of simulations with measurements, he performed additional simulations, which explained current-dependent nonlinear beam dynamics in detail. This result provides confidence in predictions of high-charge injected beam dynamics in the storage ring.

He is striving to develop novel schemes in the accelerator field. Recently he suggested a new on-axis injection scheme that uses a transverse deflecting rf cavity to kick the incoming beam into an already-populated bucket, but with a timing offset from the synchronous phase. In an extremely-small-emittance ring of 4GSRs, only on-axis injections are workable for such a small dynamic aperture; so far, three on-axis injection schemes have been proposed for 4GSR. However, they require a tight condition on the injected beam, and a kicker that has a very short pulse to avoid disturbing the stored beam. Compared with previous on-axis injection schemes, his new scheme has three advantages: no need for shorter pulse dipole kicker than bunch spacing, larger energy acceptance for injected beam and the additional benefit of generating a short x-ray pulse between the deflecting cavities.

Key references (up to 3 key publications\*)

1. S. Shin\*, S. Kwon, D-T. Kim, D-E. Kim, M. Kim, S-H. Kim, S-C. Kim, J. Kim, C. Kim, B. Park, S-S. Park, S-J. Park, E. Park, Y. Son, J. Yoon, B. Lee, E. Lee, J-W. Lee, H-S. Lee, Y. Joo, J. Choi, T. Ha, W. Hwang, I. Hwang, J-Y. Lee, B. Oh, C-H. Lee, H-S. Lee, J-Y. Kim, J. Y. Kim, J. Y. Hwang, S. H. Nam, and M. Cho, "Commissioning of the PLS-II", Journal of Instrumentation, 8, P01019 (2013).
2. Vadim Sajaev, Ryan Lindberg, Michael Borland, and Seunghwan Shin\*, "Simulations and measurements of the impact of collective effects on dynamics aperture", Phys. Rev. Accel. and beam, 22, 032802 (2019)
3. J. Kim, G. Jang, M. Yoon, B-H. Oh, J. Lee, J. Ko, Y. Parc, T. Ha, D. Kim, S. Kim, and S. Shin\*, "Injection scheme with deflecting cavity for a fourth-generation storage ring", Phys. Rev. Accel. and beam, 22, 011601 (2019)

\*) Copy of one most significant publication should be attached.

Nominator (name, affiliation, email, telephone and relation to the candidate)

Name: In Soo Ko

Affiliation: Director, Pohang Accelerator Laboratory and Professor Emeritus, POSTECH

Email: isko@postech.ac.kr

Tel: +82 54 279 1001 (O), +82 10 5066 1121 (M)

Relation to the candidate:

- A member of faculty at Department of Physics, POSTECH during Dr. Shin's graduate course.
- Currently, he is a member (Division Head) of PAL in charge of PLS-II operations and a collaborator of PAL 4GSR design.

Signature



Date

March 28, 2019

Nomination form for the 2019 Nishina Asia Award

Candidate (name, affiliation, curriculum vitae including the date of the degree of Ph.D., nationality, address, email and telephone)

Name: Jeng-Da Chai

Nationality: Taiwan

Affiliation: Department of Physics, National Taiwan University

Address: No. 1, Sec. 4, Roosevelt Road, Taipei 10617, Taiwan

Ph.D.: December 2005, University of Maryland, College Park

E-mail: [jdchai@phys.ntu.edu.tw](mailto:jdchai@phys.ntu.edu.tw)

Telephone: +886-2-3366-5586

Website: <http://web.phys.ntu.edu.tw/jdchai/>

Professional Experience:

Professor, Department of Physics, National Taiwan University (Aug. 2017 ~ present)

Associate Professor, Department of Physics, National Taiwan University (Aug. 2013 ~ Jul. 2017)

Assistant Professor, Department of Physics, National Taiwan University (Aug. 2009 ~ Jul. 2013)

Postdoctoral Fellow, Department of Chemistry, UC Berkeley (Jan. 2006 ~ Jun. 2009)

Awards and Honors:

Project for Excellent Junior Research Investigators, Ministry of Science and Technology, Taiwan (2018 ~ 2021, 2015 ~ 2018)

Excellence in Teaching Award, National Taiwan University, Taiwan (2018)

Junior Research Investigators Award, Academia Sinica, Taiwan (2017)

Outstanding Young Physicist Award, The Physical Society of the Republic of China (Taiwan) (2016)

Career Development Award, National Taiwan University, Taiwan (2015 ~ 2016, 2013 ~ 2015)

Youth Medal, China Youth Corps, Taiwan (2015).

TWAS Young Affiliate, The World Academy of Sciences (TWAS) - for the advancement of science in developing countries (2013 ~ 2017).

Young Theorist Award, National Center for Theoretical Sciences, Taiwan (2012).

EPSON Scholarship Award, The International Society for Theoretical Chemical Physics (2011).

Journal Editorial Boards:

Editorial Board, International Journal of Quantum Chemistry (Mar. 2018 ~ present)

Editorial Board, Chinese Journal of Physics (Dec. 2017 ~ present)

Citation for the Award (within 30 words)

For his development of accurate density functional methods for nanoscale applications.



## Description of the work

Dr. Jeng-Da Chai's research has mainly focused on the development of new quantum-mechanical methods suitable for the study of nanoscale systems, and their applications to materials for new energy. In particular, much of his recent research has focused on resolving the qualitative failures of semilocal density functional methods, while greatly improving their predictive power for nanoscale applications.

After getting Ph.D., Dr. Jeng-Da Chai joined Prof. Martin Head-Gordon's group at UC Berkeley as a postdoc, and developed several promising long-range corrected (LC) hybrid density functionals for nanoscale applications. Ref. [1] first proposed a general scheme for systematically modeling LC hybrid functionals, significantly improving the accuracy of LC hybrid functionals. Ref. [2] developed a very influential LC hybrid functional (cited more than 4,100 times), using the aforementioned scheme and atom-atom dispersion corrections. The resulting LC hybrid functionals ( $\omega$ B97 [1],  $\omega$ B97X [1], and  $\omega$ B97X-D [2]) were shown to significantly outperform the most popular hybrid functional (i.e., B3LYP) and many other well-known density functionals for a very wide range of applications (e.g., thermochemistry, kinetics, noncovalent interactions, frontier orbital energies, fundamental gaps, and long-range charge-transfer excitations). Since then, this seminal work has yielded substantial nanoscale applications. More importantly, it has created a new direction in the development of accurate density functionals for nanoscale applications.

Since August 2009, Dr. Jeng-Da Chai has joined the faculty of the Department of Physics at National Taiwan University, and has continued to make significant contributions to the development of accurate density functional methods for nanoscale applications.

For systems with strong static correlation effects, Kohn-Sham density functional theory (KS-DFT) employing conventional semilocal and hybrid density functionals can provide unreliable results, due to the inappropriate treatment of static correlation. To reliably predict the properties of these systems, high-level *ab initio* multi-reference electronic structure methods are typically needed. However, accurate multi-reference calculations are prohibitively expensive for large systems (especially for geometry optimization). Therefore, it remains extremely challenging to investigate the properties of strongly correlated electron systems at the nanoscale using conventional electronic structure methods. Aiming to study the ground-state properties of strongly correlated electron systems at the nanoscale with minimum computational complexity, in 2012, Dr. Jeng-Da Chai pioneered a density functional theory with fractional orbital occupations (TAO-DFT) [3], wherein strong static correlation can be properly described. Due to its computational efficiency and reasonable accuracy, TAO-DFT was recently applied to study the properties of nanoscale systems with strong static correlation effects (e.g., acenes, zigzag graphene nanoribbons, cyclacenes, Möbius cyclacenes, alternant polycyclic aromatic hydrocarbons, and hydrogen storage materials possessing radical character), all of which are extremely challenging systems for traditional electronic structure methods.

In summary, Dr. Jeng-Da Chai's research achievements in the development of accurate density functional methods for the study of electronic and optical properties of nanoscale systems (e.g., his seminal work in LC hybrid density functionals ( $\omega$ B97 [1],  $\omega$ B97X [1], and  $\omega$ B97X-D [2]) and his pioneering work in TAO-DFT [3]) have extended the applicability of electronic structure methods to an area long believed to be beyond their reach.

Key references (up to 3 key publications\*)

- [1] **Jeng-Da Chai** and Martin Head-Gordon, “Systematic Optimization of Long-Range Corrected Hybrid Density Functionals”, Journal of Chemical Physics **128**, 084106 (2008).  
[Times Cited: **1449**]
- [2] **Jeng-Da Chai** and Martin Head-Gordon, “Long-Range Corrected Hybrid Density Functionals with Damped Atom-Atom Dispersion Corrections”, Physical Chemistry Chemical Physics **10**, 6615 (2008). [Times Cited: **4128**]
- [3] **Jeng-Da Chai**, “Density Functional Theory with Fractional Orbital Occupations”, Journal of Chemical Physics **136**, 154104 (2012). [Times Cited: **49**]

\*) Copy of one most significant publication should be attached.

Nominator (name, affiliation, email, telephone and relation to the candidate)

- (1) Name: Yuan-Huei Chang
- (2) Affiliation: Department of Physics, National Taiwan University
- (3) Address: No. 1, Sec. 4, Roosevelt Road, Taipei 10617, Taiwan
- (4) E-mail: yhchang@phys.ntu.edu.tw
- (5) Telephone: +886-2-3366-5126
- (6) Relation to the Candidate: Colleague

Signature: Yuan-Huei Chang



Date: March 29, 2019

## Nomination form for the 2019 Nishina Asia Award

Candidate (name, affiliation, curriculum vitae including the date of the degree of Ph.D., nationality, address, email and telephone)
<p><b>Name:</b> Yanchao Wang</p> <p><b>Affiliation:</b> State Key Lab of Superhard Materials, Jilin University, China</p> <p><b>Nationality:</b> Chinese</p> <p><b>Address:</b> State Key Lab of Superhard Materials, Jilin University, 2699 Qianjin Str., 130012, Changchun, China</p> <p><b>Phone:</b> +86-13943087661</p> <p><b>Email:</b> wyc@calypso.cn</p> <p><b>Education:</b></p> <p>2013.09 -- Ph.D in Condensed Matter Physics, State Key Lab of Superhard Materials, Jilin Univ., China.</p> <p>2009.06 -- M.S. in Condensed Matter Physics, State Key Lab of Superhard Materials, Jilin Univ., China.</p> <p>2006.06 -- B.S. in Physics, Department of Physics, Baicheng Normal College, China.</p> <p><b>Permanent Positions Hold:</b></p> <p>2017.10 -- now      Professor, State Key Lab of Superhard Materials, Jilin Univ., China</p> <p>2013.08 -- 2017.09    Lecturer/Associate Professor, State Key Lab of Superhard Materials, Jilin Univ., China</p>
Citation for the Award (within 30 words)
For his development of efficient method (named as CALYPSO) for the prediction of crystal structures with the only given information of chemical compositions.
Description of the work
<p>One of the most challenging problems in physics, chemistry and materials science is to predict theoretically the atomic arrangement—the crystal structure of a material—with only given information of chemical composition.</p> <p>Dr. Yanchao Wang has developed an efficient CALYPSO (see more at <a href="http://www.calypso.cn">http://www.calypso.cn</a>) approach [1-2] for structure prediction at given information of chemical compositions via multi-objective swarm-intelligence optimization algorithms. The method [1] represents a significant step forward in the field, and received a great deal of interests with 1,034 citations till now [Google Scholar].</p> <p>The method has been widely used by more than 2,300 users distributed world-widely in 65 countries to design multi-dimensional materials ranging from bulk crystals to nanoclusters, two-dimensional layers, and surfaces, and the use of the method has generated &gt; 750 high-profile publications including those in Nat. Chem., PRL, and PNAS, etc.</p>

Using the developed CALYPSO method, Dr. Wang solved a number of structure-related problems by predicting more than 30 novel phases of materials under pressure, some of which received experimental confirmation. His prediction of an ionic phase of water ice at extremely high pressure [3] is particularly interesting as it is the first ionic ice seen in the literature.

Key references (up to 3 key publications\*)

- [1] **Yanchao Wang**, Jian Lv, Li Zhu, and Yanming Ma\*, “Crystal structure prediction via particle-swarm optimization”, **Phys. Rev. B** 82, 094116 (2010). **1,034 citations** in Google Scholar
- [2] **Yanchao Wang**, Jian Lv, Li Zhu, Yanming Ma\*, "CALYPSO: A method for crystal structure prediction", **Comput. Phys. Commun.** 183, 2063 (2012). **773 citations** in Google Scholar
- [3] **Yanchao Wang**, Hanyu Liu, Jian Lv, Li Zhu, Hui Wang, Yanming Ma\*, “High pressure partially ionic phase of water ice”, **Nat. Commun.** 2, 563 (2011). **175 citations** in Google Scholar

\*) Copy of one most significant publication should be attached.

Nominator (name, affiliation, email, telephone and relation to the candidate)

**Name:** Yanming Ma

**Affiliation:** College of Physics, Jilin University, China

**Email:** mym@jlu.edu.cn

**Phone:** +86-431-85168276

**Relation to the candidate:** Supervisor of Yanchao Wang

Signature

*Yanming Ma*

Date

Mar. 28, 2019

## Nomination for the 2019 Nishina Asia Award

1. Candidate (name, affiliation, curriculum vitae including the date of the degree of Ph.D., nationality, address, email and telephone)

Name: Yi-Bo Yang (杨一玻)

Affiliation: Institute of Theoretical Physics, Chinese Academy of Science (ITP-CAS), Beijing, China.

Curriculum vitae:

- Peking University Beijing, China 2001.9-2005.7, B.S.
- Institute of Theoretical Physics of CAS, Beijing, China 2005.9-2010.6, Ph.D [PhD degree granted 2010 July]
- Institute of High-Energy Physics of CAS (IHEP-CAS), Beijing, China 2010.7-2013.7, Postdoc
- University of Kentucky Lexington, KY, USA 2013.9-2017.1, Postdoc
- Michigan State University East Lansing, MI, USA 2017.1-2018.8, Postdoc
- ITP/CAS Beijing, China 2018.9-present, Associate Professor

Nationality: P. R. China

Address: Zhong Guan Cun East Street 55#, Beijing 100190, P.R. China

Email: ybyang@itp.ac.cn

Telephone: 86-010-62582510

2. Citation for the Award (within 30 words)

Advancement of Lattice QCD efforts to understand the importance of the gluon in the proton

3. Description of the work

As the fundamental theory of the strong interaction, Quantum Chromodynamics (QCD) has quite different properties at different scales. QCD is perturbatively calculable at the scale much smaller than 1 fm and has been examined precisely by the experiment; but at the hadron scale around 1 fm, the nature of QCD is hidden by the non-perturbative properties like color confinement and then the quarks are bound by the gluon to form the proton and even nuclei. The analysis of the present experiments has shown that the gluon provides considerable chunk to the proton mass and spin, and the Electron-Ion Colliders are proposed in US and China for more solid determination.

Thus whether a precise prediction can be made from the theoretical side is a crucial challenge to our understanding on the strong interaction. Lattice QCD provide a framework to define the QCD on a 4-D Euclidean lattice, and then allow the accurate calculation on the non-perturbative properties of QCD. It has been well established for the calculation on the quark in the proton, but the progress in the gluon part is very limited.

After Dr. Yi-Bo Yang's first postdoc at IHEP/CAS on the glueball with Prof. Ying Chen and et.al., he joined the Professor Keh-Fei Liu's group for the proton spin decomposition. Such a decomposition is proposed over 30 years ago, to decompose the proton spin into the contribution from the quark spin and orbital angular momentum contributions, plus those of the gluon. Among the contributions, the gluon spin is most unknown from Lattice QCD calculation. Dr. Yang led the numerical gluon spin calculation with the computer resources from NERSC, XSEDE and OLCF, and guided the collaborator on the analytical 1-loop renormalization calculation. The final result shows that "the gluons that bind quarks together in nucleons provide a considerable chunk of proton's total spin", as in the statement for this work as one of eight APS 2017 highlights. After the paper [1] is published on PRL, it is selected as Editor's suggestion and favored on Physics with Viewpoint article, reported by ScienceNews and also Forbes, and eventually selected as one of the APS 2017 highlights among the other famous experimental researches likes the progress on the gravity wave and dark matter search.

During the spin calculation, Dr. Yang find that the renormalization of the gluon operator is the major source of the systematic uncertainty, in the lattice QCD calculation of the gluon in the proton mass. The bare result with different lattice regularizations can be differ by a factor of 3 or more, such a fact makes the perturbative calculation fails in most of the cases. In the other side, the non-perturbative renormalization of the gluon operator was absent after the quark case has been developed over 30 years, since the calculation is extremely expensive and then that for a lattice with the physical quark mass will need the gross of nowadays computing power or so to reduce the statistical uncertainty to a few percent level. Using the principle of the cluster decomposition and the fast Fourier transform algorithm, Dr. Yang found the solution to reduce the cost of the above calculation by a factor of 100,000 and then make the non-perturbative renormalization to be doable for the gluon operators [2], and led the collaborators to complete the proton mass decomposition calculation with the systematic uncertainty of the renormalization under control [3]. The result is the first Lattice QCD prediction on the proton mass decomposition, and shows that the quark and gluon kinetic energy contributions to the proton mass, and also the QCD trace anomaly one are insensitive to the light quark mass. The related paper is accepted by PRL after 26 days of the submission, selected as Editor's suggestion, favored on Physics with Viewpoint article, and reported by ScienceNews and also The Inquisitor.

Besides above accomplishments, Dr. Yang lead the first lattice QCD investigation on the gluon PDF using the large momentum effective theory approach, and the glueball in the charmonium radiative decay; he also coauthored a number of the important works likes on the quark PDF, strange quark contribution to the radius and magnetic moment of the proton and so on. His contribution to the gluon structure in the proton deserves the Nishina Asia Award.

4. Key references (up to 3 key publications, copies attached)

- "Glue spin and helicity in nucleon from lattice QCD", Yi-Bo Yang , Raza Sabbir Sufian, Andrei Alexandru, Terrence Draper, Michael J. Glatzmaier, Keh-Fei Liu, Yong Zhao, Phys. Rev. Lett. 118 (2017) 102001
- "Nonperturbatively-renormalized glue momentum fraction at physical pion mass from Lattice QCD", Yi-Bo Yang , Ming Gong, Jian Liang, Huey-Wen Lin, Keh-Fei Liu, Dimitra Pefkou, Phiala Shanahan, Phys. Rev. D 98 (2018), 074506
- "Proton Mass Decomposition from the QCD Energy Momentum Tensor", Yi-Bo Yang , Jian Liang, Yu-Jiang Bi, Ying Chen, Terrence Draper, Keh-Fei Liu, Zhaofeng Liu, Phys. Rev. Lett. 121 (2018) 212001

5. Nominator (name, affiliation, email, telephone and relation to the candidate)

Dr. Hai-Jun Zhou,  
Research Professor  
Institute of Theoretical Physics, the Chinese Academy of Sciences (ITP-CAS), Beijing  
zhouhj@mail.itp.ac.cn  
0086-10-62582362

Colleague of Dr. Yi-Bo Yang at ITP-CAS

Signature  Date 2019-03-30



# Proton Mass Decomposition from the QCD Energy Momentum Tensor

Yi-Bo Yang,<sup>1,5</sup> Jian Liang,<sup>2</sup> Yu-Jiang Bi,<sup>3</sup> Ying Chen,<sup>3,4</sup> Terrence Draper,<sup>2</sup> Keh-Fei Liu,<sup>2</sup> and Zhaofeng Liu<sup>3,4</sup>

<sup>1</sup>*Department of Physics and Astronomy, Michigan State University, East Lansing, Michigan 48824, USA*

<sup>2</sup>*Department of Physics and Astronomy, University of Kentucky, Lexington, Kentucky 40506, USA*

<sup>3</sup>*Institute of High Energy Physics, Chinese Academy of Sciences, Beijing 100049, China*

<sup>4</sup>*School of Physics, University of Chinese Academy of Sciences, Beijing 100049, China*

<sup>5</sup>*Institute of Theoretical Physics, Chinese Academy of Sciences, Beijing 100190, China*



(Received 4 September 2018; published 19 November 2018)

We report results on the proton mass decomposition and also on related quark and glue momentum fractions. The results are based on overlap valence fermions on four ensembles of  $N_f = 2 + 1$  domain wall fermion configurations with three lattice spacings and three volumes, and several pion masses including the physical pion mass. With fully nonperturbative renormalization (and universal normalization on both quark and gluon), we find that the quark energy and glue field energy contribute 32(4)(4)% and 36(5)(4)% respectively in the  $\overline{\text{MS}}$  (modified minimal subtraction) scheme at  $\mu = 2$  GeV. A quarter of the trace anomaly gives a 23(1)(1)% contribution to the proton mass based on the sum rule, given 9(2)(1)% contribution from the  $u$ ,  $d$ , and  $s$  quark scalar condensates. The  $u$ ,  $d$ ,  $s$ , and glue momentum fractions in the  $\overline{\text{MS}}$  scheme are in good agreement with global analyses at  $\mu = 2$  GeV.

DOI: 10.1103/PhysRevLett.121.212001

**Introduction.**—In the standard model, the Higgs boson provides the origin of quark masses. But how it is related to the proton mass and thus the masses of nuclei and atoms is another question. The masses of the valence quarks in the proton are just  $\sim 3$  MeV per quark, which is directly related to the Higgs boson, while the total proton mass is 938 MeV. The percentages of the quark and gluon contributions to the proton mass can only be provided by solving QCD non-perturbatively and/or with information from experiment. With phenomenological input, the first decomposition was carried out by Ji [1]. As in Refs. [1,2], the Hamiltonian of QCD can be decomposed as

$$M = -\langle T_{44} \rangle = \langle H_m \rangle + \langle H_E \rangle(\mu) + \langle H_g \rangle(\mu) + \frac{1}{4} \langle H_a \rangle, \quad (1)$$

in the rest frame of the hadron state where  $M$  is the hadron mass, and

$$T_{\mu\nu} = \frac{1}{4} \bar{\psi} \gamma_{(\mu} \overleftrightarrow{D}_{\nu)} \psi + F_{\mu\alpha} F_{\nu\alpha} - \frac{1}{4} \delta_{\mu\nu} F^2 \quad (2)$$

is the energy momentum tensor (EMT) of QCD in Euclidean space [3] with  $\langle T_{44} \rangle$  as its expectation value in the hadron, and the trace anomaly gives the following:

$$M = -\langle T_{\mu\mu} \rangle = \langle H_m \rangle + \langle H_a \rangle. \quad (3)$$

The  $H_m$ ,  $H_E$ , and  $H_g$  in the above equations denote the contributions from the quark condensate, the quark energy, and the glue field energy, respectively:

$$\begin{aligned} H_m &= \sum_{u,d,s,\dots} \int d^3x m \bar{\psi} \psi, \\ H_E &= \sum_{u,d,s,\dots} \int d^3x \bar{\psi} (\vec{D} \cdot \vec{\gamma}) \psi, \\ H_g &= \int d^3x \frac{1}{2} (B^2 - E^2). \end{aligned} \quad (4)$$

The QCD anomaly term  $H_a$  is the joint contribution from the quantum anomalies of both glue and quark,

$$\begin{aligned} H_a &= H_g^a + H_m^{\gamma}, \\ H_g^a &= \int d^3x \frac{-\beta(g)}{g} (E^2 + B^2), \\ H_m^{\gamma} &= \sum_{u,d,s,\dots} \int d^3x \gamma_m m \bar{\psi} \psi. \end{aligned} \quad (5)$$

All the  $\langle H \rangle$  are defined by  $\langle N | H | N \rangle / \langle N | N \rangle$  where  $|N\rangle$  is the nucleon state in the rest frame. Note that  $\langle H_E + H_g \rangle$ ,  $\langle H_m \rangle$  and  $\langle H_a \rangle$  are scale and renormalization scheme independent, but  $\langle H_E \rangle(\mu)$  and  $\langle H_g \rangle(\mu)$  separately have scale and scheme dependence.

Published by the American Physical Society under the terms of the [Creative Commons Attribution 4.0 International](#) license. Further distribution of this work must maintain attribution to the author(s) and the published article's title, journal citation, and DOI. Funded by SCOAP<sup>3</sup>.

The nucleon mass  $M$  can be calculated from the nucleon two-point function. If one calculates further  $\langle H_m \rangle$  and  $\langle H_E \rangle(\mu)$ , then  $\langle H_g \rangle(\mu)$  and  $\langle H_a \rangle$  can be obtained through Eqs. (1) and (3). The approach has been adopted to decompose  $S$ -wave meson masses, from light mesons to charmoniums, to gain insight about contributions of each term [2]. But the mixing between  $\langle H_E \rangle(\mu)$  and  $\langle H_m \rangle$  will be nontrivial under the lattice regularization when there is any breaking of the quark equation of motion at finite spacing. On the other hand, if we obtain the renormalized quark momentum fraction  $\langle x \rangle_q^R$  in the continuum limit, and define the renormalized quark energy  $\langle H_E^R \rangle$  in term of  $\langle x \rangle_q^R$  and  $\langle H_m \rangle$  with the help of the equation of motion, i.e.,

$$\langle H_E^R \rangle = \frac{3}{4} \langle x \rangle_q^R M - \frac{3}{4} \langle H_m \rangle, \quad (6)$$

then the additional mixing can be avoided. Similarly, the renormalized glue field energy can be accessed from the glue momentum fraction  $\langle x \rangle_g^R$  by

$$\langle H_g^R \rangle = \frac{3}{4} \langle x \rangle_g^R M. \quad (7)$$

In the present Letter, we use the lattice derivative operator for the quark EMT and a combination of plaquettes for the gauge EMT and address their normalization in addition to renormalization and mixing. We calculate the proton mass and the renormalized  $\langle x \rangle_{q,g}$  on four lattice ensembles, and extrapolate the results to the physical pion mass with a global fit including finite lattice spacing and volume corrections. Then we combine previously calculated  $\langle H_m \rangle$  [4] to obtain  $\langle H_a \rangle$  from Eq. (3), and the full decomposition of the proton energy in the rest frame as shown in Eq. (1).

*Numerical setup.*—We use overlap valence fermions on  $(2+1)$  flavor RBC/UKQCD domain wall fermion gauge configurations from four ensembles on  $24^3 \times 64$  (24I),  $32^3 \times 64$  (32I) [5],  $32^3 \times 64$  (32ID), and  $48^3 \times 96$  (48I) [6] lattices. These ensembles cover three values of the lattice spacing and volume respectively, and four values of the quark mass in the sea, which allows us to implement a global fit on our results to control the systematic uncertainties as in Ref. [4,7]. Other parameters of the ensembles used are listed in Table I.

The effective quark propagator of the massive overlap fermion is the inverse of the operator  $(D_c + m)$  [8,9], where  $D_c$  is chiral, i.e.,  $\{D_c, \gamma_5\} = 0$  [10], and its detailed definition can be found in our previous work [11–13]. We used four quark masses from the range  $m_\pi \in (250, 400)$  MeV on the 24I and 32I ensembles, and six or five quark masses from  $m_\pi \in (140, 400)$  MeV on the 48I/32ID ensembles respectively, which have larger volumes and thus allow a lighter pion mass with the constraint  $m_\pi L > 3.8$ . One step of the hypercubic (HYP) smearing [14] is applied on all the configurations to improve the

TABLE I. The parameters for the RBC/UKQCD configurations [6]: spatial and temporal size, lattice spacing, sea strange quark mass under  $\overline{\text{MS}}$  scheme at 2 GeV, pion mass with the degenerate light sea quark, and the number of configurations.

Symbol	$L^3 \times T$	a (fm)	$m_s^{(s)}$ (MeV)	$m_\pi$ (MeV)	$N_{cfg}$
32ID	$32^3 \times 64$	0.1431(7)	89.4	171	200
24I	$24^3 \times 64$	0.1105(3)	120	330	203
48I	$48^3 \times 96$	0.1141(2)	94.9	139	81
32I	$32^3 \times 64$	0.0828(3)	110	300	309

signal. Numerical details regarding the calculation of the overlap operator, eigenmode deflation for the inversion of the quark matrix, and the  $Z_3$  grid smeared sources with low-mode substitution (LMS) to increase statistics are given in Refs. [11–13,15].

*Proton mass.*—We first calculate the proton mass on these four ensembles and apply the  $\text{SU}(4|2)$  mixed action HB $\chi$ PT functional form [16] to fit the results,

$$M(m_\pi^v, m_\pi^{\text{sea}}, a, L) = M_0 + C_1(m_\pi^v)^2 + C_2(m_\pi^{\text{sea}})^2 - \frac{(g_A^2 - 4g_A g_1 - 5g_1^2)\pi}{3(4\pi f_\pi)^2} (m_\pi^v)^3 - \frac{(8g_A^2 + 4g_A g_1 + 5g_1^2)\pi}{3(4\pi f_\pi)^2} (m_\pi^{pq})^3 + C_3^{I/D} a^2 + C_4 \frac{(m_\pi^v)^2}{L} e^{-m_\pi^v L}, \quad (8)$$

where  $M_0$ ,  $C_{1,2,3,4}$ , the axial vector coupling  $g_A$ , and an additional partially quenched one  $g_1$  are free parameters;  $f_\pi = 0.122(9)$  GeV is the pion decay constant;  $m_\pi^{v,\text{sea}}$  is the valence and sea pion mass, respectively;  $m_\pi^{pq} = \sqrt{(m_\pi^v)^2 + (m_\pi^{\text{sea}})^2 + \Delta_{\text{mix}} a^2}$  is the partially quenched mass with the mixed action term  $\Delta_{\text{mix}} a^2$ ; and  $a$  is the lattice spacing. The  $\mathcal{O}(m_\pi^3)$  logarithm function  $\mathcal{F}$  in the original functional form is dropped since it turns out to be not useful to constrain the fit. Note that we used  $C_3^I$  for the 24I/48I/32I ensembles and  $C_3^{ID}$  for 32ID ensemble as they used different gauge actions. We get the prediction of the proton mass at the physical point as  $M(m_\pi^{\text{phys}}, m_\pi^{\text{phys}}, 0, \infty) = 0.960(13)$  GeV with  $\chi^2/\text{d.o.f.} = 0.52$ . From the fit, we can also get the light quark mass sigma term  $H_{m,u+d} \simeq (\partial M / \partial m_\pi) m_\pi / 2 = 52(8)$  MeV, which is consistent with our previous direct calculation  $46(7)(2)$  MeV [4]. The  $g_A$  we get from the fit is 0.9(2) which is consistent with the experimental result 1.2723(23) [17] within  $2\sigma$ . Alternatively, using the experimental value of  $g_A$  predicts the proton mass as 0.931(8) with a  $\chi^2/\text{d.o.f.}$  of 1.5. The results of the proton mass with the partially quenching effect ( $m_\pi^{\text{sea}} \neq m_\pi^v$ ) subtracted are plotted in Fig. 1 as a function of the valence pion mass, together with the blue band for our prediction in the continuum limit. The difference between

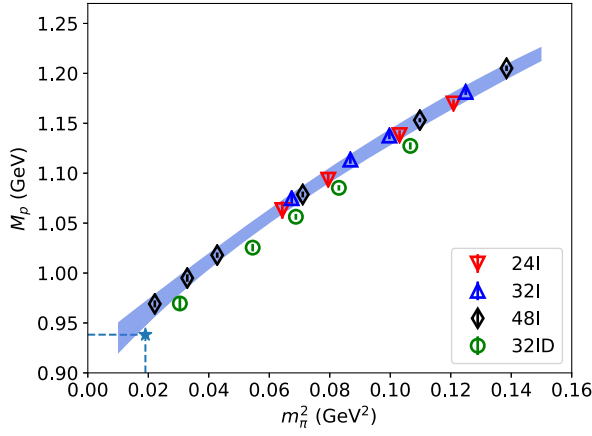


FIG. 1. The proton mass as a function of the pion mass at different lattice spacings and volumes, after partially quenching effects are subtracted. The star shows the physical proton mass.

the results with different symbols reflects the discretization errors and finite volume effects, which are reasonably small, as shown in Fig. 1.

**Momentum fraction.**—The quark and gluon momentum fractions in the nucleon can be defined by the traceless diagonal part of the EMT matrix element in the rest frame [18],

$$\begin{aligned} \langle x \rangle_{q,g} &\equiv -\frac{\langle N | \frac{4}{3} \bar{T}_{44}^{q,g} | N \rangle}{M \langle N | N \rangle}, \\ \bar{T}_{44}^q &= \int d^3x \bar{\psi}(x) \frac{1}{2} \left( \gamma_4 \vec{D}_4 - \frac{1}{4} \sum_{i=0,1,2,3} \gamma_i \vec{D}_i \right) \psi(x), \\ \bar{T}_{44}^g &= \int d^3x \frac{1}{2} [E(x)^2 - B(x)^2]. \end{aligned} \quad (9)$$

In practice, we calculated ratios of the three-point function to the two-point function

$$R^{q,g}(t_f, t) = \frac{\langle 0 | \int d^3y \Gamma^e \chi_S(\vec{y}, t_f) \bar{T}_{44}^{q,g}(t) \sum_{\vec{x} \in G} \bar{\chi}_S(\vec{x}, 0) | 0 \rangle}{\langle 0 | \int d^3y \Gamma^e \chi_S(\vec{y}, t_f) \sum_{\vec{x} \in G} \bar{\chi}_S(\vec{x}, 0) | 0 \rangle}, \quad (10)$$

where  $\chi_S$  is the standard proton interpolation field with Gaussian smearing applied to all three quarks, and  $\Gamma^e$  is the unpolarized projection operator of the nucleon. All the correlation functions from the source points  $\vec{x}$  in the grid  $G$  are combined to improve the signal-to-noise ratio (SNR) [13]. When  $t_f$  is large enough,  $R^{q,g}(t_f, t)$  approaches the bare nucleon matrix element  $\langle N | \bar{T}_{44}^{q,g} | N \rangle$ .

For each quark mass on each ensemble, we construct  $R(t_f, t)$  for several sink-source separations  $t_f$  from 0.7 fm to 1.5 fm and all the current insertion times  $t$  between the source and sink, combine all the data to do the two-state fit, and then obtain the matrix elements we want with the excited-states contamination removed properly. The more detailed discussion of the simulation setup and the two-state fit can be found in our previous work [4,7,19].

To improve the signal in the disconnected insertion part of  $\langle x \rangle_{q,g}$ , all the time slices are looped over for the proton propagator. For  $\langle x \rangle_g$ , the cluster-decomposition error reduction (CDER) technique is applied, as described in Refs. [20,21].

The renormalized momentum fractions  $\langle x \rangle^R$  in the  $\overline{\text{MS}}$  scheme at scale  $\mu$  are

$$\begin{aligned} \langle x \rangle_{u,d,s}^R &= Z_{QQ}^{\overline{\text{MS}}}(\mu) \langle x \rangle_{u,d,s} + \delta Z_{QQ}^{\overline{\text{MS}}}(\mu) \sum_{q=u,d,s} \langle x \rangle_q \\ &\quad + Z_{QG}^{\overline{\text{MS}}}(\mu) \langle x \rangle_g, \\ \langle x \rangle_g^R &= Z_{GQ}^{\overline{\text{MS}}}(\mu) \sum_{q=u,d,s} \langle x \rangle_q + Z_{GG}^{\overline{\text{MS}}}(\mu) \langle x \rangle_g, \end{aligned} \quad (11)$$

where  $\langle x \rangle_{u,d,s,g}$  is the bare momentum fraction under the lattice regularization, and the renormalization constants in the  $\overline{\text{MS}}$  at scale  $\mu$  are defined through the RI/MOM scheme

$$\begin{aligned} &\begin{pmatrix} Z_{QQ}^{\overline{\text{MS}}}(\mu) + N_f \delta Z_{QQ}^{\overline{\text{MS}}}(\mu) & N_f Z_{QG}^{\overline{\text{MS}}}(\mu) \\ Z_{GQ}^{\overline{\text{MS}}}(\mu) & Z_{GG}^{\overline{\text{MS}}}(\mu) \end{pmatrix} \\ &\equiv \left\{ \begin{bmatrix} Z_{QQ}(\mu_R) + N_f \delta Z_{QQ} & N_f Z_{QG}(\mu_R) \\ Z_{GQ}(\mu_R) & Z_{GG}(\mu_R) \end{bmatrix} \right. \\ &\quad \times \left. \begin{pmatrix} R_{QQ}(\frac{\mu}{\mu_R}) + \mathcal{O}(N_f \alpha_s^2) & N_f R_{QG}(\frac{\mu}{\mu_R}) \\ R_{GQ}(\frac{\mu}{\mu_R}) & R_{GG}(\frac{\mu}{\mu_R}) \end{pmatrix} \right\}^{-1} \Big|_{a^2 \mu_R^2 \rightarrow 0} \end{aligned} \quad (12)$$

and  $Z_{QQ}(\mu) = [(Z_{QQ}(\mu_R) R_{QQ}(\mu/\mu_R))]_{a^2 \mu_R^2 \rightarrow 0}^{-1}$ . Note that the isovector matching coefficient  $R_{QQ}(\mu/\mu_R)$  has been obtained at the three-loop level [22] while just the one-loop level results of the other  $R$ 's are available [23].

We list the renormalization constants for  $\bar{T}_{44}^{q,g}$  at  $\overline{\text{MS}}$  2 GeV in Table II and the details of the nonperturbative renormalization (NPR) calculation are discussed in the Supplementary Material [24], based on the previous research of Refs. [25–27].

After the renormalization, the total momentum fraction is generally larger than 1 by 20–30% on the four ensembles due to the discretization error. We apply a uniform normalization on both the quark and gluon momentum fractions at each quark mass of each ensemble, and plot these normalization factors  $\bar{Z} = \langle x \rangle_{u+d+s+g}^{-1}$  in the lower-right panel of Fig. 2.  $\bar{Z}$  should approach unity as can be seen by comparing the normalization of the 24I ( $a = 0.1105$  fm) and the 32I ( $a = 0.0828$  fm) lattices, which have about the same quark mass, for  $m_\pi^2 > 0.08$  GeV<sup>2</sup>.

Then the pion mass dependence of the renormalized and normalized  $\langle x \rangle_{u,d,s,g}^R$  are fitted with the following empirical form simultaneously,

$$\begin{aligned} \langle x \rangle^R(m_\pi^v, m_\pi^{\text{sea}}, a, L) &= \langle x \rangle_0^R + D_1[(m_\pi^v)^2 - (m_\pi^0)^2] \\ &\quad + D_2[(m_\pi^v)^2 - (m_\pi^{\text{sea}})^2] \\ &\quad + D_3^{I/ID} a^2 + D_4 e^{-m_\pi^* L}, \end{aligned} \quad (13)$$

TABLE II. The nonperturbative renormalization (NPR) constants on different ensembles, at  $\overline{\text{MS}}$  2 GeV. The 24I and 48I ensembles have the same lattice spacing and thus share the renormalization constants. The two uncertainties are the statistical and systematic ones, respectively, with the details provided in the Supplementary Material [24].

Symbol	$Z_{QQ}$	$\delta Z_{QQ}$	$Z_{QG}$	$Z_{GQ}$	$Z_{GG}$
32ID	1.25(0)(2)	0.018(2)(2)	0.017(17)	0.57(3)(6)	1.29(5)(9)
24I/48I	1.24(0)(2)	0.012(2)(2)	0.007(14)	0.35(3)(6)	1.07(4)(4)
32I	1.25(0)(2)	0.008(2)(2)	0.000(14)	0.18(2)(2)	1.10(4)(5)

and the  $\chi^2/\text{d.o.f.}$  is 0.20. Our prediction of the  $\langle x \rangle_{u,d,s,g}^R$  are 0.307(30)(18), 0.160(27)(40), 0.051(26)(5), and 0.482(69)(48), respectively, where the first error is the statistical one and the second error includes the systematic uncertainties from the chiral, continuum, and infinite volume interpolation or extrapolation. The systematic uncertainties from the

two-state fit and CDER for  $\langle x \rangle_g$  haven't been taken into account yet and will be investigated in the future. With the normalization factors shown in lower-right panel of Fig. 2, all the predictions of the momentum fractions are consistent with the phenomenological global fit at  $\overline{\text{MS}}$  2 GeV, e.g., CT14 [28] values  $\langle x \rangle_u^R = 0.348(3)$ ,  $\langle x \rangle_d^R = 0.190(3)$ ,  $\langle x \rangle_s^R = 0.035(5)$ , and  $\langle x \rangle_g^R = 0.416(5)$ . The other global fits results [29–33], summarized in Ref. [34], are consistent with CT14. After the partially quenching effect term proportional to  $D_2$  is subtracted, the  $\langle x \rangle_{u,d,s,g}^R$  at different ensembles and valence quark masses are illustrated in Fig. 2 as a function of  $m_\pi^2$ , in the upper-left panel for the  $u$  and  $d$  cases and the upper-right panel for the  $s$  and  $g$  cases. The bands on the figures show our predictions in the continuum limit with their uncertainties (blue for the statistics and cyan for the total).

We also predict the isovector momentum fraction  $\langle x \rangle_{u-d}^R$  as 0.151(28)(29), which is consistent with the CT14 result 0.158(6) [28], in the lower-left panel of Fig. 2.

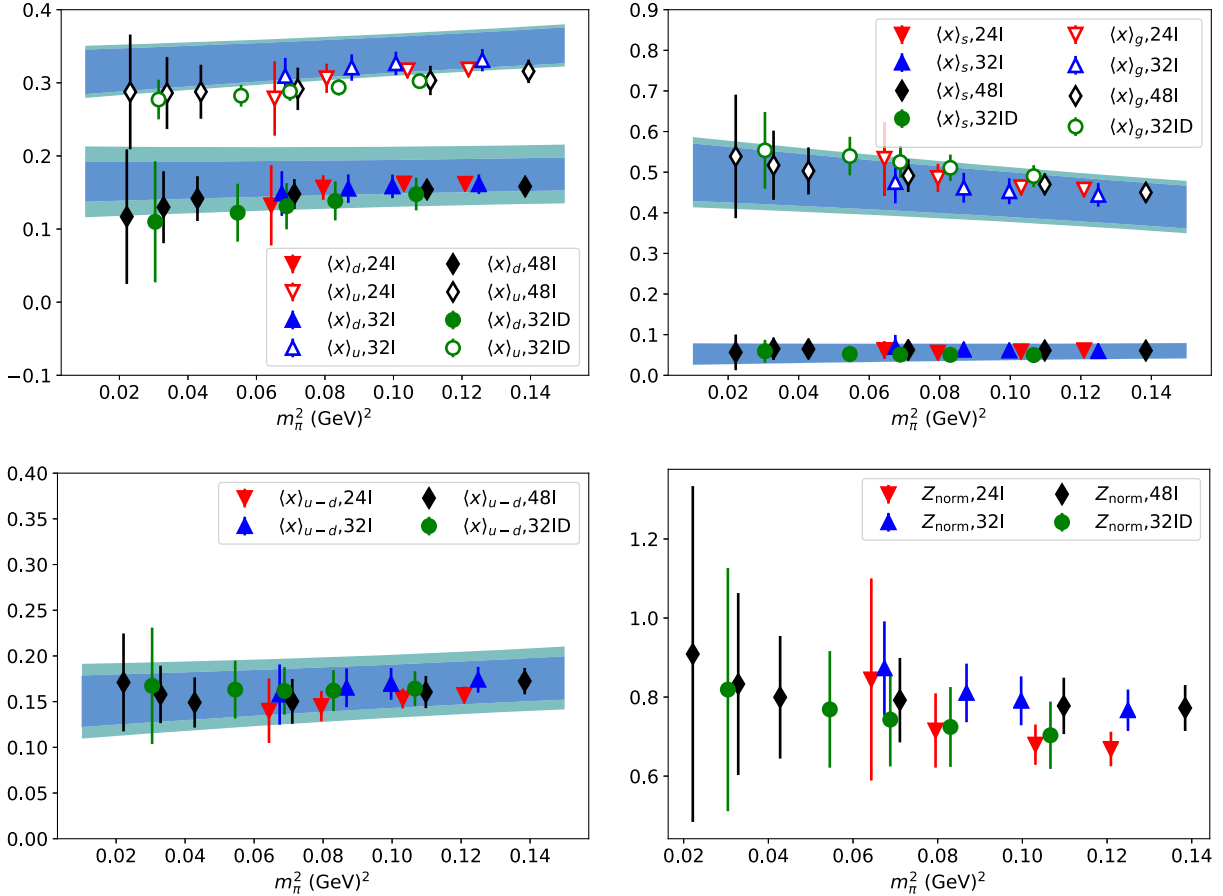


FIG. 2. The momentum fractions of different quark flavors and glue in the proton, at  $\overline{\text{MS}}$  2 GeV. The two upper panels show the  $u$ ,  $d$ ,  $s$ , and  $g$  momentum fractions, respectively, and two lower ones show the  $u-d$  case (left panel), and also the normalization factors for the momentum fraction sum rule (right panel). The bands on the figures show our predictions in the continuum limit of the momentum fractions with their statistical (blue) and total (cyan) uncertainties. The data points correspond to our simulation results at different valence quark masses on different ensembles, with the partially quenching effect subtracted.



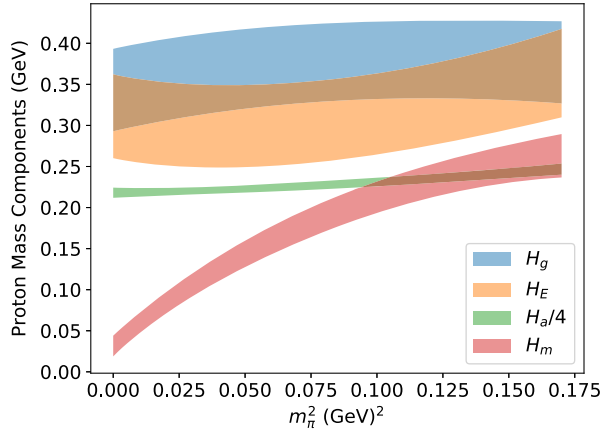


FIG. 3. The valence pion mass dependence of the proton mass decomposition in terms of the quark condensate  $\langle H_m \rangle$ , quark energy  $\langle H_E \rangle$ , glue field energy  $\langle H_g \rangle$ , and trace anomaly  $\langle H_a \rangle/4$ .

*Final proton mass decomposition.*—With these momentum fractions at  $\overline{\text{MS}}$  2 GeV, we can apply Eqs. (6) and (7) to obtain the quark and glue energy contributions in the proton mass (or more precisely, the proton energy in the rest frame). Combined with the quark scalar condensate and trace anomaly contributions, the entire proton mass decomposition is illustrated in Fig. 3 as a function of the valence pion mass. As shown in the figure, the major quark mass dependence comes from the quark condensate term, and the other components are almost independent of the quark mass. At the physical point, the quark and glue energy contributions are 32(4)(4)% and 36(5)(4)% respectively. With the quark scalar condensate contribution of 9(2)(1)% [4], we can obtain that a quarter of the trace anomaly contributes 23(1)(1)% with  $N_f = 2 + 1$ .

In summary, we present a simulation strategy to calculate the proton mass decomposition. The renormalization and mixing between the quark and glue energy can be calculated nonperturbatively, and the quark scalar condensate contribution and the trace anomaly are renormalization group invariant. Based on this strategy, the lattice simulation is carried out on four ensembles with three lattice spacings and volumes, and several pion masses, including the physical pion mass, to control the respective systematic uncertainties. With nonperturbative renormalization and normalization, the individual  $u$ ,  $d$ ,  $s$ , and glue momentum fractions agree with those from the global fit in the  $\overline{\text{MS}}$  scheme at 2 GeV. Quark energy, gluon energy, and quantum anomaly contributions to the proton mass are fairly insensitive to the pion mass up to 400 MeV within our statistical and systematic uncertainties.

We thank the RBC and UKQCD collaborations for providing us their domain wall fermion gauge configurations. Y.Y. is supported by the US National Science Foundation under Grant No. PHY 1653405 “CAREER: Constraining Parton Distribution Functions for

New-Physics Searches.” Y. C. and Z. L. acknowledge the support of the National Science Foundation of China under Grants No. 11575196, No. 11575197, and No. 11335001. This work is partially supported by DOE Grant No. DE-SC0013065 and by the DOE TMD topical collaboration. This research used resources of the Oak Ridge Leadership Computing Facility at the Oak Ridge National Laboratory, which is supported by the Office of Science of the U.S. Department of Energy under Contract No. DE-AC05-00OR22725. This work used Stampede time under the Extreme Science and Engineering Discovery Environment (XSEDE), which is supported by National Science Foundation Grant No. ACI-1053575. We also thank the National Energy Research Scientific Computing Center (NERSC) for providing HPC resources that have contributed to the research results reported within this Letter. We acknowledge the facilities of the USQCD Collaboration used for this research in part, which are funded by the Office of Science of the U.S. Department of Energy.

- 
- [1] X.-D. Ji, *Phys. Rev. Lett.* **74**, 1071 (1995).
  - [2] Y.-B. Yang, Y. Chen, T. Draper, M. Gong, K.-F. Liu, Z. Liu, and J.-P. Ma, *Phys. Rev. D* **91**, 074516 (2015).
  - [3] S. Caracciolo, G. Curci, P. Menotti, and A. Pelissetto, *Ann. Phys. (N.Y.)* **197**, 119 (1990).
  - [4] Y.-B. Yang, A. Alexandru, T. Draper, J. Liang, and K.-F. Liu ( $\chi$ QCD Collaboration), *Phys. Rev. D* **94**, 054503 (2016).
  - [5] Y. Aoki *et al.* (RBC and UKQCD Collaborations), *Phys. Rev. D* **83**, 074508 (2011).
  - [6] T. Blum *et al.* (RBC and UKQCD Collaborations), *Phys. Rev. D* **93**, 074505 (2016).
  - [7] R. S. Sufian, Y.-B. Yang, A. Alexandru, T. Draper, J. Liang, and K.-F. Liu, *Phys. Rev. Lett.* **118**, 042001 (2017).
  - [8] T.-W. Chiu, *Phys. Rev. D* **60**, 034503 (1999).
  - [9] K.-F. Liu, *Int. J. Mod. Phys. A* **20**, 7241 (2005).
  - [10] T.-W. Chiu and S. V. Zenkin, *Phys. Rev. D* **59**, 074501 (1999).
  - [11] A. Li *et al.* ( $\chi$ QCD Collaboration), *Phys. Rev. D* **82**, 114501 (2010).
  - [12] M. Gong *et al.* ( $\chi$ QCD Collaboration), *Phys. Rev. D* **88**, 014503 (2013).
  - [13] Y.-B. Yang, A. Alexandru, T. Draper, M. Gong, and K.-F. Liu, *Phys. Rev. D* **93**, 034503 (2016).
  - [14] A. Hasenfratz and F. Knechtli, *Phys. Rev. D* **64**, 034504 (2001).
  - [15] J. Liang, Y.-B. Yang, K.-F. Liu, A. Alexandru, T. Draper, and R. S. Sufian, *Phys. Rev. D* **96**, 034519 (2017).
  - [16] B. C. Tiburzi, *Phys. Rev. D* **72**, 094501 (2005); **79**, 039904(E) (2009).
  - [17] C. Patrignani *et al.* (Particle Data Group), *Chin. Phys. C* **40**, 100001 (2016).
  - [18] R. Horsley, R. Mollo, Y. Nakamura, H. Perlt, D. Pleiter, P. E. L. Rakow, G. Schierholz, A. Schiller, F. Winter, and J. M. Zanotti (UKQCD, QCDSF), *Phys. Lett. B* **714**, 312 (2012).
  - [19] Y.-B. Yang, R. S. Sufian, A. Alexandru, T. Draper, M. J. Glatzmaier, K.-F. Liu, and Y. Zhao, *Phys. Rev. Lett.* **118**, 102001 (2017).

- [20] K.-F. Liu, J. Liang, and Y.-B. Yang, *Phys. Rev. D* **97**, 034507 (2018).
- [21] Y.-B. Yang, M. Gong, J. Liang, H.-W. Lin, K.-F. Liu, D. Pefkou, and P. Shanahan, [arXiv:1805.00531](https://arxiv.org/abs/1805.00531).
- [22] J. A. Gracey, *Nucl. Phys.* **B667**, 242 (2003).
- [23] Y.-B. Yang, M. Glatzmaier, K.-F. Liu, and Y. Zhao, [arXiv:1612.02855](https://arxiv.org/abs/1612.02855).
- [24] See Supplemental Material at <http://link.aps.org/supplemental/10.1103/PhysRevLett.121.212001> for the details of the calculation and error estimation of the non-perturbative renormalization of the quark and glue energy momentum tensor.
- [25] C. Alexandrou, M. Constantinou, T. Korzec, H. Panagopoulos, and F. Stylianou, *Phys. Rev. D* **83**, 014503 (2011).
- [26] Z. Liu, Y. Chen, S.-J. Dong, M. Glatzmaier, M. Gong, A. Li, K.-F. Liu, Y.-B. Yang, and J.-B. Zhang ( $\chi$ QCD Collaboration), *Phys. Rev. D* **90**, 034505 (2014).
- [27] Y. Bi, H. Cai, Y. Chen, M. Gong, K.-F. Liu, Z. Liu, and Y.-B. Yang, *Phys. Rev. D* **97**, 094501 (2018).
- [28] S. Dulat, T.-J. Hou, J. Gao, M. Guzzi, J. Huston, P. Nadolsky, J. Pumplin, C. Schmidt, D. Stump, and C. P. Yuan, *Phys. Rev. D* **93**, 033006 (2016).
- [29] L. A. Harland-Lang, A. D. Martin, P. Motylinski, and R. S. Thorne, *Eur. Phys. J. C* **75**, 204 (2015).
- [30] H. Abramowicz *et al.* (ZEUS and H1 Collaborations), *Eur. Phys. J. C* **75**, 580 (2015).
- [31] A. Accardi, L. T. Brady, W. Melnitchouk, J. F. Owens, and N. Sato, *Phys. Rev. D* **93**, 114017 (2016).
- [32] S. Alekhin, J. Blümlein, S. Moch, and R. Placakyte, *Phys. Rev. D* **96**, 014011 (2017).
- [33] R. D. Ball *et al.* (NNPDF Collaboration), *Eur. Phys. J. C* **77**, 663 (2017).
- [34] H.-W. Lin *et al.*, *Prog. Part. Nucl. Phys.* **100**, 107 (2018).



# Nonperturbatively renormalized glue momentum fraction at the physical pion mass from lattice QCD

Yi-Bo Yang,<sup>1</sup> Ming Gong,<sup>2</sup> Jian Liang,<sup>3</sup> Huey-Wen Lin,<sup>1</sup> Keh-Fei Liu,<sup>3</sup> Dimitra Pefkou,<sup>4</sup> and Phiala Shanahan<sup>4,5</sup>

( $\chi$ QCD Collaboration)

<sup>1</sup>*Department of Physics and Astronomy, Michigan State University, East Lansing, Michigan 48824, USA*

<sup>2</sup>*Institute of High Energy Physics, Chinese Academy of Sciences, Beijing 100049, China*

<sup>3</sup>*Department of Physics and Astronomy, University of Kentucky, Lexington, Kentucky 40506, USA*

<sup>4</sup>*Department of Physics, College of William and Mary, Williamsburg, Virginia 23187-8795, USA*

<sup>5</sup>*Thomas Jefferson National Accelerator Facility, Newport News, Virginia 23606, USA*

 (Received 9 May 2018; revised manuscript received 20 August 2018; published 12 October 2018)

We present the first nonperturbatively renormalized determination of the glue momentum fraction  $\langle x \rangle_g$  in the nucleon, based on lattice-QCD simulations at the physical pion mass using the cluster-decomposition error reduction technique. We provide the first practical strategy to renormalize the gauge energy-momentum tensor nonperturbatively in the regularization-independent momentum-subtraction (RI/MOM) scheme and convert the results to the  $\overline{\text{MS}}$  scheme with one-loop matching. The simulation results show that the cluster-decomposition error reduction technique can reduce the statistical uncertainty of its renormalization constant by a factor of  $\mathcal{O}(300)$  in calculations using a typical state-of-the-art lattice volume, and the nonperturbatively renormalized  $\langle x \rangle_g$  is shown to be independent of the lattice definitions of the gauge energy-momentum tensor up to discretization errors. We determine the renormalized  $\langle x \rangle_g^{\overline{\text{MS}}}(2 \text{ GeV})$  to be 0.47(4)(11) at the physical pion mass, which is consistent with the experimentally determined value.

DOI: [10.1103/PhysRevD.98.074506](https://doi.org/10.1103/PhysRevD.98.074506)

## I. INTRODUCTION

A longstanding problem raised by deep-inelastic scattering and Drell-Yan experiments on the nucleon is that the gluons contribute almost as large a fraction of the nucleon momentum as the quarks [1,2], contradicting the naive quark model. The momentum fractions of the quarks and glue equal the second moments of their respective parton distribution functions (PDFs)  $f_p(x)$  ( $p = u, \bar{u}, d, \bar{d}, s, \dots, g$ ),

$$\langle x \rangle_p = \int_0^1 dx x f_p(x), \quad (1)$$

where the PDF can be determined from global fits of experimental results with certain assumptions about their functional forms. The recent CT14NNLO global PDF fit [2] yields  $\langle x \rangle_g^{\overline{\text{MS}}}(2 \text{ GeV}) = 0.42(2)$ , and the value at the TeV scale will be around 0.5, which is irrespective of its value at

lower scales. Besides the importance in understanding the nucleon momentum, the value of  $\langle x \rangle_g$  is also an important input to obtain the glue contributions to the nucleon mass and spin [3,4], so calculating it from a first-principle lattice-QCD simulation is of fundamental interest, in addition to providing an independent input and check of the experimental PDF determinations.

Lattice calculations of  $\langle x \rangle_g$  in the nucleon [4–7] have been significantly refined in the last ten years. However, values of  $\langle x \rangle_g^{\overline{\text{MS}}}(2 \text{ GeV})$  vary widely; two quenched calculations found 0.43(9) and 0.33(6) [4,5], and recent dynamical  $N_f = 2$  calculation obtained 0.267(22)(30) [6,7].

The recent quenched (Refs. [4,5]) and dynamical (Refs. [6,7]) lattice calculations of  $\langle x \rangle_g$  used different lattice definitions of the gauge energy-momentum tensor (EMT) with the one-loop renormalization based on the lattice perturbation theory (LPT). It is known that LPT is poorly convergent at one-loop level without smearing of the gauge EMT [8,9], and LPT calculations beyond one-loop level are extremely difficult. Whether smearing of the gauge EMT can improve the convergence of LPT remains an open question, but it was found in Ref. [10] that hypercubic (HYP) smearing [11] of the glue operator can change the bare glue matrix

*Published by the American Physical Society under the terms of the [Creative Commons Attribution 4.0 International](https://creativecommons.org/licenses/by/4.0/) license. Further distribution of this work must maintain attribution to the author(s) and the published article's title, journal citation, and DOI. Funded by SCOAP<sup>3</sup>.*

element by a factor of  $\sim 3$ . Nonperturbative renormalization (NPR) of  $\langle x \rangle_g$  is thus essential to check whether different lattice definitions of the gauge EMT and smearing can provide a consistent prediction of  $\langle x \rangle_g$ .

In this work, we present the first NPR of the gauge EMT using the cluster-decomposition error reduction (CDER). We confirm that nonperturbatively renormalized  $\langle x \rangle_g$  is independent of the lattice definition of the gauge EMT and whether the HYP smearing is applied to it.

The glue NPR technique that we introduce will be applicable for the quantities beyond the  $\langle x \rangle_g$ . State-of-the-art calculations of the glue spin contribution to the proton spin [10] and the glue transversity in hadrons [12] have been presented recently; the renormalization of the glue operators in these calculations are determined at the one-loop level or neglected entirely. Approaches that target the entire glue PDF instead of the moments, like large-momentum effective theory [13] and the lattice cross section approach [14], have been explored recently. NPR will be also essential to obtain accurate predictions for those quantities.

In the rest of the paper, we will start from the simulation strategy of NPR in Sec. II. Then, in Sec. III, this strategy is tested in several cases including the quenched, 2-flavor, and  $2 + 1$ -flavor ones. Based on those tests, a prediction of the renormalized  $\langle x \rangle_g$  is provided in Sec. IV, with controllable systematic uncertainties from NPR. Our findings in this work are summarized in Sec. V, and the additional discussion on the cases with more than one step of HYP smearing is presented in the Appendix.

## II. NPR SIMULATION STRATEGY

At tree level, the gauge EMT  $\bar{T}_{g,\mu\nu} \equiv F_{\mu\rho}F_{\nu\rho} - \frac{1}{4}g_{\mu\nu}F^2$  includes nine Lorentz structures,

$$\begin{aligned} \bar{T}_{g,\mu\nu}^{(0)} = & (2p_\mu p_\nu g_{\rho\tau} - p_\mu p_\rho g_{\nu\tau} + p^2 g_{\rho\mu} g_{\nu\tau} - p_\tau p_\nu g_{\rho\mu} \\ & - p_\nu p_\rho g_{\mu\tau} + p^2 g_{\rho\nu} g_{\mu\tau} - p_\tau p_\mu g_{\rho\nu} \\ & + g_{\mu\nu}(p_\tau p_\rho - p^2 g_{\tau\rho})) A_\rho(p) A_\tau(-p), \end{aligned} \quad (2)$$

where  $\mu$  and  $\nu$  denote the external Lorentz indices of the EMT and  $\rho$  (or  $\tau$ ) is the Lorentz index of the external gluon state  $A_{\rho/\tau}$ . As discussed in Ref. [15],  $2p_\mu p_\nu g_{\rho\tau}$  is the only structure free of mixing with the unphysical terms of the gauge EMT (gauge dependent term and ghost term) and is thus the best choice to consider the renormalization of the gauge EMT without the mixing calculation with unphysical terms.

While taking the physical condition  $p_\rho = p_\tau = 0$ ,  $p^2 = 0$  [15] in the Minkowski space will isolate this term, the on-shell condition  $p^2 = 0$  is not satisfied on the lattice. One can, however, choose other conditions on the lattice to isolate this term. More precisely, the RI/MOM renormalization constant of the off-diagonal pieces of the gauge

EMT at the renormalization scale  $\mu_R^2 = p^2$  can be defined using the following approach, which is analogous to that commonly used for the quark bilinear operators [16],

$$\begin{aligned} Z^{-1}(\mu_R^2) &= \left( \frac{N_c^2 - 1}{2} Z_g^{\text{RI}}(\mu_R^2) \right)^{-1} \\ &\times \frac{V \langle \bar{T}_{g,\mu\nu} \text{Tr}[A_\rho(p) A_\rho(-p)] \rangle}{2p_\mu p_\nu \langle \text{Tr}[A_\rho(p) A_\rho(-p)] \rangle^2} \bigg|_{\substack{p^2=\mu_R^2, \\ \rho \neq \mu \neq \nu, \\ p_\rho=0}} \\ &= \frac{p^2 \langle \bar{T}_{g,\mu\nu} \text{Tr}[A_\rho(p) A_\rho(-p)] \rangle}{2p_\mu p_\nu \langle \text{Tr}[A_\rho(p) A_\rho(-p)] \rangle^2} \bigg|_{\substack{p^2=\mu_R^2, \\ \rho \neq \mu \neq \nu, \\ p_\rho=0}}, \end{aligned} \quad (3)$$

where the index  $\rho$  is not summed and  $V$  is the physical volume of the lattice. The final expression on the right-hand side of Eq. (3) does not depend on the renormalization constant

$$Z_g^{\text{RI}} \frac{\langle \text{Tr}[A_\rho(p) A_\rho(-p)] \rangle}{V} = \frac{N_c^2 - 1}{2} \frac{1}{p^2} \quad (4)$$

in the RI/MOM scheme, as it is cancelled by the inverse of the  $\langle \text{Tr}[A_\rho(p) A_\rho(-p)] \rangle$  in its definition.

The Landau gauge-fixed gluon field  $A_\rho(p)$  used above is defined from the gauge links  $U_\mu(x)$  as

$$A_\rho(p) = a^4 \sum_x e^{ip \cdot (x + \frac{1}{2}\hat{\rho})} \left[ \frac{U_\rho(x) - U_\rho^\dagger(x)}{2ig_0 a} \right]_{\text{traceless}}. \quad (5)$$

Note that, even though the operator  $\bar{T}$  may be HYP smeared, no smearing will be applied to the gauge field  $A_\rho(p)$ , since the gauge action is not smeared and no reweighting is applied to the configurations. Similarly, the RI/MOM renormalization constants of the traceless diagonal pieces of the gauge EMT can be defined by

$$Z_T^{-1}(\mu_R^2) = \frac{p^2 \langle (\bar{T}_{\mu\mu} - \bar{T}_{\nu\nu}) \text{Tr}[A_\rho(p) A_\rho(-p)] \rangle}{2p_\mu^2 \langle \text{Tr}[A_\rho(p) A_\rho(-p)] \rangle^2} \bigg|_{\substack{p^2=\mu_R^2, \\ \rho \neq \mu \neq \nu, \\ p_\rho=0, \\ p_\nu=0}}. \quad (6)$$

The bare lattice gauge EMT can be defined by the clover definition of the field tensor  $F_{\mu\nu}$  [4,5],

$$\begin{aligned} \bar{T}_{g,\mu\nu}^{(a)} &= 2a^4 \sum_x \text{Tr} \left[ F_{\mu\rho} F_{\nu\rho} - \frac{1}{4} g_{\mu\nu} F^2 \right] (x), \\ F_{\mu\nu}(x) &= \frac{i}{8a^2 g} [\mathcal{P}_{[\mu,\nu]} + \mathcal{P}_{[\nu,-\mu]} + \mathcal{P}_{[-\mu,-\nu]} + \mathcal{P}_{[-\nu,\mu]}] (x), \end{aligned} \quad (7)$$

where the plaquette  $\mathcal{P}_{\mu,\nu}(x) = U_\mu(x) U_\nu(x + a\hat{\mu}) U_\mu^\dagger(x + a\hat{\nu}) U_\nu^\dagger(x)$  with  $U_{-\nu}(x) = U_\nu^\dagger(x - a\hat{\nu})$  and  $P_{[\mu,\nu]} \equiv P_{\mu,\nu} - P_{\nu,\mu}$ . The bare traceless diagonal component  $\bar{T}_{g,\mu\mu}$  also has a simpler definition (the plaquette definition) [6,7]:

$$\bar{T}_{g,\mu\mu}^{(b)} = \frac{-4}{g^2} \left( \sum_{\nu \neq \mu, x} \text{Tr}[\mathcal{P}_{\mu,\nu}(x)] - \frac{1}{4} \sum_{\rho \neq \nu, x} \text{Tr}[\mathcal{P}_{\rho,\nu}(x)] \right). \quad (8)$$

Different definitions and choices of smearing on the links  $U_\mu(x)$  in these definitions of  $\bar{T}_g$  yield different bare hadron matrix elements, but the renormalized results should agree up to  $\mathcal{O}(a^2)$  correction.

After the renormalization constant  $Z^{-1}(\mu_R^2)$  is obtained perturbatively or nonperturbatively under the lattice regularization at  $\mu_R^2 = p^2$ , the matching factor to convert the result to the  $\overline{\text{MS}}$  scheme should be calculated using dimensional regularization. At the  $\mu_R$  used in this work, the one-loop corrections to match the  $\overline{\text{MS}}$  scheme at 2 GeV are at a few percent level [17]. The mixing with the quark EMT is also small [17] and will be considered as a systematic uncertainty; more detailed discussions of the matching and mixing effects can also be found there.

Calculation of the correlation function

$$C_3(p) = \langle \bar{T}_{\mu\nu} \text{Tr}[A_\rho(p)A_\rho(-p)] \rangle \\ = \left\langle \int d^4x d^4y d^4z e^{ip(x-y)} \bar{T}_{\mu\nu}(z) \text{Tr}[A_\rho(x)A_\rho(y)] \right\rangle \quad (9)$$

is numerically challenging, even when the gluon propagator has been determined at better than the 1% level. Figure 1 illustrates this difficulty: the light-colored bands in the background show the direct calculations of  $Z_T^{-1}(a^2\hat{p}^2 \equiv 4\sum_\mu \sin^2 \frac{ap_\mu}{2})$  (with the condition that two components of  $p$  are zero and  $\sum_\mu p_\mu^4 / (\sum_\mu p_\mu^2)^2 < 0.55$ ) based on the definition in Eq. (9), on 356 configurations of the 2 + 1-flavor RBC/UKQCD domain-wall fermion Iwasaki gauge ensemble “48I” with lattice spacing  $a = 0.114$  fm,  $m_\pi = 140$  MeV and lattice volume  $L^3 \times V = 48^3 \times 96$

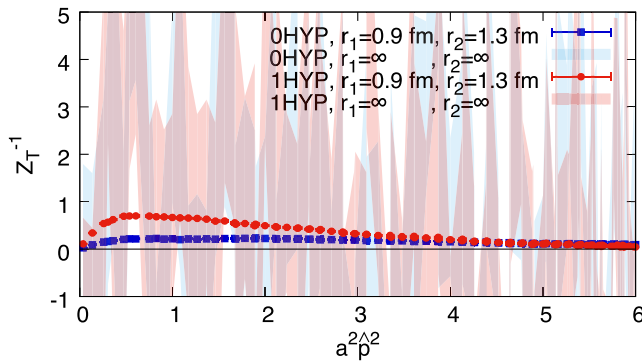


FIG. 1. The glue operator renormalization constants  $Z_T^{-1}$  in  $\overline{\text{MS}}$  at 2 GeV with and without CDER (i.e., cutoffs on the distance between the gauge fields/operator). Without CDER, the errors are large, and the signal cannot be resolved (bands in the background). The errors can be reduced by a factor of  $\sim 300$  with  $r_1 = 0.9$  fm,  $r_2 = 1.3$  fm, shown by the red dots (blue boxes) for  $Z_T^{-1}$  with (without) HYP smearing.

( $L = 5.5$  fm) [18]. The statistical uncertainties are very large, and  $Z_T^{-1}$  cannot be resolved at any scale.

However, we can apply the CDER technique to reduce the errors [19]. The cluster-decomposition principle enunciates that correlators fall off exponentially in the distance between operator insertions and implies that integrating the correlator over this distance beyond the correlation length will only garner noise and not signal. The CDER technique will cut off the volume integral beyond a characteristic length, and then one can gain a factor of  $\sqrt{V}$  in the signal-to-noise ratio [19]. Applying CDER to  $C_3(p)$  in Eq. (9) introduces two cutoffs,  $r_1$  between the glue operator and one of the gauge fields and  $r_2$  between the gauge fields in the gluon propagator, and then leads to the cutoff correlator:

$$C_3^{\text{CDER}}(p) \equiv \left\langle \int_{|r|<r_1} d^4r \int_{|r'|<r_2} d^4r' \int d^4x \right. \\ \left. \times e^{ip \cdot r'} \bar{T}_{\mu\nu}(x+r) \text{Tr}[A_\rho(x)A_\rho(x+r')] \right\rangle. \quad (10)$$

For example, with cutoffs  $r_1 = 0.9$  fm,  $r_2 = 1.3$  fm, the statistical uncertainty can be reduced by a factor of approximately 300. This is close to the square root of  $V^2$  over the product of four-dimensional spheres with radii  $r_1$  and  $r_2$ ,  $2V/(\pi^2 r_1^2 r_2^2) \simeq 263$ . Using these parameters, a very clear signal can be resolved, shown as the red dots and blue boxes in Fig. 1, for  $Z_T^{-1}$  with and without HYP smearing, respectively. The values of  $Z_T^{-1}$  differ by a factor of  $\sim 3$  for the calculations with or without the HYP smearing, at  $a^2\hat{p}^2 \sim 1$ .

A naive cost estimate for the partial triple sum on the volume  $V$  in Eq. (10) is  $\mathcal{O}(V r_1^4 r_2^4)$ , but the practical cost can be reduced to  $\mathcal{O}(V \log V)$  by applying the fast Fourier transform several times [19] using the following strategy:

- (1) Construct  $O'_{\mu\nu}(x) = \int_{|r'|<r_2} d^4r' \bar{T}_{\mu\nu}(x+r')$  by Fourier transforming  $\bar{T}_{\mu\nu}(x)$  and  $f(x) = \theta(r_2 - |x|)$ , multiply the transformed functions together in momentum space, and then perform the anti-Fourier transform.
- (2) Calculate  $B'_{\rho\mu\nu}(x) = A_\rho(x) \bar{T}'_{\mu\nu}(x)$ .
- (3) Apply the cluster decomposition to  $\int d^4x d^4y e^{ip \cdot (x-y)} B'_{\rho\mu\nu}(x) A_\rho(y)$  [19]: perform the Fourier transform (FT) for both  $A$  and  $B$ , applying the anti-FT to  $A(p)B(-p)$ ; apply the cut  $g(x) = \theta(r_1 - |x|)$  in coordinate space; and then FT the product.

The CDER with symmetric cutoffs

$$C_3(p) \approx \left\langle \int_{|r|<r_1} d^4r \int_{|r''|<r_3} d^4r'' \int d^4x \right. \\ \left. \times e^{ip \cdot (r+r'')} \bar{T}_{\mu\nu}(x) \text{Tr}[A_\rho(x-r)A_\rho(x+r'')] \right\rangle \quad (11)$$

can also be efficient if a  $V \log V$  implementation can be obtained.

### III. TESTS ON CDER

Since the number of configurations in the 48I ensemble at  $m_\pi = 140$  MeV is limited, we turn to three ensembles with smaller volume and larger statistics to check the systematic uncertainties of the CDER approach. To reduce statistical uncertainties then provide a stronger check, we will apply one step of HYP smearing on the gauge EMTs used in this section.

#### A. Quenched ensemble 24Q

We calculated  $Z(1\text{-HYP})$  without CDER on decorrelated 70,834 configurations of a quenched Wilson gauge ensemble “24Q” with  $a = 0.098$  fm and  $L^3 \times V = 24^3 \times 64$  and compared them with those on 708 of the 70,834 configurations (pick 1 per 100 configuration numbers) with CDER. The CDER results with  $r_1 \geq 0.8$  fm and  $r_2 \geq 1.1$  fm agree with the CDER-free results for all  $a^2 \hat{p}^2$ . Figures 2–4 show the  $Z^{-1}$  and  $Z_T^{-1}$  results with  $a^2 \hat{p}^2 = 2.00$ , 2.48, and 3.00, respectively. In those figures, the red bands show the results on 70,834 configurations without CDER, and the black boxes show the results with  $r_1 = 0.7 \times r_2 = R$  agree with

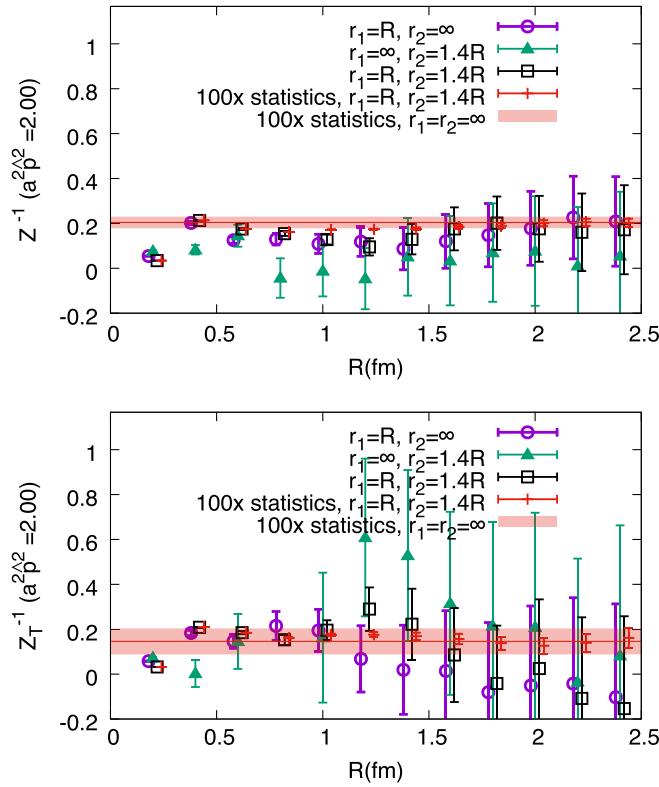


FIG. 2. The cutoff  $R$  dependence for  $r_{1,2}$  of the renormalization constant  $Z^{-1}(2 \text{ GeV})$  and  $Z_T^{-1}(2 \text{ GeV})$  on the 24Q ensemble with  $a^2 p^2 = 2.00$ . Calculations on 300 configurations with  $r_1 \geq 0.7$  fm and  $r_2 \geq 1.0$  fm are consistent with those using 70,834 configurations without any cutoff. The result is less sensitive to the cutoff  $r_1$  than  $r_2$ ; thus, most of the variance reduction comes from reducing  $r_1$ , while reducing  $r_2$  is also useful. The green/black/red data are shifted horizontally to enhance legibility.

the red bands for all the  $R$ 's not smaller than 0.7 fm. Results with the cutoff on either  $r_1$  or  $r_2$  set to  $\infty$  (the green triangles and purple dots) are also shown in the figures, and it is obvious from the leftmost data points that the cutoff effects on  $r_2$  are as strong as those on  $r_1$  when  $r_1 = 0.7 \times r_2$ . Thus, setting the  $r_{1,2}$  with this relation can be a proper choice to simplify the parameter tuning. The results also demonstrate that cutoffs on either  $r_1$  or  $r_2$  also reduce the statistical uncertainties of  $Z^{-1}$ . As shown in Figs. 2–4, the full-statistics CDER results (red crosses) actually saturate at  $R > 0.8$  fm or so and are consistent with both the full-statistics non-CDER results and the 1%-statistics CDER results as expected.

#### B. Two-flavor ensembles 24C/12C

We also studied the dynamical case. We calculated  $Z^{-1}(1\text{-HYP})$  with CDER on 2,123 configurations of the two-flavor clover fermion Lüscher-Weisz gauge ensemble “24C” with lattice spacing  $a = 0.117$  fm,  $m_\pi = 450$  MeV, and  $L^3 \times V = 24^3 \times 64$  [20]. For comparison, we repeat the calculation of  $Z^{-1}$  on 21,166 configurations on the 12C ensemble (with the same lattice setup as 24C except a smaller volume  $12^3 \times 24$ ) without CDER. Figure 5 shows similar  $R$ -dependence plots for the dynamical case with 24C and 12C lattices ( $a = 0.117$  fm,  $m_\pi = 450$  MeV,  $L^3 \times V$  equal to  $24^3 \times 64$  and  $12^3 \times 24$ , respectively).

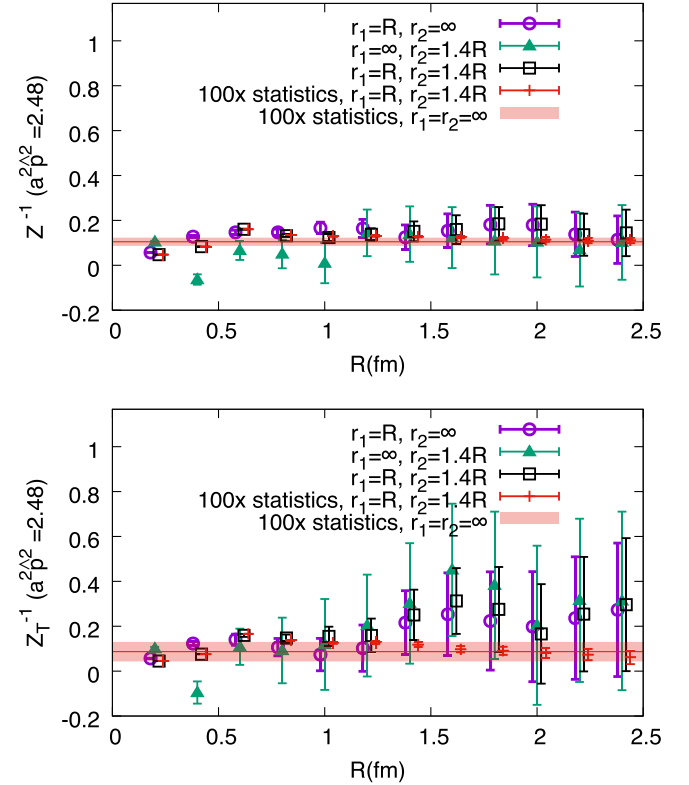


FIG. 3. The cutoff  $R$  dependence of the renormalization constant  $Z^{-1}(2 \text{ GeV})$  and  $Z_T^{-1}(2 \text{ GeV})$  on the 24Q ensemble with  $a^2 p^2 = 2.48$ .

Candidate (name, affiliation, curriculum vitae including the date of the degree of Ph.D., nationality, address, email and telephone)

Curriculum Vitae of

***Jun Zhao***

***Citizenship:*** China

***Current Appointments:***

Xie Xide Junior Chair Professor, Dept. of Physics, Fudan University, Shanghai, China (from 2014)

***Past Appointments:***

Professor, Dept. of Physics, Fudan University, Shanghai (2012-2014)

Miller Research Fellow, University of California at Berkeley (2010-2012)

***Education:***

Dept. of Physics and Astronomy, the University of Tennessee, Knoxville (August 2005 - May 2010)

Degree: Ph.D. in Physics (May, 2010)

Thesis: Neutron Scattering Study of High Temperature Superconductors

Advisor: Professor Pengcheng Dai

Institute of Physics, Chinese Academy of Sciences, Beijing, China (September 2002 to July 2005)

Degree: M.S. in Physics

Advisor: Professor Zhongxian Zhao

Physics Department, Tsinghua University, Beijing, China (September 1998 - July 2002)

Degree: B. S. in Physics

***HONORS AND AWARDS:***

Sir Martin Wood China Prize (2018)

Wanren Program Leading Scientist, Department of Organization, China (2018)

Chang Jiang Distinguished Professor, Ministry of Education, China (2017)

Qiushi Outstanding Young Scholar Award, Qiushi Foundations, Hong Kong (2014)

Pujiang Scholar Award, City of Shanghai, China (2013)

Thousand Young Talents Investigator Award, Department of Organization, China (2012)

Miller Fellowship, University of California, Berkeley (2010-2012)



Outstanding Dissertation in Magnetism Award (for doctoral thesis of outstanding quality and achievements in magnetism), American Physical Society (2010)

Address:

Advanced Materials Laboratory 435, 2205 Songhu Rd.

Shanghai 200438, China

Tel: +86-15921879158

E-mail: zhaoj@fudan.edu.cn

Website: <http://jzhao.fudan.edu.cn/>

Publication Citations:

<https://scholar.google.com/citations?hl=en&user=Ue1WSaYAAAAJ>

Citation for the Award (within 30 words)

The elucidation of magnetic properties of iron-based superconductors.

Description of the work

The discovery of iron-based high temperature superconductors (iron pnictides and iron chalcogenides) opened a new avenue of research that could help to unravel one of the biggest mysteries in condensed matter physics—the mechanism of high temperature superconductivity. Prof. Jun Zhao has made outstanding contributions in understanding magnetic correlations and their relationship to high temperature superconductivity in iron-based materials.

Shortly after the discovery of the iron-based superconductors, Prof. Jun Zhao and his collaborators used neutron powder diffraction to study the magnetic and structural phase diagram for iron pnictides. They discovered that the electronic phase diagram of the iron pnictides is very similar to that of the cuprates. Like the cuprates, the parent compounds of the iron pnictides are antiferromagnets, where superconductivity arises from the proximity of the antiferromagnetic ground state through chemical doping. To understand the nature of the antiferromagnetic ground state of the parent compounds, Prof. Jun Zhao and collaborators used inelastic neutron scattering to map out the entire energy spectrum of spin wave excitations in the parent compounds of iron pnictides. They solved the effective magnetic exchange Hamiltonian and found that the magnetic interactions are anisotropic in the  $ab$  plane, which suggests the presence of magnetic nematicity; in addition, they found that the magnetism in iron pnictides has both local moment and conduction electron characters. Recently, Prof. Zhao's group also used inelastic neutron scattering to show that the structurally simplest iron-chalcogenide superconductor FeSe displays both spin fluctuations at two different wavevectors  $(\pi,0)$  and  $(\pi,\pi)$ , both of which are coupled with nematicity, indicating that FeSe is a novel nematic quantum paramagnet. The elucidation of the interplay between spin fluctuations, nematicity and superconductivity in these materials are important for establishing the mechanism behind high temperature superconductivity.



In addition to the work described above, Prof. Zhao's group has been active in studying the magnetic correlations in complex magnetic materials, such as the spin liquids, hidden-order materials and heli-magnetic superconductors. Very recently, Prof. Zhao's group reported neutron scattering measurements that reveal continuous spinon excitations and hidden order quantum excitations in the triangular-lattice antiferromagnets  $\text{YbMgGaO}_4$  and  $\text{TmMgGaO}_4$ , respectively. Moreover, Prof. Zhao's group discovered that, for the first time, a spin re-orientation transition coincides with the occurrence of superconductivity in the exotic heli-magnetic superconductor  $\text{CrAs}$ .

Prof Jun Zhao's works have had a large impact in the condensed matter physics community. I strongly recommend him for the Nishina Asia Award without any reservations.

Key references (up to 3 key publications\*)

1. Structural and magnetic phase diagram of  $\text{CeFeAsO}_{1-x}\text{F}_x$  and its relationship to high-temperature superconductivity

Jun Zhao, Q. Huang, C. de la Cruz, S. Li, J. W. Lynn, Y. Chen, M. A. Green, G. F. Chen, G. Li, Z. Li, J. L. Luo, N. L. Wang, Pengcheng Dai,  
Nature Materials 75, 953-959 (2008)

2. Strong interplay between stripe spin fluctuations, nematicity and superconductivity in FeSe.

Qisi Wang, Yao Shen, Bingying Pan, Yiqing Hao, Mingwei Ma, Fang Zhou, P. Steffens, K. Schmalzl, T. R. Forrest, M. Abdel-Hafiez, Xiaojia Chen, D. A. Chareev, A. N. Vasiliev, P. Bourges, Y. Sidis, Huibo Cao and Jun Zhao.  
Nature Materials 15, 159-163 (2016)

3. Magnetic ground state of FeSe

Qisi Wang, Yao Shen, Bingying Pan, Xiaowen Zhang, K. Ikeuchi, K. Iida, A. D. Christianson, H. C. Walker, D. T. Adroja, M. Abdel-Hafiez, Xiaojia Chen, D. A. Chareev, A. N. Vasiliev and Jun Zhao  
Nature Communications 7, 12182 (2016)

\*) Copy of one most significant publication should be attached.

Nominator (name, affiliation, email, telephone and relation to the candidate)

Yuanbo Zhang

Professor of Physics, Fudan University, China

zhyb@fudan.edu.cn

Phone: +86-18616137929

Relation to the candidate: Colleague at Fudan University

Signature:

A handwritten signature in black ink, appearing to be 'Zhang' followed by a stylized surname.

Date: 2019/03/29

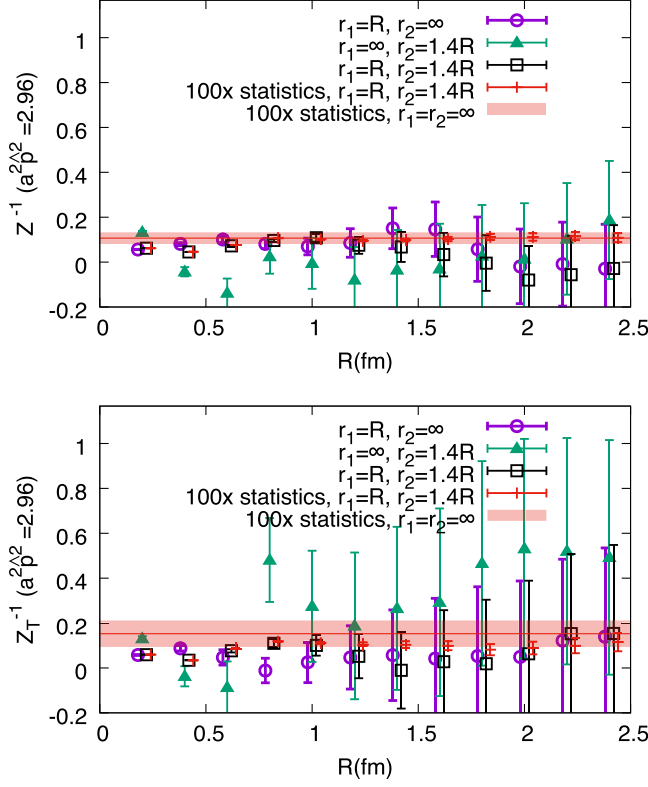


FIG. 4. The cutoff  $R$  dependence of the renormalization constant  $Z^{-1}(2 \text{ GeV})$  and  $Z_T^{-1}(2 \text{ GeV})$  on the 24Q ensemble with  $a^2 p^2 = 2.96$ .

The red bands show the results on 21,166 configurations without any cutoff, and the data points show the CDER results. They are all consistent for all the  $R$ 's not smaller than 0.9 fm. The uncertainty of the full-statistics CDER results are not much smaller than the non-CDER ones since the volume is too small to make the CDER efficient.

For the cutoffs on the radii  $r_1$  and  $r_2$ , they should correspond to the respective correlation lengths between the relevant operators.  $r_1$  is between the gauge field and the EMT operator. Taking the vector meson  $\omega(780)$  as an estimate, the correlation length  $3/m_\omega \sim 0.76 \text{ fm}$  (at three times the Compton wavelength, the Yukawa potential has fallen by 95%) is close to 0.9 fm that we take for  $r_1$ . On the other hand, the gluon has a “dynamical mass”  $m_g \sim 550 \text{ MeV}$  in the small momentum region [21,22]. This gives an estimate of the correlation length of  $3/m_g \sim 1.2 \text{ fm}$ , which is close to the 1.3 fm cutoff used for  $r_2$ .

As in Fig. 6, we should choose  $r_1 \geq 0.9 \text{ fm}$  and  $r_2 \geq 1.3 \text{ fm}$  on 24C (black crosses) to get the results consistent with those on 12C without CDER (the red boxes). If we fit the CDER result of  $Z^{-1}$  on 24C with a polynomial form including  $a^{2n} \hat{p}^{2n}$  ( $n \leq 2$ ) terms in the range  $a^2 \hat{p}^2 \in [1.5, 5]$ , the result is 2.63(5) with  $\chi^2/\text{d.o.f.} = 0.80$ . Figure 6 also shows  $Z^{-1}(1\text{-HYP})$  with either smaller  $r_1$  (the purple band) or  $r_2$  (the green band). These two cases have distinct systematic bias in the form of oscillation in  $a^2 \hat{p}^2$  although

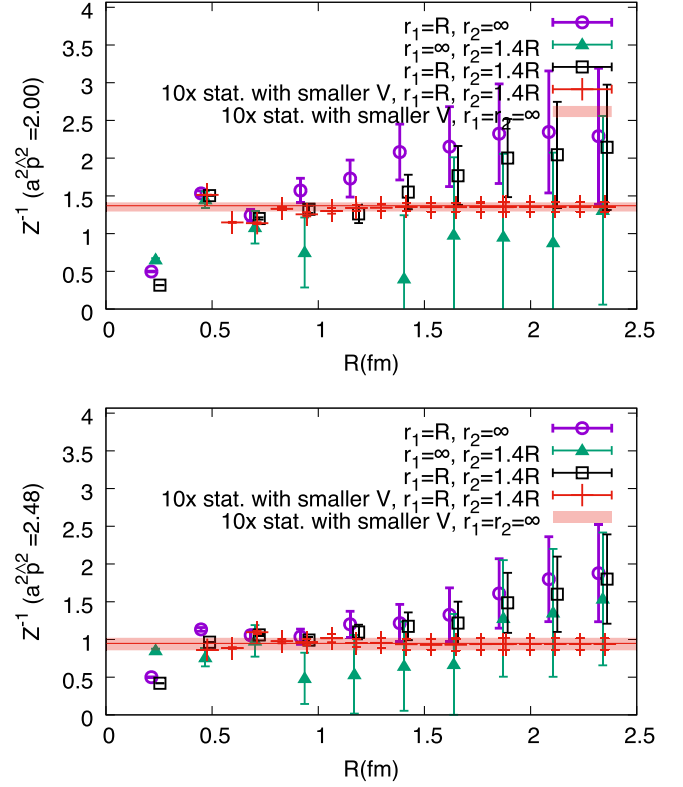


FIG. 5. The cutoff  $R$  dependence of the renormalization constant  $Z^{-1}(2 \text{ GeV})$  on the 24C/12C ensembles with  $a^2 p^2 = 2.00$  and 2.48.

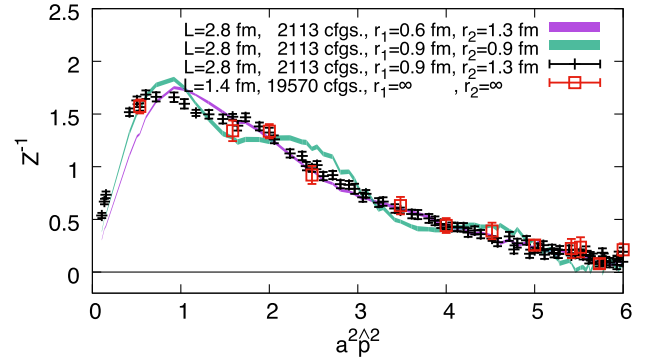


FIG. 6. The  $\overline{\text{MS}}$  renormalization constant  $Z^{-1}(2 \text{ GeV})$  on the 24C ensemble as a function of  $a^2 \hat{p}^2$ , with different cutoffs on the gluon field-operator correlation ( $r_1$ ) and propagator ( $r_2$ ). A high-statistics calculation without cutoff on a lattice with smaller volume but the same parameters is also presented (red boxes) for comparison.

the statistical uncertainties are smaller. If we fit the corresponding data with previous fitting setup, the  $\chi^2/\text{d.o.f.}$  will be 6.1 and 28.9 in two cases respectively and then are not acceptable. Thus, whether  $\chi^2/\text{d.o.f.}$  is around 1 can provide consistent criteria on the systematic uncertainties introduced by CDER, especially in the case (likes 48I) we cannot resolve any signal without CDER.

### C. 2+1-flavor ensembles 48I

Before the end of this section, a few  $R$ -dependence tests on 48I, the ensemble we will use for the final result, are provided in Fig. 7.

In the upper panel of Fig. 7, the  $Z_T^{-1}$  (2 GeV) case with  $a^2\hat{p}^2 = 2.00$  is presented using a similar style as the previous plots in this section, while the bands are based on the results with the CDER cutoffs  $r_1 = 0.7 \times r_2 = 0.9$  fm. It is obvious that the cutoffs on  $r_{1,2}$  are necessary as the errors with either an  $r_1$  or  $r_2$  cutoff only are very large. The central panel of Fig. 7 shows the cutoff  $R$  dependence with  $r_1 = 0.7 \times r_2 = R$  at  $a^2\hat{p}^2 = 2.00, 2.48, 2.97$ , and  $3.48$ . All the data points with  $R > 0.9$  fm are consistent with the band based on the data point at  $R = 0.9$ . In the lower panel

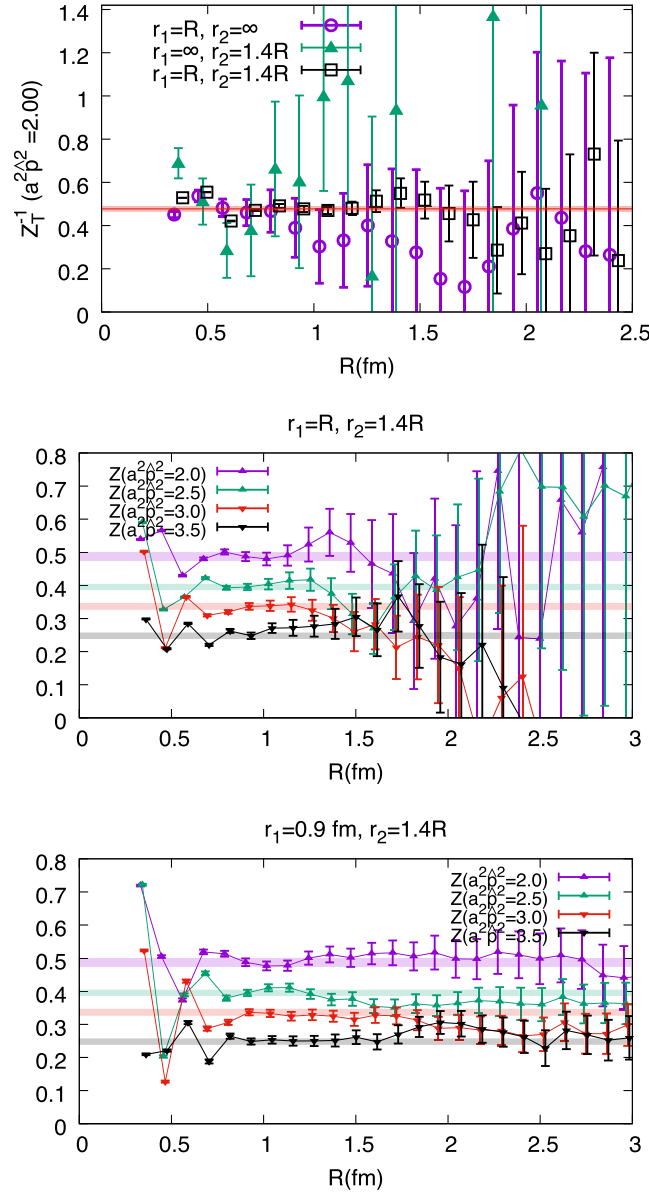


FIG. 7. The cutoff  $R$  dependence of the renormalization constant  $Z_T^{-1}$  (2 GeV) on the 48I ensemble.

of Fig. 7, the cutoff  $R = 0.7 \times r_2$  dependences at different  $a^2\hat{p}^2$  are presented with fixed  $r_1 = 0.9$  fm. Thus, the uncertainty with larger  $r_2$  is smaller, and then consistency is more obvious. As an estimate of the systematic uncertainty due to the choice of  $r_2$ , we take the 2% fluctuation of the gluon propagator at  $r_2 = 1.3$  fm as the systematic error in our final prediction.

### IV. RENORMALIZED $\langle x \rangle_g$ ON 48I

Given the success of CDER in resolving a clean signal of  $Z_T^{-1}$ , it is nevertheless important to confirm that the renormalized  $\langle x \rangle_g$  is independent of the lattice definition of  $\bar{T}_g$  or whether the HYP smearing is applied, up to  $\mathcal{O}(a^2)$  corrections. Figure 8 gives the CDER results on the 48I ensemble as the functions of  $a^2\hat{p}^2$ . The red dots and blue boxes show  $Z_T^{-1}$  with and without HYP smearing, respectively, using the clover definition in Eq. (7); the green triangles show the HYP-smeared case using the plaquette definition in Eq. (8),  $\bar{Z}_T^{-1}$ . The  $a^2\hat{p}^2$  dependence and the  $a^2\hat{p}^2 \rightarrow 0$  limit of the renormalization constants are different between the different definitions, while the presumed rotation symmetry breaking between  $Z^{-1}$  (black triangles) and  $Z_T^{-1}$  is consistent with zero within the uncertainties. With the functional form  $Z_T^{-1}(a^2\hat{p}^2) = Z_T^{-1}(0) + C_1 a^2\hat{p}^2 + C_2 a^4\hat{p}^4$ , we fit the range  $a^2\hat{p}^2 \in [1.5, 5]$  (the lighter area in Fig. 8) and obtain  $Z_T^{-1}(0\text{-HYP}) = 0.257(25)(5)$ ,  $Z_T^{-1}(1\text{-HYP}) = 0.946(26)(19)$ , and  $\bar{Z}_T^{-1}(1\text{-HYP}) = 1.05(35)(21)$ , where the second error is an estimate of the systematic uncertainty from the 2% truncation error of the gluon propagator at  $r_2 \sim 1.3$  fm. The  $\chi/\text{d.o.f.}$  for all the cases are smaller than 1.

To determine the bare  $\langle x \rangle_g$ , the following ratio is calculated in the rest frame of the nucleon on 81 configurations of the 48I ensemble with a partially quenched valence overlap fermion for the pion mass  $m_\pi \in [135, 372]$  MeV,

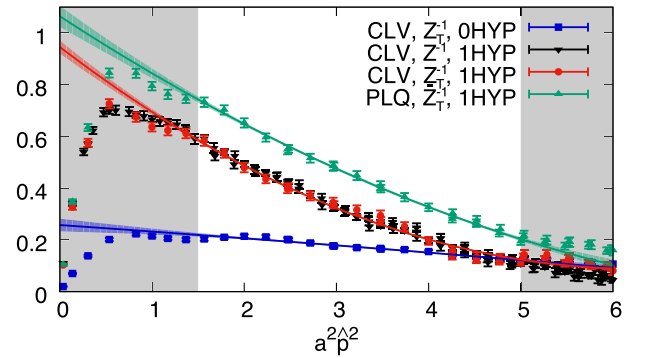


FIG. 8. The  $\bar{\text{MS}}$  at 2 GeV renormalization constants as functions of  $a^2\hat{p}^2$ , for the gauge EMT operators. The red dots and blue boxes show the  $Z_T^{-1}$  with and without HYP smearing using the clover definition (CLV), and the green triangles show the HYP-smeared case using the plaquette definition (PLQ). The result of  $Z^{-1}$  with HYP smearing and the clover definition (purple triangles) are also plotted for the comparison.

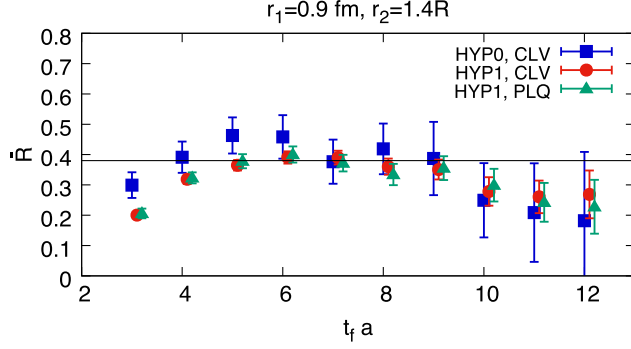


FIG. 9. The renormalized  $\bar{R}(t_f)$  with and without the HYP smearing (the red dots and blue boxes, respectively) using the clover definition and also the HYP-smeared case with the plaquette definition (the green triangles). The HYP-smeared data are shifted horizontally to enhance the legibility, and a black line at 0.38 is placed on the figure to guide the eyes. All results agree with each other within  $2\sigma$  for  $t_f \geq 4$ .

$$R(t_f, t) = \frac{4\langle 0 | \Gamma^e \int d^3 y \chi(\vec{y}, t_f) \bar{T}_{g,44}(t) \bar{\chi}(\vec{0}, 0) | 0 \rangle}{3M_N \langle 0 | \Gamma^e \int d^3 y \chi(\vec{y}, t_f) \bar{\chi}(\vec{0}, 0) | 0 \rangle}, \quad (12)$$

where  $\chi$  is the nucleon interpolation field,  $\Gamma^e$  is the unpolarized projection operator of the proton, and  $M_N$  is the nucleon mass. When  $t_f$  is large enough, the derivative of the  $t$ -summed ratio  $R(t_f, t)$  becomes the glue momentum fraction in the nucleon, as applied in the recent high-accuracy nucleon matrix element calculation [23],

$$\begin{aligned} \bar{R}(t_f) &\equiv \sum_{0 < t < t_f} R(t_f, t) - \sum_{0 < t < t_f - 1} R(t_f - 1, t) \\ &= \langle x \rangle_g^{\text{bare}} + \mathcal{O}(e^{-\delta m t_f}), \end{aligned} \quad (13)$$

up to the excited-state contamination at  $\mathcal{O}(e^{-\delta m t_f})$ . The calculation setup is the same as for our previous work on the glue spin [10]: a  $4 \times 4 \times 4$  smeared grid source with low mode substitution [24] is used for the nucleon two-point functions, and all the time slices are looped over to increase statistics. We followed the same strategy in Ref. [19] to apply CDER to the numerator of  $R(t_f, t)$ . With a cutoff around 1 fm, which is enough as demonstrated in the NPR cases studied here, the statistical uncertainties of  $\bar{R}(t_f)$  can be reduced by a factor of  $\sim 10$ . The systematic uncertainties in bare  $\bar{R}(t_f)$  due to CDER will be investigated in the future following the strategy in Ref. [19]. The renormalized  $\bar{R}(t_f)$  at  $m_\pi = 372$  MeV is shown in Fig. 9 as a check with the best signals we have. The errors from  $Z_T$  and the bare  $\bar{R}(t_f)$  are combined in quadrature. As shown in that figure, even though the renormalization constants with or without HYP smearing differ by a factor of  $\sim 3$  as we saw in Fig. 8, the renormalized  $\bar{R}^R(t_f) \equiv Z_T \bar{R}(t_f)$  are consistent within  $2\sigma$  for  $t_f \geq 4$ .

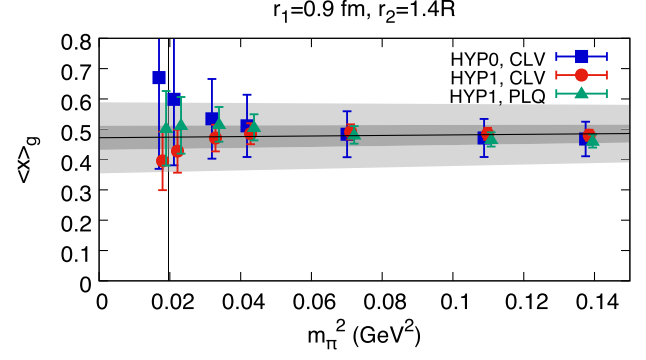


FIG. 10. The renormalized glue momentum fraction  $\langle x \rangle_g$  as a function of  $m_\pi^2$ . The HYP-smeared data are slightly shifted horizontally to enhance the legibility. The results with different definitions are consistent with each other, and the  $m_\pi^2$  dependence is mild. The dark and light gray bands show the statistical and total uncertainties, respectively, at a combined linear fit of the  $m_\pi^2$  dependence.

We fit  $\bar{R}(t_f)$  to a constant in the range  $t_f \geq 7a$  to obtain  $\langle x \rangle_g$  and plot its  $m_\pi^2$  dependence in Fig. 10. With a linear fit to  $m_\pi^2$  for  $m_\pi < 400$  MeV on the 1-HYP-smeared data with the clover definition, we obtain  $\langle x \rangle_g^{\overline{\text{MS}}}(2 \text{ GeV})$  at the physical pion mass as  $0.47(4)(11)$ . The variance of the values from three definitions, the uncertainties of the renormalization constants, and the mixing effect from the quark momentum fraction  $\langle x \rangle_q$  (which is estimated by  $1 - \langle x \rangle_g$  times the one-loop mixing coefficient  $0.1528$  [17]) are combined in quadrature as the systematic uncertainty. The prediction is consistent with the global fitting result CT14 [2]  $0.42(2)$  in  $\overline{\text{MS}}$  at the same scale. The major systematic uncertainty is the mixing from the quark and can be eliminated with a similar nonperturbative calculation with the quark external states.

## V. SUMMARY

In summary, we have presented a systematic implementation of NPR for the glue momentum fraction  $\langle x \rangle_g$ . We demonstrated that the CDER technique can provide an unbiased improvement on the lattice with the cutoffs  $r_1 \sim 0.9$  fm and  $r_2 \sim 1.3$  fm and that the renormalized  $\langle x \rangle_g$  is insensitive to the lattice definition of the gauge EMT or HYP smearing within uncertainties.

Our calculation also shows that HYP smearing can make the  $a^2 \hat{p}^2$  dependence of the renormalization constant much stronger than the case without HYP smearing, even though the  $a^2 \hat{p}^2$ -extrapolated value can be closer to 1. The cases with more steps of HYP smearing are shown in the Appendix.

## ACKNOWLEDGMENTS

We thank W. Detmold, L. Jin, and P. Sun for useful discussions and the RBC and UKQCD collaborations for providing us their domain-wall fermion gauge configurations.

H. L. and Y. Y. are supported by the U.S. National Science Foundation under Grant No. PHY 1653405, “CAREER: Constraining Parton Distribution Functions for New-Physics Searches.” This work is partially supported by DOE Grant No. DE-SC0013065 and the DOE TMD topical collaboration. This research used resources of the Oak Ridge Leadership Computing Facility at the Oak Ridge National Laboratory, which is supported by the Office of Science of the U.S. Department of Energy under Contract No. DE-AC05-00OR22725. This work used Stampede time under the Extreme Science and Engineering Discovery Environment, which is supported by National Science Foundation Grant No. ACI-1053575. We also thank National Energy Research Scientific Computing Center for providing HPC resources that have contributed to the research results reported within this paper. We acknowledge the facilities of the USQCD Collaboration, which are funded by the Office of Science of the U.S. Department of Energy, used for this research in part. This work is supported in part by the National Science Foundation of China (NSFC) under the project No. 11775229, and by the Youth Innovation Promotion Association of CAS (2015013). Part of this work was performed using computing facilities at the College of William and Mary which were provided by contributions from the National Science Foundation, the Commonwealth of Virginia Equipment Trust Fund and the Office of Naval Research.

### APPENDIX: THE DISCRETIZATION ERROR WITH MORE STEPS OF HYP SMEARING

In this section, we repeat the NPR and matrix elements calculation on 48I, but with two and five steps of HYP smearing.

As shown in the left panel of Fig. 11,  $Z_T^{-1}$  becomes increasingly nonlinear on  $a^2\hat{p}^2$  when more HYP-smearing

steps are applied on the gauge EMT. Without HYP smearing, the  $a^2\hat{p}^2$  dependence of  $Z_T^{-1}$  can be well described by a linear term, and the coefficient of the next order  $a^4\hat{p}^4$  term is consistent with zero. With more HYP-smearing steps, the coefficients of the  $a^2\hat{p}^2$  and  $a^4\hat{p}^4$  terms increase significantly. Since all momenta  $p$  on the external legs of the gauge EMT will be integrated in the hadron matrix element,  $a^{2n}\hat{p}^{2n}$  corrections will result in  $\mathcal{O}(a^{2n})$  discretization errors at finite lattice spacing. From the renormalized  $\bar{R}(t_f)$  in the right panel of Fig. 11, the results with two steps of HYP smearing still agree with the results with 1 step of HYP smearing, but if we jump to the five-step HYP smearing used by some previous studies, the  $a^{2n}\hat{p}^{2n}$  corrections will be much larger, and the renormalized result will have large systematic uncertainties from determining  $Z_T^{-1}$  (green triangles and blue boxes).

In the 5-HYP case, with the same range  $a^2\hat{p}^2 \in [1.5, 5]$  and the polynomial form up to the  $a^4\hat{p}^4$  term,  $Z_T^{-1}(5\text{-HYP}) = 0.663(35)$  is obtained with  $\chi^2 = 0.8$  (the default fit). If the  $a^6\hat{p}^6$  term is added and the range is switched to  $a^2\hat{p}^2 \in [1, 4]$ ,  $Z_T^{-1}(5\text{-HYP})$  will jump to 1.11(11) with  $\chi^2 = 0.4$  (the tuned fit). The data of  $Z_T^{-1}(5\text{-HYP})$  (the green triangles) with the band from the default fit (the green band) and tuned fit (the blue band) are plotted in the left panel of Fig. 11, and the renormalized  $\bar{R}(t_f)$  with both fits of  $Z_T^{-1}$  are shown in the right panel. The errors from  $Z_T$  and the bare  $\bar{R}(t_f)$  are combined in quadrature. It is obvious that the renormalized  $\bar{R}(t_f)$  with five-step HYP smearing (green triangles) based on the default fit of  $Z_T^{-1}$  is much higher than those with one and two steps of HYP smearing. Even though the consistency can be improved if the tuned fit of  $Z_T^{-1}$  is applied (the blue boxes), the systematic uncertainties from the fit of  $Z_T^{-1}$  will make the final uncertainties in the five-step HYP-smearing case larger than the cases with fewer steps of HYP smearing.

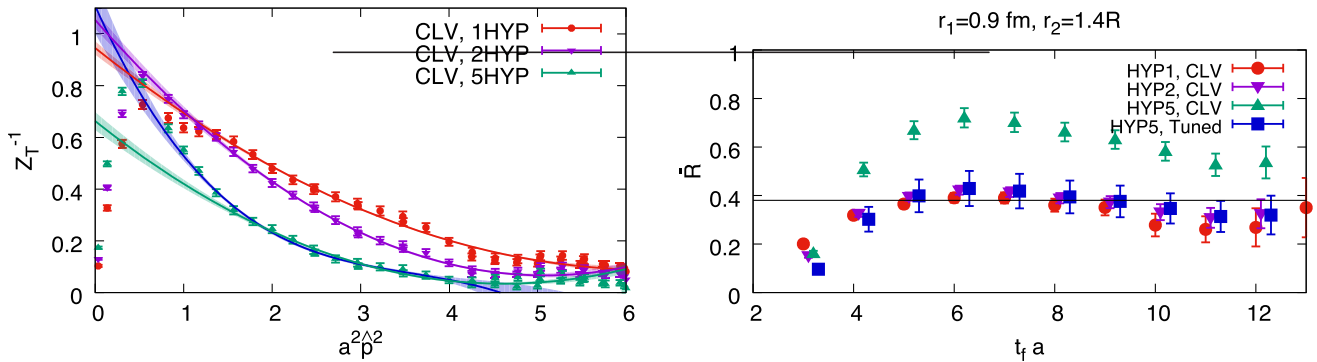


FIG. 11. The  $\bar{\text{MS}}$  2 GeV renormalization constants  $Z_T^{-1}$  and renormalized  $\bar{R}(t_f)$  with one, two, and five steps of HYP smearing are shown as the red dots, purple reversed triangles, and green triangles, respectively. Both the blue and green bands are the fit of the 5-HYP data, with the regions  $a^2\hat{p}^2 \in [1, 4]$  and  $[1.5, 5]$ , respectively. The renormalized  $\bar{R}(t_f)$  in the 2-HYP case is still consistent with the 1-HYP case even though the  $a^2\hat{p}^2$  dependence of  $Z_T^{-1}$  is quite different for  $t_f \geq 3$ , but the 5-HYP case will be very sensitive to the fit of  $Z_T^{-1}$  and then has a large systematic uncertainties.



- [1] M. Gluck, E. Reya, and I. Schienbein, *Eur. Phys. J. C* **10**, 313 (1999).
- [2] S. Dulat, T.-J. Hou, J. Gao, M. Guzzi, J. Huston, P. Nadolsky, J. Pumplin, C. Schmidt, D. Stump, and C. P. Yuan, *Phys. Rev. D* **93**, 033006 (2016).
- [3] X.-D. Ji, *Phys. Rev. Lett.* **74**, 1071 (1995).
- [4] M. Deka *et al.*, *Phys. Rev. D* **91**, 014505 (2015).
- [5] R. Horsley, R. Millo, Y. Nakamura, H. Perlt, D. Pleiter, P. E. L. Rakow, G. Schierholz, A. Schiller, F. Winter, and J. M. Zanotti (UKQCD and QCDSF Collaborations), *Phys. Lett. B* **714**, 312 (2012).
- [6] C. Alexandrou, M. Constantinou, K. Hadjiyiannakou, K. Jansen, H. Panagopoulos, and C. Wiese, *Phys. Rev. D* **96**, 054503 (2017).
- [7] C. Alexandrou, M. Constantinou, K. Hadjiyiannakou, K. Jansen, C. Kallidonis, G. Koutsou, A. Vaquero Avilés-Casco, and C. Wiese, *Phys. Rev. Lett.* **119**, 142002 (2017).
- [8] G. Corbo, E. Franco, and G. C. Rossi, *Phys. Lett. B* **236**, 196 (1990).
- [9] S. Capitani and G. Rossi, *Nucl. Phys. B* **433**, 351 (1995).
- [10] Y.-B. Yang, R. S. Sufian, A. Alexandru, T. Draper, M. J. Glatzmaier, K.-F. Liu, and Y. Zhao, *Phys. Rev. Lett.* **118**, 102001 (2017).
- [11] A. Hasenfratz, R. Hoffmann, and F. Knechtli, *Nucl. Phys. B, Proc. Suppl.* **106**, 418 (2002).
- [12] W. Detmold and P. E. Shanahan, *Phys. Rev. D* **94**, 014507 (2016); **95**, 079902(E) (2017).
- [13] X. Ji, *Sci. China Phys. Mech. Astron.* **57**, 1407 (2014).
- [14] Y.-Q. Ma and J.-W. Qiu, *Phys. Rev. Lett.* **120**, 022003 (2018).
- [15] J. C. Collins and R. J. Scalise, *Phys. Rev. D* **50**, 4117 (1994).
- [16] G. Martinelli, C. Pittori, C. T. Sachrajda, M. Testa, and A. Vladikas, *Nucl. Phys. B* **445**, 81 (1995).
- [17] Y.-B. Yang, M. Glatzmaier, K.-F. Liu, and Y. Zhao, *arXiv*: 1612.02855.
- [18] T. Blum *et al.* (RBC and UKQCD Collaborations), *Phys. Rev. D* **93**, 074505 (2016).
- [19] K.-F. Liu, J. Liang, and Y.-B. Yang, *Phys. Rev. D* **97**, 034507 (2018).
- [20] K. Orginos, A. Parreno, M. J. Savage, S. R. Beane, E. Chang, and W. Detmold, *Phys. Rev. D* **92**, 114512 (2015).
- [21] O. Oliveira and P. Bicudo, *J. Phys. G* **38**, 045003 (2011).
- [22] A. Cucchieri, D. Dudal, T. Mendes, and N. Vandersickel, *Phys. Rev. D* **85**, 094513 (2012).
- [23] C. C. Chang, A. Nicholson, E. Rinaldi, E. Berkowitz, N. Garron, D. A. Brantley, H. Monge-Camacho, C. J. Monahan, C. Bouchard, M. A. Clark, B. Joó, T. Kurth, K. Orginos, P. Vranas, and A. Walker-Loud, *Nature* **558**, 91 (2018).
- [24] A. Li *et al.* ( $\chi$ QCD Collaboration), *Phys. Rev. D* **82**, 114501 (2010).



## Glue Spin and Helicity in the Proton from Lattice QCD

Yi-Bo Yang,<sup>1</sup> Raza Sabbir Sufian,<sup>1</sup> Andrei Alexandru,<sup>2</sup> Terrence Draper,<sup>1</sup> Michael J. Glatzmaier,<sup>1</sup>  
 Keh-Fei Liu,<sup>1</sup> and Yong Zhao<sup>3,4</sup>

( $\chi$ QCD Collaboration)

<sup>1</sup>Department of Physics and Astronomy, University of Kentucky, Lexington, Kentucky 40506, USA

<sup>2</sup>Department of Physics, The George Washington University, Washington, D.C. 20052, USA

<sup>3</sup>Maryland Center for Fundamental Physics, University of Maryland, College Park, Maryland 20742, USA

<sup>4</sup>Nuclear Science Division, Lawrence Berkeley National Laboratory, Berkeley, California 94720, USA  
 (Received 12 October 2016; revised manuscript received 6 December 2016; published 6 March 2017)

We report the first lattice QCD calculation of the glue spin in the nucleon. The lattice calculation is carried out with valence overlap fermions on  $2+1$  flavor domain-wall fermion gauge configurations on four lattice spacings and four volumes including an ensemble with physical values for the quark masses. The glue spin  $S_G$  in the Coulomb gauge in the modified minimal subtraction ( $\overline{\text{MS}}$ ) scheme is obtained with one-loop perturbative matching. We find the results fairly insensitive to lattice spacing and quark masses. We also find that the proton momentum dependence of  $S_G$  in the range  $0 \leq |\vec{p}| < 1.5$  GeV is very mild, and we determine it in the large-momentum limit to be  $S_G = 0.251(47)(16)$  at the physical pion mass in the  $\overline{\text{MS}}$  scheme at  $\mu^2 = 10$  GeV<sup>2</sup>. If the matching procedure in large-momentum effective theory is neglected,  $S_G$  is equal to the glue helicity measured in high-energy scattering experiments.

DOI: 10.1103/PhysRevLett.118.102001

**Introduction.**—Deep-inelastic scattering experiments reveal that, contrary to the naive quark model, the quark spin contribution to the proton spin is quite small, about 30% [1–3]. In an effort to search for the missing proton spin, recent analyses [4,5] of the high-statistics 2009 STAR [6] and PHENIX [7] experiments at RHIC showed evidence of nonzero glue helicity  $\Delta G$  in the proton. For  $Q^2 = 10$  GeV<sup>2</sup>, the glue helicity distribution  $\Delta g(x, Q^2)$  is found to be positive and away from zero in the momentum fraction region  $x < 0.05$ . However, the results are limited by very large uncertainty in this region.

The recent COMPASS analysis explored  $\Delta g(x)$  from the scaling violation of  $\Delta q(x)$ , and the highly distinct solutions of  $\Delta g(x)$  can be obtained with different parametrizations of  $\Delta q(x)$  [8]. Therefore, it hints that if a high precision  $\Delta g(x)$  can be obtained directly, it will benefit our understanding of the parametrizations of  $\Delta q(x)$  and provide more information about the role of quark spin in the proton.

Given the importance of  $\Delta g(x)$  to explain the origin of the proton spin, and the fact that significant efforts are devoted to its precise experimental determination, a theoretical understanding and calculation of  $\Delta G$  is highly desired.  $\Delta G$  is defined as the first moment of the glue helicity distribution  $\Delta g(x)$  [9],

$$\Delta G = \int dx \frac{i}{2xP^+} \int \frac{d\xi^-}{2\pi} e^{-ixP^+\xi^-} \times \langle PS | F_a^{+\alpha}(\xi^-) \mathcal{L}^{ab}(\xi^-, 0) \tilde{F}_{\alpha,b}^+(0) | PS \rangle, \quad (1)$$

where the light front coordinates are  $\xi^\pm = (\xi^0 \pm \xi^3)/\sqrt{2}$ . The proton plane wave state is written as  $|PS\rangle$ , with momentum  $P^\mu = (P, 0, 0, P)$  and polarization  $S$ . The light-cone gauge-link  $\mathcal{L}(\xi^-, 0) = P \exp[-ig \int_0^{\xi^-} A^+(\eta^-, 0_\perp) d\eta^-]$  is defined in the adjoint representation. It connects the gauge field tensor and its dual,  $\tilde{F}^{\alpha\beta} = \frac{1}{2} \epsilon^{\alpha\beta\mu\nu} F_{\mu\nu}$ , to construct a gauge-invariant operator. After integrating over  $x$ , one can define the gauge-invariant gluon helicity operator in a nonlocal form [10,11],

$$\tilde{S}_g = \left[ \vec{E}^a(0) \times \left( \vec{A}^a(0) - \frac{1}{\nabla^+} (\vec{\nabla} A^{+,b}) \mathcal{L}^{ba}(\xi^-, 0) \right) \right]^z, \quad (2)$$

where  $\nabla^+ = \partial/\partial\xi^-$ . It is the gauge-invariant extension of the operator  $\vec{E} \times \vec{A}$  in the light-cone gauge  $A^+ = 0$ , but one cannot evaluate this expression on the lattice directly due to its real-time dependence.

On the other hand,  $\tilde{S}_g$  is equal to the infinite momentum frame (IMF) limit of a universality class of operators [12] whose matrix elements can be matched to  $\Delta G$  through a factorization formula in large-momentum effective theory (LMET) [13,14]. The gluon spin operator proposed in Ref. [15,16] with the non-Abelian transverse condition belongs to this universality class and has been proven to be equivalent to the gauge-invariant extension of  $\vec{E} \times \vec{A}$  in the Coulomb gauge  $\vec{\partial} \cdot \vec{A} = 0$  [17,18],

$$\vec{S}_g = 2 \int d^3x \text{Tr}(\vec{E}_c \times \vec{A}_c), \quad (3)$$

where the factor 2 is from the normalization of the SU(3) group generators and  $\vec{E}_c$  and  $\vec{A}_c$  are the chromoelectric field and gauge potential in the Coulomb gauge with their lattice versions to be addressed in the following.

$\vec{S}_g$  is not Lorentz covariant and has nontrivial frame dependence [11]. It is shown in Ref. [12] that when boosted to the IMF, the Coulomb gauge fixing condition (as well as the temporal condition  $A^0 = 0$ ) [12] becomes  $A^+ = 0$ , and then the longitudinal component of  $\vec{S}_g$  in either gauge is equivalent to the glue helicity operator  $\tilde{S}_g$  with a proper matching to cancel the intrinsic frame dependence of  $\vec{S}_g$ . On the lattice, the Coulomb condition can be obtained numerically [19] and the glue spin operator  $\vec{S}_g$  in the Coulomb gauge can be calculated without numerical difficulty.

The major task of this work is calculating the matrix element of  $\vec{S}_g$  in the proton, which will be indicated as  $S_G$ , in the rest and moving frames. The results are then renormalized at one-loop order in lattice perturbation theory and matched to the modified minimal subtraction ( $\overline{\text{MS}}$ ) scheme at  $\mu^2 = 10 \text{ GeV}^2$ , to investigate their frame dependence and address the matching to the helicity.

*Numerical details.*—A preliminary attempt [20] to calculate  $S_G$  was carried out on 2 + 1 flavor dynamical domain-wall configurations on a  $24^3 \times 64$  lattice (24I) with the sea pion mass at 330 MeV and on a  $32^3 \times 64$  lattice with sea pion mass at 300 MeV [21]. In this work, we improve the statistics on the ensembles mentioned above and carry out the calculation on another three ensembles with different lattice spacings, volumes, and sea quark masses to check the corrections to the glue spin from various systematic uncertainties. We use the 2-2-2 smeared stochastic grid source on all the ensembles (except 48I, where the 4-4-4 smeared stochastic grid source is used), and apply the low-mode substitution [22,23] to make the signal-to-noise ratio close to that with 8 (64 on the 48I ensemble) independent smeared point sources. Furthermore, we loop over all the time slices for the two-point functions of the nucleon to increase statistics. The statistics used for this grid source measurement is roughly equivalent to evaluating a large number of quasi-independent smeared point source measurements ranging from 103,936 on the 24I lattice to 497,664 on the 48I lattice. The parameters of the ensembles used in this work are listed in Table I, and more details of the simulation setups can be found in the Supplemental Material [24].

The Coulomb gauge fixing condition used here is enforced by requiring that the spatial sum of the backward difference of the hypercubic (HYP)-smeared gauge links [26] be zero,

TABLE I. The parameters for the RBC and UKQCD configurations [25].  $m_\pi^{(s)}$  is the pion mass of the light sea quark in the 2 + 1 flavor configuration, and  $N_{\text{cfg}}$  is the number of configurations used in the simulation.

Symbol	$L^3 \times T$	$a$ (fm)	$m_\pi^{(s)}$ (MeV)	$N_{\text{cfg}}$
32ID	$32^3 \times 64$	0.1431(7)	170	200
48I	$48^3 \times 96$	0.1141(2)	140	81
24I	$24^3 \times 64$	0.1105(3)	330	203
32I	$32^3 \times 64$	0.0828(3)	300	309
32If	$32^3 \times 64$	0.0627(3)	370	238

$$\sum_{\mu=x,y,z} [U_\mu^c(x) - U_\mu^c(x - a\hat{\mu})] = 0, \quad (4)$$

where  $U_\mu^c(x)$  is the Coulomb gauge fixed Wilson link from  $x + a\hat{\mu}$  to  $x$ . The gauge fixed potential  $A_c$  is defined by

$$A_{c,\mu} = \left( \frac{U_\mu^c(x) - U_\mu^{c\dagger}(x) + U_\mu^c(x - a\hat{\mu}) - U_\mu^{c\dagger}(x - a\hat{\mu})}{4ia g} \right)_{\text{traceless}}, \quad (5)$$

with  $g$  as the bare coupling constant, and the chromoelectric field used in this work is given by the clover definition,

$$F_{\mu\nu}^c = \frac{i}{8a^2 g} (\mathcal{P}_{\mu,\nu} - \mathcal{P}_{\nu,\mu} + \mathcal{P}_{\nu,-\mu} - \mathcal{P}_{-\mu,\nu} + \mathcal{P}_{-\mu,-\nu} - \mathcal{P}_{-\nu,-\mu} + \mathcal{P}_{-\nu,\mu} - \mathcal{P}_{\mu,-\nu}), \quad (6)$$

where  $\mathcal{P}_{\mu,\nu} = U_\mu^c(x) U_\nu^c(x + a\hat{\mu}) U_\mu^{c\dagger}(x + a\hat{\nu}) U_\nu^{c\dagger}(x)$ .

In order to extract  $S_G$ , we compute the ratio of the disconnected three-point function with the gluon operator insertion to the nucleon propagator with the source and sink of the nucleon located at 0 and  $t_f$ , respectively. The glue spin operator is inserted at the time slice  $t$ , which is between 0 and  $t_f$ . Then the ratio in a moving frame  $\vec{p} = (0, 0, p_3)$  along the  $z$  direction is

$$R(t_f, t) = \frac{\langle 0 | \Gamma_3^m \int d^3y e^{-ip_3 y_3} \chi(\vec{y}, t_f) S_G^3(t) \bar{\chi}(\vec{0}, 0) | 0 \rangle}{\langle 0 | \Gamma^e \int d^3y e^{-ip_3 y_3} \chi(\vec{y}, t_f) \bar{\chi}(\vec{0}, 0) | 0 \rangle}, \quad (7)$$

where  $\chi$  is the nucleon interpolation field and  $\Gamma^e$  and  $\Gamma_3^m$  are the unpolarized projection operator of the proton and the polarized one along the  $z$  direction, respectively. When  $t_f$  is large enough,  $R(t_f, t)$  is equal to the proton matrix element of the longitudinal glue spin operator  $S_G$  plus  $t$ -dependent corrections,

$$R(t_f, t) = S_G + C_1 e^{-\Delta E(t_f - t)} + C_2 e^{-\Delta E t} + C_3 e^{-\Delta E t_f}, \quad (8)$$

where  $\Delta E$  is the energy difference between the first excited state and the ground state and  $C_{1,2,3}$  are the spectral weights involving the excited state.

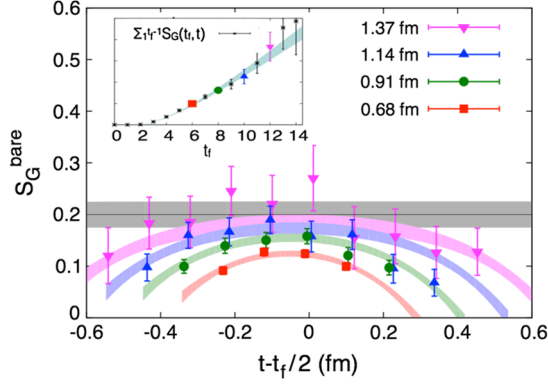


FIG. 1. The ratio  $R(t_f, t)$  as a function of the source-sink separation  $t_f$  and the current time slice  $t$ , for the bare glue spin matrix element in the proton  $S_G^{\text{bare}}$  is plotted at the unitary point on the 24I ensemble. The gray band shows the result extrapolated to infinite separation, which corresponds to the prediction of  $S_G$ . The excited-state contamination is small when the source-sink separation is larger than 1 fm. The inset shows that the prediction of  $\sum_t R(t_f, t)$  from the two-state fit (the band) in Eq. (8) agrees well with the data points.

We plot the ratio  $R(t_f, t)$  for the unitary point on the 24I ensemble, as a function of  $t - t_f/2$  for several  $t_f$ , in Fig. 1. The curves predicted by the fit agree with the data, and the  $\chi^2/\text{d.o.f.}$  is smaller than 1.4 for all the other quark masses on five ensembles. From the fit, we see that the excited-state contamination is small when the source-sink separation is larger than 1 fm. The final prediction of  $S_G$  (the gray band) is consistent with the blue and purple data points at  $t \sim t_f/2$ . Similar plots for the other ensembles can be found in the Supplemental Material [24].

It is observed that the central values of the glue spin matrix elements as a function of HYP-smearing steps are unchanged after two or three steps of smearing, as shown in Fig. 2 (for the case of the unitary point on the ensemble

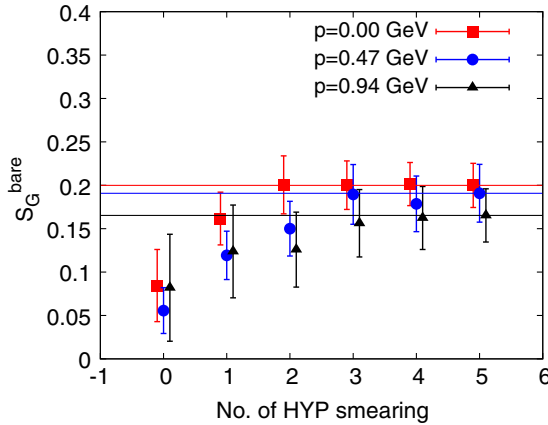


FIG. 2. The HYP-smearing steps dependence of the bare glue spin  $S_G$  at the unitary point on the ensemble 24I, for  $p = 0$  (red squares),  $p = 0.47$  GeV (blue dots), and  $p = 0.94$  GeV (black triangles). The values of  $S_G$  are unchanged after two or three steps of smearing.

24I), while the SNR can be improved when more HYP-smearing steps are applied. In this work, five steps of HYP smearing are used for the glue spin operator on each ensemble, and the nucleon two-point correlators with the source located on all the time slices are generated to increase the SNR. Since the tadpole improvement factor is  $1/u_0^5 \sim 2$  for the  $S_g$  operator without any HYP smearing, the enlargement of the result after the HYP smearing is understandable. Note that the HYP smearing here just affects the glue spin operator, but the gauge action is unchanged since no reweighting is applied on configuration averages.

**Results.**—The renormalized matrix element  $S_G$  including mixing from the quark spin is [27]

$$S_G^{\overline{\text{MS}}} = \left\{ 1 - \frac{g^2}{16\pi^2} \left[ N_f \left( \frac{2}{3} \log(\mu^2 a^2) + 1.27 \right) - C_A \left( \frac{4}{3} \log(\mu^2 a^2) + f_{gg}(g^2) \right) \right] \right\} S_G^L + \frac{g^2 C_F}{16\pi^2} \left( \frac{5}{3} \log(\mu^2 a^2) + 7.31 \right) \Delta\Sigma^L + O(g^4), \quad (9)$$

where the superscripts  $\overline{\text{MS}}$  and  $L$  indicate the quantities under the  $\overline{\text{MS}}$  scheme and that under lattice regularization, respectively. We applied the cactus improvement [28] to resum the major tadpole contributions to get a better convergence in the one-loop correction of the glue spin. Then the resummed finite piece  $f_{gg}(g^2)$  depends on the bare coupling  $g^2$  weakly and is in the range of 1.7–2.4 for the values of  $g^2$  we used in this work. The details are addressed in Ref. [27]. Since the value of the mixing term involving  $\Delta\Sigma^L$  in Eq. (9) is at the same order of the present statistical error of  $S_G^L$ , the uncertainty due to  $\Delta\Sigma^L$  for the gauge ensembles considered here will be even smaller. Therefore, we approximate the quark spin  $\Delta\Sigma^L$  by the experimental value  $\Delta\Sigma^{\overline{\text{MS}}}$ , which is  $\sim 30\%$  of the total proton spin from the global analysis of deep-inelastic scattering data [1–3].

After matching to the values under the  $\overline{\text{MS}}$  scheme at  $\mu^2 = 10 \text{ GeV}^2$ , we find that the valence quark mass dependence is mild regardless of the proton momentum. In Fig. 3, we show results in the rest frame for various valence quark masses on all the five ensembles, with five pairs of volumes and lattice spacings. Their dependence is also mild. To obtain  $S_G$  in a relatively large-momentum frame, we calculate  $S_G$  for all the momenta smaller than  $\pi/(4a)$  on all the five ensembles. To show the frame dependence, we extrapolate  $S_G$  on all the ensembles in different momentum frames to the physical value of the valence pion mass, as shown in Fig. 4. Some points are not shown in the figure if their uncertainties are larger than the signal.



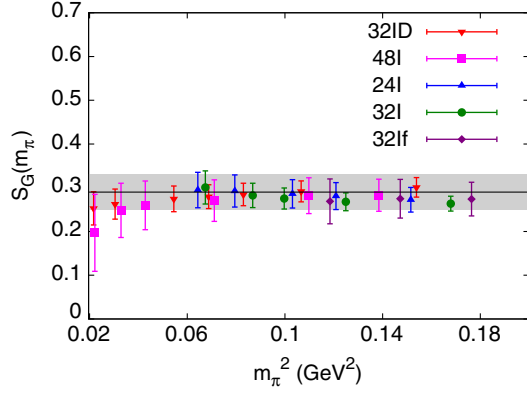


FIG. 3. The valence pion mass dependence of  $S_G$  at  $\mu^2 = 10 \text{ GeV}^2$ , in the rest frame of the proton. These dependencies are fairly mild and can be well described with a linear fit. The gray band shows the result based on the global fit with the empirical form in Eq. (11).

The glue helicity in the proton  $\Delta G$  corresponds to the glue longitudinal spin component  $S_G$  in the IMF. The LMET [14] shows a large finite correction at the one-loop level:

$$S_G(|\vec{p}|, \mu) = \left[ 1 + \frac{g^2 C_A}{16\pi^2} \left( \frac{7}{3} \log \frac{(\vec{p})^2}{\mu^2} - 10.2098 \right) \right] \Delta G(\mu) + \frac{g^2 C_F}{16\pi^2} \left( \frac{4}{3} \log \frac{(\vec{p})^2}{\mu^2} - 5.2627 \right) \Delta \Sigma(\mu) + O(g^4) + O\left(\frac{1}{(\vec{p})^2}\right). \quad (10)$$

At  $\mu^2 = 10 \text{ GeV}^2$  and  $|\vec{p}| = 1.5 \text{ GeV}$ , the factor before  $\Delta G$  is 0.22, which is much smaller than unity and indicates a convergence problem for the perturbative series even after one resums the large logarithms. (The factor is 0.80 if the finite piece 10.2098 is removed.) On the other hand, the largest momentum we have on the lattice with acceptable signal is comparable to the proton mass, so the power corrections in Eq. (10) cannot be neglected and one cannot simply apply this matching condition. Nevertheless, the mild dependence of  $S_G$  on the proton momentum as in Fig. 4 leads us to suggest that it could be a small effect to match to the IMF; i.e.,  $S_G \approx \Delta G + O(1/(\vec{p})^2)$ .

Therefore, we neglect the one-loop LMET matching and use the following empirical form to fit our data:

$$S_G(|\vec{p}|) = S_G(\infty) + \frac{C_1}{M^2 + (\vec{p})^2} + C_2(m_{\pi, vv}^2 - m_{\pi, \text{phys}}^2) + C_3(m_{\pi, ss}^2 - m_{\pi, \text{phys}}^2) + C_4 a^2, \quad (11)$$

where  $m_{\pi, \text{phys}} = 0.139 \text{ GeV}$  and  $M = 0.939 \text{ GeV}$  are the physical pion and proton mass, respectively, and  $m_{\pi, vv/ss}$  are the valence and sea pion masses, respectively. The

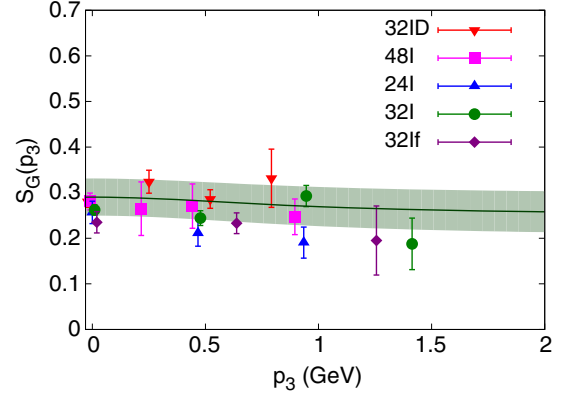


FIG. 4. The results extrapolated to the physical pion mass as a function of the absolute value of  $\vec{p} = (0, 0, p_3)$ , on all the five ensembles. All the results have been converted to  $\overline{\text{MS}}$  at  $\mu^2 = 10 \text{ GeV}^2$ . The data on several ensembles are shifted horizontally to enhance the legibility. The green band shows the frame dependence of the global fit [with the empirical form in Eq. (11)] of the results.

$1/(\vec{p})^2$  correction in Eq. (10) is replaced by  $1/[M^2 + (\vec{p})^2]$  to include all the data in the fitting. Since all the coefficients other than  $S_G(\infty)$  are small, the cross terms and the higher-order terms are ignored. The overall  $\chi^2/\text{d.o.f.}$  is 1.21 with 110 degrees of freedom. In Fig. 4, the band of the global fit with the empirical form in Eq. (11) shows that the frame dependence is mild and the central value is changed by less than 10% from its value in the rest frame to that at  $|\vec{p}| \sim 1.5 \text{ GeV}$ ; the change is smaller than the statistical uncertainty.

Since the Coulomb gauge fixing on the lattice has a built-in  $O(a)$  correction, we repeated the fit with a linear term in  $a$ . The central value is changed by about 1%, while the uncertainty is larger. We take the variance of the central values from two fits as an estimate of this uncertainty. Similarly, the uncertainty from the volume dependence  $e^{-m_{\pi vv} L}$  is estimated in the same way and added to the systematic uncertainties in quadrature. In addition, the value of the quark spin  $\Delta \Sigma$  is varied by 20% to cover the value  $\sim 0.30$  [1] and that from Ref. [3]. The final result is  $S_G(\infty, \mu^2 = 10 \text{ GeV}^2) = 0.251(47)(16)$  with two errors from the statistical and systematic uncertainties.

**Summary and outlook.**—In this work, we calculated the glue spin in the proton for the first time based on  $\vec{E} \times \vec{A}$  in the Coulomb gauge [15,16], with various quark masses, lattice spacings, volumes, and proton momenta. The results show mild dependencies on these quantities. After one-loop perturbative matching from the lattice theory to the continuum and neglecting the matching effect between the glue spin and helicity, we conclude that the gluon helicity  $\Delta G(\mu^2 = 10 \text{ GeV}^2) \approx S_G(\infty, \mu^2 = 10 \text{ GeV}^2) = 0.251(47)(16)$ , which is 50(9)(3)% of the total proton spin. The cactus improvement [28] we used in Eq. (9) indicates that uncertainties can be considerable in perturbative QCD,

and its reliability should be checked with nonperturbative renormalization in the future.

On the LMET side, the convergence problem warrants the matching condition to be calculated at the two-loop level or higher. On the other hand, if the glue spin in the temporal gauge can be calculated on the lattice, then its LMET matching in Eq. (10) can be avoided at the one-loop level [12]. This possibility is worthy of further investigation [27].

We thank X. D. Ji and F. Yuan for useful comments and the RBC and UKQCD Collaborations for providing us their domain-wall fermion gauge configurations. This work is supported in part by the U.S. DOE Grant No. DE-SC0013065. A. A. is supported in part by the National Science Foundation CAREER Grant No. PHY-1151648 and by U.S. DOE Grant No. DE-FG02-95ER40907. Y. Z. is supported in part by the U.S. Department of Energy Office of Science, Office of Nuclear Physics under Awards No. DE-FG02-93ER-40762 and No. DE-AC02-05CH11231. Y.-B. Y. also thanks the Institute of High Energy Physics, Chinese Academy of Science for its partial support and hospitality. This material is based upon work supported by the U.S. Department of Energy, Office of Science, Office of Nuclear Physics, within the framework of the TMD Topical Collaboration. This research used resources of the Oak Ridge Leadership Computing Facility at the Oak Ridge National Laboratory, which is supported by the Office of Science of the U.S. Department of Energy under Contract No. DE-AC05-00OR22725. This work also used the Extreme Science and Engineering Discovery Environment (XSEDE), which is supported by National Science Foundation Grant No. ACI-1053575.

- 
- [1] A. Accardi *et al.*, *Eur. Phys. J. A* **52**, 268 (2016).
  - [2] D. de Florian, R. Sassot, M. Stratmann, and W. Vogelsang, *Phys. Rev. D* **80**, 034030 (2009).
  - [3] C. A. Aidala, S. D. Bass, D. Hasch, and G. K. Mallot, *Rev. Mod. Phys.* **85**, 655 (2013).
  - [4] D. de Florian, R. Sassot, M. Stratmann, and W. Vogelsang, *Phys. Rev. Lett.* **113**, 012001 (2014).

- [5] E. R. Nocera, R. D. Ball, S. Forte, G. Ridolfi, and J. Rojo (NNPDF Collaboration), *Nucl. Phys.* **B887**, 276 (2014).
- [6] P. Djawotho (STAR Collaboration), *Nuovo Cimento Soc. Ital. Fis.* **36C**, 35 (2013).
- [7] A. Adare *et al.* (PHENIX Collaboration), *Phys. Rev. D* **90**, 012007 (2014).
- [8] C. Adolph *et al.* (COMPASS Collaboration), *Phys. Lett. B* **753**, 18 (2016).
- [9] A. V. Manohar, *Phys. Lett. B* **255**, 579 (1991).
- [10] Y. Hatta, *Phys. Rev. D* **84**, 041701 (2011).
- [11] X. Ji, J.-H. Zhang, and Y. Zhao, *Phys. Rev. Lett.* **111**, 112002 (2013).
- [12] Y. Hatta, X. Ji, and Y. Zhao, *Phys. Rev. D* **89**, 085030 (2014).
- [13] X. Ji, *Sci. China Phys. Mech. Astron.* **57**, 1407 (2014).
- [14] X. Ji, J.-H. Zhang, and Y. Zhao, *Phys. Lett. B* **743**, 180 (2015).
- [15] X.-S. Chen, X.-F. Lu, W.-M. Sun, F. Wang, and T. Goldman, *Phys. Rev. Lett.* **100**, 232002 (2008).
- [16] X.-S. Chen, W.-M. Sun, X.-F. Lu, F. Wang, and T. Goldman, *Phys. Rev. Lett.* **103**, 062001 (2009).
- [17] C. Lorce, *Phys. Rev. D* **87**, 034031 (2013).
- [18] Y. Zhao, K.-F. Liu, and Y. B. Yang, *Phys. Rev. D* **93**, 054006 (2016).
- [19] M. Schröck and H. Vogt, *Comput. Phys. Commun.* **184**, 1907 (2013).
- [20] R. S. Sufian, M. J. Glatzmaier, Y.-B. Yang, K.-F. Liu, and M. Sun ( $\chi$  QCD), *Proc. Sci.*, LATTICE2014 (2014) 166.
- [21] Y.-B. Yang, R. S. Sufian, A. Alexandru, T. Draper, M. J. Glatzmaier, and K.-F. Liu ( $\chi$  QCD Collaboration), *Proc. Sci.*, LATTICE (2015) 129.
- [22] A. Li *et al.* ( $\chi$  QCD Collaboration), *Phys. Rev. D* **82**, 114501 (2010).
- [23] M. Gong *et al.* ( $\chi$  QCD Collaboration), *Phys. Rev. D* **88**, 014503 (2013).
- [24] See Supplemental Material at <http://link.aps.org/supplemental/10.1103/PhysRevLett.118.102001> for the details of the numerical simulation setup and the two-state fits used to obtain the glue spin matrix element.
- [25] T. Blum *et al.* (RBC and UKQCD Collaborations), *Phys. Rev. D* **93**, 074505 (2016).
- [26] A. Hasenfratz and F. Knechtli, *Phys. Rev. D* **64**, 034504 (2001).
- [27] Y.-B. Yang and Y. Zhao (to be published).
- [28] M. Constantinou, H. Panagopoulos, and A. Skouroupathis, *Phys. Rev. D* **74**, 074503 (2006).



Nomination form for the 2019 Nishina Asia Award

Candidate (name, affiliation, curriculum vitae including the date of the degree of Ph.D., nationality, address, email and telephone)

**Name:** Feng-Kun Guo

**Affiliation:** Institute of Theoretical Physics, Chinese Academy of Sciences

**Nationality:** China

**Address:** Institute of Theoretical Physics, CAS, Zhong Guan Cun East Street 55, Beijing 100190, China

**Email:** fkguo@itp.ac.cn    **Telephone:** +86-10-62648752

**Appointments:**

- 01.2019 – Professor, Institute of Theoretical Physics, CAS
- 09.2015 – 12.2018 Associate Professor, Institute of Theoretical Physics, CAS
- 10.2010 – 09.2015 Senior Research Fellow, University of Bonn
- 10.2007 – 09.2010 VIQCD Postdoctoral Fellow, Forschungszentrum Jülich

**Education:**

- 09.2002 – 07.2007 Ph.D. in physics, Institute of High Energy Physics, CAS; Thesis: “Heavy Quarkonium  $\pi\pi$  Transitions and New Hadronic States”; Advisor: Prof. Peng-Nian Shen
- 09.1998 – 07.2002 B.S. in physics, Shandong University

**Honors:**

- 2018 Key Project, National Natural Science Foundation of China
- 2018 IoP Publishing Top Cited Author Award (China)
- 2017 Most Valued Reviewer for 2017 (Phys. Lett. B)
- 2017 EPJ Distinguished Referee in 2017 (nominated by Eur. Phys. J. A)
- 2017 Chin. Phys. C Top Reviewer Award
- 2015 EPJ Distinguished Referee in 2015 (nominated by Eur. Phys. J. C)
- 2015 The Thousand Talents Plan for Young Professionals

Citation for the Award (within 30 words)

For his outstanding theoretical contributions to understanding the nature of new hadrons discovered since 2003.

## Description of the work

Quantum chromodynamics (QCD) is the fundamental theory for the strong interaction, which is the interaction generating the majority of the mass of the visible universe. The experimentally accessible strongly interacting particles are called hadrons composed of quarks and gluons, with the proton and neutron as two examples. However, because quarks and gluons are confined within hadrons, one has to understand hadron spectroscopy in order to understand how the strong interaction in the nonperturbative regime works. The central question in this aspect is thus: How is the emerging hadron spectrum organized? The potential quark model provided historically an answer to this question. However, dozens of new hadrons have been discovered since the year 2003 at high-energy experiments at the B factories (Belle, BESIII, CLEO) playing a central role. Their properties are at odds with the quark model expectations, and thus have inspired intensive theoretical and experimental investigations. Feng-Kun Guo has worked vigorously in this field, and produced a number of influential papers. Both experimental and theoretical developments in the field, with a special focus on hadronic molecules which are strongly interacting systems formed of two hadrons, have been summarized comprehensively in the recent review by him (coauthored with his collaborators) published in Rev. Mod. Phys. [1]. The review has become a standard reference in the field.

Among the very first new unusual hadrons are the charmed mesons with positive parity discovered in 2003. They exhibit several mysterious properties. In the pioneering work [2], Feng-Kun Guo studied these mesons by investigating the interactions between ground state charmed mesons and light mesons that are the Goldstone bosons of the spontaneous chiral symmetry breaking in QCD. Consequently, the positive-parity charmed mesons are dynamically generated as hadronic molecules. In his sequential works, combining chiral effective field theory with results from large-scale lattice QCD simulations and experimental results, he has shown that all the mysteries can be naturally resolved.

In addition to the charmed mesons, the other major groups of new hadrons were observed in the charmonium mass region, denoted as XYZ states due to their mysterious properties. Feng-Kun Guo showed that approximate symmetries of QCD for heavy quarks could provide invaluable insights into revealing the nature of these XYZ states, and made a series of predictions in [3] and other publications. These predictions have led to experimental investigations, and some of them have been verified such as the observation of the X(3872) in the radiative decay of the Y(4260) made by BESIII.

Prof. Guo continuously produces influential papers with insightful ideas, and his work has helped to understand the nature of these new hadrons and plays a major role in establishing a clearer pattern for them. Feng-Kun Guo has become a world leading scientist in this field, and clearly deserves the Nishina Asia Award. I strongly recommend him.

Key references (up to 3 key publications\*)

- [1] \* Feng-Kun Guo, Christoph Hanhart, Ulf-G. Meißner, Qian Wang, Qiang Zhao, Bing-Song Zou, *Hadronic molecules*, **Rev. Mod. Phys.** **90** (2018) 015004.
- [2] Feng-Kun Guo, Peng-Nian Shen, Huan-Ching Chiang, Rong-Gang Ping, Bing-Song Zou, *Dynamically generated  $0^+$  heavy mesons in a heavy chiral unitary approach*, **Phys. Lett. B** **641** (2006) 278.
- [3] Feng-Kun Guo, Carlos Hidalgo-Duque, Juan Nieves, Manuel Pavon Valderrama, *Consequences of heavy quark symmetries for hadronic molecules*, **Phys. Rev. D** **88** (2013) 054007.

\*) Copy of one most significant publication should be attached.

Nominator (name, affiliation, email, telephone and relation to the candidate)

**Name:** Makoto Oka

**Affiliation:** Advanced Science Research Center, Japan Atomic Energy Agency

**Email:** oka@post.j-parc.jp

**Telephone:** 029-282-5093

**Relation to the candidate:** I first met him in a conference in Spain and have known him for these 5 years. I invited him to a workshop at JAEA in 2018.

Signature



Date

March, 29, 2019